

Published in final edited form as:

Nature. 2020 February ; 578(7793): 82–93. doi:10.1038/s41586-020-1969-6.

Users may view, print, copy, and download text and data-mine the content in such documents, for the purposes of academic research, subject always to the full Conditions of use:http://www.nature.com/authors/editorial_policies/license.html#terms

Correspondence and requests for materials should be addressed to P.J.C. (pc8@sanger.ac.uk), G.G. (gadgetz@broadinstitute.org), J.O.K. (korb@embl.de), J.M.S. (jstuart@ucsc.edu) or L.D.S. (lincoln.stein@gmail.com).

§A list of members and their affiliations appears in the online version of the paper

Author contributions

A structured author contribution list is available in the online version of the paper.

Writing committee leads: Peter J Campbell, Gad Getz, Jan O Korb, Joshua M Stuart, Jennifer L Jennings, Lincoln D Stein. Head of project management: Jennifer L Jennings. Sample Collection: Major contributions from Marc D Perry, Hardeep K Nahal-Bose; Led by BF Francis Ouellette. Histopathology harmonisation: Major contribution from Constance H Li; Further contributions from Esther Rheinbay, G Petur Nielsen, Dennis C Sgroi, Chin-Lee Wu, William C Faquin, Vikram Deshpande, Paul C Boutros, Alexander J Lazar, Katherine A Hoadley; Led by Lincoln D Stein, David N Louis. Uniform processing, somatic, germline variant calling: Major contribution from L Jonathan Dursi; Further contributions from Christina K Yung, Matthew H Bailey, Gordon Saksena, Keiran M Raine, Ivo Buchhalter, Kortine Kleinheinz, Matthias Schlesner, Junjun Zhang, Wenyi Wang, David A Wheeler; Led by Li Ding, Jared T Simpson. Core alignment, variant calling by cloud computing: Major contributions from Christina K Yung, Brian D O'Connor, Sergei Yakneen, Junjun Zhang; Further contributions from Kyle Ellrott, Kortine Kleinheinz, Naoki Miyoshi, Keiran M Raine, Adam P Butler, Romina Royo, Gordon Saksena, Matthias Schlesner, Solomon I Shorser, Miguel Vazquez. Integration, phasing, validation of germline variant callsets: Major contributions from Tobias Rausch, Grace Tiao, Sebastian M Waszak, Bernardo Rodriguez-Martin, Suyash Shringarpure, Dai-Ying Wu; Further contributions from Sergei Yakneen, German M Demidov, Olivier Delaneau, Shuto Hayashi, Seiya Imoto, Nina Habermann, Ayellet V Segre, Erik Garrison, Andy Cafferkey, Eva G Alvarez, Jose Maria Heredia-Genestar, Francesc Muiyas, Oliver Drechsel, Alicia L Bruzos, Javier Temes, Jorge Zamora, L Jonathan Dursi, Adrian Baez-Ortega, Hyung-Lae Kim, Matthew H Bailey, R Jay Mashl, Kai Ye, Ivo Buchhalter, Anthony DiBiase, Kuan-lin Huang, Ivica Letunic, Michael D McLellan, Steven J Newhouse, Matthias Schlesner, Tal Shmaya, Sushant Kumar, David C Wedge, Mark H Wright, Venkata D Yellapantula, Mark Gerstein, Ekta Khurana, Tomas Marques-Bonet, Arcadi Navarro, Carlos D Bustamante, Jared T Simpson, Li Ding, Reiner Siebert, Hidewaki Nakagawa, Douglas F Easton; Led by Stephan Ossowski, Jose MC Tubio, Gad Getz, Francisco M De La Vega, Xavier Estivill, Jan O Korb. Validation, benchmarking, merging of somatic variant calls: Major contribution from L Jonathan Dursi; Further contributions from David A Wheeler, Christina K Yung; Led by Li Ding, Jared T Simpson. Data, code availability: Major contribution from Junjun Zhang; Further contributions from Christina K Yung, Sergei Yakneen, Denis Yuen, George L Mihaiescu, Larsson Omberg; Led by Vincent Ferretti. Pan-cancer burden of somatic mutations: Major contribution from Junjun Zhang; Led by Peter J Campbell. Panorama of driver mutations in human cancer: Led by Radhakrishnan Sabarinathan, Oriol Pich, Abel Gonzalez-Perez. PCAWG tumours with no apparent driver mutations: Major contribution from Esther Rheinbay; Further contributions from Amaro Taylor-Weiner, Radhakrishnan Sabarinathan; Led by Peter J Campbell, Gad Getz. Patterns, oncogenicity of kataegis, chromoplexy: Major contributions from Matthew W Fittall, Jonas Demeulemeester, Maxime Tarabichi; Further contributions from Nicola D Roberts, Peter J Campbell, Jan O Korb; Led by Peter Van Loo. Patterns, oncogenicity of chromothripsis: Major contributions from Maxime Tarabichi, Jonas Demeulemeester, Matthew W Fittall; Further contributions from Isidro Cortes-Ciriano, Lara Urban, Peter Park, Peter J Campbell, Jan O Korb; Led by Peter Van Loo. Timing clustered mutational processes during tumour evolution: Major contributions from Jonas Demeulemeester, Maxime Tarabichi, Matthew W Fittall; Further contributions from Jan O Korb, Peter J Campbell; Led by Peter Van Loo. Germline effects on somatic mutation: Major contributions from Sebastian M Waszak, Bin Zhu, Bernardo Rodriguez-Martin, Esa Pitkanen, Tobias Rausch; Further contributions from Yilong Li, Natalie Saini, Leszek J Klimczak, Joachim Weischenfeldt, Nikos Sidiropoulos, Ludmil B Alexandrov, Francesc Muiyas, Raquel Rabionet, Georgia Escaramis, Adrian Baez-Ortega, Mattia Bosio, Aliaksei Z Holik, Hana Susak, Eva G Alvarez, Alicia L Bruzos, Javier Temes, Aparna Prasad, Nina Habermann, Serap Erkek, Lara Urban, Claudia Calabrese, Benjamin Raeder, Eoghan Harrington, Simon Mayes, Daniel Turner, Sissel Juul, Steven A Roberts, Lei Song, Roelof Koster, Lisa Mirabello, Xing Hua, Tomas J Tanskanen, Marta Tojo, David C Wedge, Jorge Zamora, Jieming Chen, Lauri A Aaltonen, Gunnar Ratsch, Roland F Schwarz, Atul J Butte, Alvis Brazma, Peter J Campbell, Stephen J Chanock, Nilanjan Chatterjee, Oliver Stegle, Olivier Harismendy; Led by G Steven Bova, Dmitry A Gordenin, Jose MC Tubio, Douglas F Easton, Xavier Estivill, Jan O Korb. Replicative Immortality: Major contribution from David Haan; Further contributions from Lina Sieverling, Lars Feuerbach; Led by Lincoln D Stein, Joshua M Stuart. Ethical considerations of genomic cloud computing: Led by Don Chalmers, Yann Joly, Bartha Knoppers, Fruzsina Molnar-Gabor, Jan O Korb, Mark Phillips, Adrian Thorogood, David Townend. Online resources for data access, visualisation, exploration, analysis: Major contributions from Mary Goldman, Junjun Zhang, Nuno A Fonseca; Further contributions from Qian Xiang, Brian Craft, Elena Pineiro-Yanez, Alfonso Munoz, Robert Petryszak, Anja Fullgrabe, Fatima Al-Shahrour, Maria Keays, David Haussler, John Weinstein, Wolfgang Huber, Alfonso Valencia, Irene Papatheodorou, Jingchun Zhu; Led by Brian O'Connor, Lincoln D Stein, Alvis Brazma, Vincent Ferretti, Miguel Vazquez. Pilot-63 Analysis Validation Process: Major contribution from L Jonathan Dursi; Further contributions from Christina K Yung, Matthew H Bailey, Gordon Saksena, Keiran M Raine, Ivo Buchhalter, Kortine Kleinheinz, Matthias Schlesner, Yu Fan, David Torrents, Matthias Bieg, Paul C Boutros, Ken Chen, Zechen Chong, Kristian Cibulskis, Oliver Drechsel, Roland Eils, Robert S Fulton, Josep Gelpi, Mark Gerstein, Santiago Gonzalez, Gad Getz, Ivo G Gut, Faraz Hach, Michael Heinold, Taobo Hu, Vincent Huang, Barbara Hutter, Hyung-Lae Kim, Natalie Jager, Jongsun Jung, Sushant Kumar, Yogesh Kumar, Christopher Lalansingh, Ignaty Leshchiner, Ivica Letunic, Dimitri Livitz, Eric Z Ma, Yosef Maruvka, R Jay Mashl, Michael D McLellan, Ana Milovanovic, Morten Muhlig Nielsen, Brian O'Connor, Stephan Ossowski, Nagarajan Paramasivam, Jakob Skou Pedersen, Marc D Perry, Montserrat Puigros, Romina Royo, Esther Rheinbay, S Cenk Sahinalp, Iman Sarrafi, Chip Stewart, Miranda D Stobbe, Grace Tiao, Jeremiah A Wala, Jiayin Wang, Wenyi Wang, Sebastian M Waszak, Joachim Weischenfeldt, Michael Wendl, Johannes Werner,

Pan-cancer analysis of whole genomes

Zhenggang Wu, Hong Xue, Sergei Yakneen, Takafumi N Yamaguchi, Kai Ye, Venkata Yellapantula, Junjun Zhang, David A Wheeler; Led by Li Ding, Jared T Simpson. Processing of Validation Data: Major contributions from Christina K Yung, Brian D O'Connor, Sergei Yakneen, Junjun Zhang; Further contributions from Kyle Ellrott, Kortine Kleinheinz, Naoki Miyoshi, Keiran M Raine, Romina Royo, Gordon Saksena, Matthias Schlesner, Solomon I Shorser, Miguel Vazquez, Joachim Weischenfeldt, Denis Yuen, Adam P Butler, Brandi N Davis-Dusenbery, Roland Eils, Vincent Ferretti, Robert L Grossman, Olivier Harismendy, Youngwook Kim, Hidewaki Nakagawa, Steven J Newhouse, David Torrents; Led by Lincoln D Stein. Whole Genome Sequencing Somatic Variant Calling: Major contribution from Junjun Zhang; Further contributions from Christina K Yung, Solomon I Shorser. Whole Genome Alignment: Keiran M Raine, Junjun Zhang, Brian O'Connor. DKFZ Pipeline: Kortine Kleinheinz, Tobias Rausch, Jan O Korbel, Ivo Buchhalter, Michael C Heinold, Barbara Hutter, Natalie Jager, Nagarajan Paramasivam, Matthias Schlesner. EMBL Pipeline: Joachim Weischenfeldt. Sanger Pipeline: Keiran M Raine, Jonathan Hinton, David R Jones, Andrew Menzies, Lucy Stebbings, Adam P Butler. Broad Pipeline: Gordon Saksena, Dimitri Livitz, Esther Rheinbay, Julian M Hess, Ignaty Leshchiner, Chip Stewart, Grace Tiao, Jeremiah A Wala, Amaro Taylor-Weiner, Mara Rosenberg, Andrew J Dunford, Manaswi Gupta, Marcin Imielinski, Matthew Meyerson, Rameen Beroukhim, Gad Getz. MuSE Pipeline: Yu Fan, Wenyi Wang. Consensus Somatic SNV/Indel Annotation: Andrew Menzies, Matthias Schlesner, Juri Reimand, Priyanka Dhingra, Ekta Khurana. Somatic SNV, indel Merging: Major contribution from L Jonathan Dursi; Further contributions from Christina K Yung, Matthew H Bailey, Gordon Saksena, Keiran M Raine, Ivo Buchhalter, Kortine Kleinheinz, Matthias Schlesner, Yu Fan, David Torrents, Matthias Bieg, Paul C Boutros, Ken Chen, Zechen Chong, Kristian Cibulskis, Oliver Drechsel, Roland Eils, Robert S Fulton, Josep Gelpi, Mark Gerstein, Santiago Gonzalez, Gad Getz, Ivo G Gut, Faraz Hach, Michael Heinold, Taobo Hu, Vincent Huang, Barbara Hutter, Hyung-Lae Kim, Natalie Jager, Jongsun Jung, Sushant Kumar, Yogesh Kumar, Christopher Lalansingh, Ignaty Leshchiner, Ivica Letunic, Dimitri Livitz, Eric Z Ma, Yosef Maruvka, R Jay Mashl, Michael D McLellan, Ana Milovanovic, Morten Muhlig Nielsen, Brian O'Connor, Stephan Ossowski, Nagarajan Paramasivam, Jakob Skou Pedersen, Marc D Perry, Montserrat Puiggros, Romina Royo, Esther Rheinbay, S Cenk Sahinalp, Iman Sarrafi, Chip Stewart, Miranda D Stobbe, Grace Tiao, Jeremiah A Wala, Jiayin Wang, Wenyi Wang, Sebastian M Waszak, Joachim Weischenfeldt, Michael Wendl, Johannes Werner, Zhenggang Wu, Hong Xue, Sergei Yakneen, Takafumi N Yamaguchi, Kai Ye, Venkata Yellapantula, Junjun Zhang, David A Wheeler; Major contributions from Li Ding, Jared T Simpson. Somatic SV Merging: Joachim Weischenfeldt, Francesco Favero, Yilong Li. Somatic Copy Number Alteration Merging: Stefan Dentre, Jeff Wintersinger, Ignaty Leshchiner. Oxidative Artefact Filtration: Dimitri Livitz, Ignaty Leshchiner, Chip Stewart, Esther Rheinbay, Gordon Saksena, Gad Getz. Strand Bias Filtration: Matthias Bieg, Ivo Buchhalter, Johannes Werner, Matthias Schlesner. miniBAM generation: Jeremiah Wala, Gordon Saksena, Rameen Beroukhim, Gad Getz. Germline Variant Identification from WGS: Major contributions from Tobias Rausch, Grace Tiao, Sebastian M Waszak, Bernardo Rodriguez-Martin, Suyash Shringarpure, Dai-Ying Wu; Further contributions from Sergei Yakneen, German M Demidov, Olivier Delaneau, Shuto Hayashi, Seiya Imoto, Nina Habermann, Ayellet V Segre, Erik Garrison, Andy Cafferkey, Eva G Alvarez, Alicia L Bruzos, Jorge Zamora, Jose Maria Heredia-Genestar, Francesc Muiyas, Oliver Drechsel, L Jonathan Dursi, Adrian Baez-Ortega, Hyung-Lae Kim, Matthew H Bailey, R Jay Mashl, Kai Ye, Ivo Buchhalter, Vasilisa Rudneva, Ji Wan Park, Eun Pyo Hong, Seong Gu Heo, Anthony DiBiase, Kuan-lin Huang, Ivica Letunic, Michael D McLellan, Steven J Newhouse, Matthias Schlesner, Tal Shmaya, Sushant Kumar, David C Wedge, Mark H Wright, Venkata D Yellapantula, Mark Gerstein, Ekta Khurana, Tomas Marques-Bonet, Arcadi Navarro, Carlos D Bustamante, Jared T Simpson, Li Ding, Reiner Siebert, Hidewaki Nakagawa, Douglas F Easton; Led by Stephan Ossowski, Jose MC Tubio, Gad Getz, Francisco M De La Vega, Xavier Estivill, Jan O Korbel. RNA-Seq analysis: Major contributions from Nuno A Fonseca, Andre Kahles, Kjong-Van Lehmann, Lara Urban, Cameron M Soulette, Yuichi Shiraiishi, Fenglin Liu, Yao He, Deniz Demircioglu, Natalie R Davidson, Claudia Calabrese, Junjun Zhang, Marc D Perry, Qian Xiang; Further contributions from Liliana Greger, Siliang Li, Dongbing Liu, Stefan G Stark, Fan Zhang, Samirkumar B Amin, Peter Bailey, Aurelien Chateigner, Isidro Cortes-Ciriano, Brian Craft, Serap Erkek, Milana Frenkel-Morgenstern, Mary Goldman, Katherine A Hoadley, Yong Hou, Matthew R Huska, Ekta Khurana, Helena Kilpinen, Jan O Korbel, Fabien C Lamaze, Chang Li, Xiaobo Li, Xinyue Li, Xingmin Liu, Maximillian G Marin, Julia Markowski, Tannistha Nandi, Morten Muhlig Nielsen, Akinyemi I Ojesina, Qiang Pan-Hammarstrom, Peter J Park, Chandra Sekhar Pedamallu, Jakob Pedersen, Reiner Siebert, Hong Su, Patrick Tan, Bin Tean Teh, Jian Wang, Sebastian M Waszak, Heng Xiong, Sergei Yakneen, Chen Ye, Christina Yung, Xiuqing Zhang, Liangtao Zheng, Jingchun Zhu, Shida Zhu, Philip Awadalla, Chad J Creighton, Matthew Meyerson, BF Francis Ouellette, Kui Wu, Huanming Yang; Led by Jonathan Goke, Roland F Schwarz, Oliver Stegle, Zemin Zhang, Alvis Brazma, Gunnar Ratsch, Angela N Brooks. Clustering of tumour genomes based on telomere maintenance-related features: Major contribution from David Haan; Led by Lincoln D Stein, Joshua M Stuart. Clustered mutational processes in PCAWG: Major contributions from Jonas Demeulemeester, Maxime Tarabichi, Matthew W Fittall; Led by Peter J Campbell, Jan O Korbel, Peter Van Loo. Tumours without detected driver mutations: Esther Rheinbay, Amaro Taylor-Weiner, Radhakrishnan Sabarinathan, Peter J Campbell, Gad Getz. Panorama of driver mutations in human cancer: Major contributions from Radhakrishnan Sabarinathan, Oriol Pich; Further contributions from Inigo Martincorena, Carlota Rubio-Perez, Malene Juul, Jeremiah Wala, Steven Schumacher, Ofer Shapira, Nikos Sidiropoulos, Sebastian M Waszak, David Tamborero, Loris Mularoni, Esther Rheinbay, Henrik Hornshoj, Jordi Deu-Pons, Ferran Muiños, Johanna Bertl, Qianyun Guo, Chad J Creighton, Joachim Weischenfeldt, Jan O Korbel, Gad Getz, Peter J Campbell, Jakob Pedersen, Rameen Beroukhim; Led by Abel Gonzalez-Perez. Pilot- benchmarking, variant consensus development, validation: Major contribution from L Jonathan Dursi; Further contributions from Christina K Yung, Matthew H Bailey, Gordon Saksena, Keiran M Raine, Ivo Buchhalter, Kortine Kleinheinz, Matthias Schlesner, Yu Fan, David Torrents, Matthias Bieg, Paul C Boutros, Ken Chen, Zechen Chong, Kristian Cibulskis, Oliver Drechsel, Roland Eils, Robert S Fulton, Josep Gelpi, Mark Gerstein, Santiago Gonzalez, Gad Getz, Ivo G Gut, Faraz Hach, Michael Heinold, Taobo Hu, Vincent Huang, Barbara Hutter, Hyung-Lae Kim, Natalie Jager, Jongsun Jung, Sushant Kumar,

The ICGC/TCGA Pan-Cancer Analysis of Whole Genomes Consortium[§]

Yogesh Kumar, Christopher Lalansingh, Ignaty Leshchiner, Ivica Letunic, Dimitri Livitz, Eric Z Ma, Yosef Maruvka, R Jay Mashl, Michael D McLellan, Ana Milovanovic, Morten Muhlig Nielsen, Brian O'Connor, Stephan Ossowski, Nagarajan Paramasivam, Jakob Skou Pedersen, Marc D Perry, Montserrat Puiggros, Romina Royo, Esther Rheinbay, S Cenk Sahinalp, Iman Sarrafi, Chip Stewart, Miranda D Stobbe, Grace Tiao, Jeremiah A Wala, Jiayin Wang, Wenyi Wang, Sebastian M Waszak, Joachim Weischenfeldt, Michael Wendl, Johannes Werner, Zhenggang Wu, Hong Xue, Sergei Yakneen, Takafumi N Yamaguchi, Kai Ye, Venkata Yellapantula, Junjun Zhang, David A Wheeler; Led by Li Ding, Jared T Simpson. Production somatic variant calling on the PCAWG Compute Cloud: Major contributions from Christina K Yung, Brian D O'Connor, Sergei Yakneen, Junjun Zhang; Further contributions from Kyle Ellrott, Kortine Kleinheinz, Naoki Miyoshi, Keiran M Raine, Romina Royo, Gordon Saksena, Matthias Schlesner, Solomon I Shorser, Miguel Vazquez, Joachim Weischenfeldt, Denis Yuen, Adam P Butler, Brandi N Davis-Dusenbery, Roland Eils, Vincent Ferretti, Robert L Grossman, Olivier Harismendy, Youngwook Kim, Hidewaki Nakagawa, Steven J Newhouse, David Torrents; Led by Lincoln D Stein. PCAWG data portals: Major contributions from Mary Goldman, Junjun Zhang, Nuno A Fonseca, Isidro Cortes-Ciriano; Further contributions from Qian Xiang, Brian Craft, Elena Pineiro-Yanez, Brian D O'Connor, Wojciech Bazant, Elisabet Barrera, Alfonso Munoz, Robert Petryszak, Anja Fullgrabe, Fatima Al-Shahrour, Maria Keays, David Haussler, John Weinstein, Wolfgang Huber, Alfonso Valencia, Irene Papatheodorou, Jingchun Zhu; Led by Vincent Ferretti, Miguel Vazquez.

The corresponding authors declare the following competing financial interests: G.G. receives research funds from IBM and Pharmacyclics and is an inventor on patent applications related to MuTect, ABSOLUTE, MutSig, MSMuTect and POLYSOLVER. The other corresponding authors have no competing financial interests to declare. Other authors declare competing financial interests: details are available in the online version of the paper.

Data availability

The PCAWG-generated alignments, somatic variant calls, annotations and derived data sets are available for general research use for browsing and download at <http://dcc.icgc.org/pcawg/> (Box 1; Supplementary Table 4). In accordance with the data access policies of the ICGC and TCGA projects, most molecular, clinical and specimen data are in an open tier which does not require access approval. To access potentially identifying information, such as germline alleles and underlying read data, researchers will need to apply to the TCGA Data Access Committee (DAC) via dbGaP (<https://dbgap.ncbi.nlm.nih.gov/aa/wga.cgi?page=login>) for access to the TCGA portion of the data set, and to the ICGC Data Access Compliance Office (DACO; <http://icgc.org/daco>) for the ICGC portion. In addition, to access somatic single nucleotide variants derived from TCGA donors, researchers will also need to obtain dbGaP authorisation.

Beyond the core sequence data and variant call-sets, the analyses in this paper used a number of datasets that were derived from the variant calls (Supplementary Table 4). The individual data sets are available at Synapse (<https://www.synapse.org/>), and are denoted with synXXXXX accession numbers; all these datasets are also mirrored at <https://dcc.icgc.org>, with full links, filenames, accession numbers and descriptions detailed in Supplementary Table 4. The datasets encompass: clinical data from each patient including demographics, tumour stage and vital status (syn10389158); harmonised tumour histopathology annotations using a standardised hierarchical ontology (syn1038916); inferred purity and ploidy values for each tumour sample (syn8272483); driver mutations for each patient from their cancer genome spanning all classes of variant, and coding versus non-coding drivers (syn11639581); mutational signatures inferred from PCAWG donors (syn11804065), including APOBEC mutagenesis (syn7437313); and transcriptional data from RNA-sequencing, including gene expression levels (syn5553985, syn5553991, syn8105922) and gene fusions (syn10003873, syn7221157).

Code availability

Computational pipelines for calling somatic mutations are available to the public at <https://dockstore.org>. A range of data visualisation and exploration tools are also available for PCAWG data (Box 1).

Author list: Participants in PCAWG Consortium

These authors jointly supervised this work:

Peter J Campbell, Gad Getz, Jan O Korbel, Joshua M Stuart and Lincoln D Stein.

Writing Committee

Writing Committee Leads

Peter J Campbell^{1,2}, Gad Getz^{3,4,5,6}, Jan O Korbel^{7,8}, Joshua M Stuart⁹, Jennifer L Jennings^{10,11} and Lincoln D Stein^{12,13}

Sample Collection

Marc D Perry^{14,15}, Hardeep K Nahal-Bose¹⁵ and BF Francis Ouellette^{16,17}

Histopathology harmonisation

Constance H Li^{12,18}, Esther Rheinbay^{3,6,19}, G Petur Nielsen¹⁹, Dennis C Sgroi¹⁹, Chin-Lee Wu¹⁹, William C Faquin¹⁹, Vikram Deshpande¹⁹, Paul C Boutros^{12,18,20,21}, Alexander J Lazar²², Katherine A Hoadley^{23,24}, Lincoln D Stein^{12,13} and David N Louis¹⁹

Uniform processing, somatic and germline variant calling

L Jonathan Dursi^{12,25}, Christina K Yung¹⁵, Matthew H Bailey^{26,27}, Gordon Saksena³, Keiran M Raine¹, Ivo Buchhalter^{28,29,30}, Kortine Kleinheinz^{28,30}, Matthias Schlesner^{28,31}, Junjun Zhang¹⁵, Wenyi Wang³², David A Wheeler^{33,34}, Li Ding^{26,27,35} and Jared T Simpson^{12,36}

Core alignment and variant calling by cloud computing

Christina K Yung¹⁵, Brian D O'Connor^{15,37}, Sergei Yakneen⁸, Junjun Zhang¹⁵, Kyle Ellrott³⁸, Kortine Kleinheinz^{28,30}, Naoki Miyoshi³⁹, Keiran M Raine¹, Adam P Butler¹, Romina Royo⁴⁰, Gordon Saksena³, Matthias Schlesner^{28,31}, Solomon I Shorser¹² and Miguel Vazquez^{40,41}

Integration, phasing, and validation of germline variant callsets

Abstract

Tobias Rausch⁸, Grace Tiao³, Sebastian M Waszak⁸, Bernardo Rodriguez-Martin^{42,43,44}, Suyash Shringarpure⁴⁵, Dai-Ying Wu⁴⁶, Sergei Yakneen⁸, German M Demidov^{47,48,49}, Olivier Delaneau^{50,51,52}, Shuto Hayashi³⁹, Seiya Imoto^{39,39}, Nina Habermann⁸, Ayellet V Segre^{3,53}, Erik Garrison¹, Andy Cafferkey⁷, Eva G Alvarez^{42,43,44}, José María Heredia-Genestar⁵⁴, Francesc Muiyas^{47,48,49}, Oliver Drechsel^{47,49}, Alicia L Bruzos^{42,43,44}, Javier Temes^{42,43}, Jorge Zamora^{1,42,43,44}, L Jonathan Dursi^{12,25}, Adrian Baez-Ortega⁵⁵, Hyung-Lae Kim⁵⁶, Matthew H Bailey^{26,27}, R Jay Mashl^{27,57}, Kai Ye^{58,59}, Ivo Buchhalter^{28,29,30}, Anthony DiBiase⁶⁰, Kuan-lin Huang^{27,61}, Ivica Letunic⁶², Michael D McLellan^{26,27,35}, Steven J Newhouse⁷, Matthias Schlesner^{28,31}, Tal Shmaya⁴⁶, Sushant Kumar^{63,64}, David C Wedge^{1,65,66}, Mark H Wright⁴⁵, Venkata D Yellapantula^{67,68}, Mark Gerstein^{63,64,69}, Ekta Khurana^{70,71,72,73}, Tomas Marques-Bonet^{74,75,76,77}, Arcadi Navarro^{74,75,76}, Carlos D Bustamante^{45,78}, Jared T Simpson^{12,36}, Li Ding^{26,27,35}, Reiner Siebert^{79,80}, Hidewaki Nakagawa⁸¹, Douglas F Easton^{82,83}, Stephan Ossowski^{47,48,49}, Jose MC Tubio^{42,43,44}, Gad Getz^{3,4,5,6}, Francisco M De La Vega^{45,46,78}, Xavier Estivill^{47,84} and Jan O Korbel^{7,8}

Validation, benchmarking and merging of somatic variant calls

L Jonathan Dursi^{12,25}, David A Wheeler^{33,34}, Christina K Yung¹⁵, Li Ding^{26,27,35} and Jared T Simpson^{12,36}

Data and code availability

Junjun Zhang¹⁵, Christina K Yung¹⁵, Sergei Yakneen⁸, Denis Yuen¹², George L Mihaiescu¹⁵, Larsson Omberg⁸⁵ and Vincent Ferretti^{15,86}

Pan-cancer burden of somatic mutations

Junjun Zhang¹⁵ and Peter J Campbell^{1,2}

Panorama of driver mutations in human cancer

Radhakrishnan Sabarinathan^{87,88,89}, Oriol Pich^{87,89} and Abel Gonzalez-Perez^{87,89}

PCAWG tumours with no apparent driver mutations

Esther Rheinbay^{3,6,19}, Amaro Taylor-Weiner⁹⁰, Radhakrishnan Sabarinathan^{87,88,89}, Peter J Campbell^{1,2} and Gad Getz^{3,4,5,6}

Patterns and oncogenicity of kataegis and chromoplexy

Matthew W Fittall⁹¹, Jonas Demeulemeester^{91,92}, Maxime Tarabichi^{1,91}, Nicola D Roberts¹, Peter J Campbell^{1,2}, Jan O Korbel^{7,8} and Peter Van Loo^{91,92}

Patterns and oncogenicity of chromothripsis

Maxime Tarabichi^{1,91}, Jonas Demeulemeester^{91,92}, Matthew W Fittall⁹¹, Isidro Cortés-Ciriano^{93,94,95}, Lara Urban^{7,8}, Peter Park^{94,95}, Peter J Campbell^{1,2}, Jan O Korbel^{7,8} and Peter Van Loo^{91,92}

Timing clustered mutational processes during tumour evolution

Jonas Demeulemeester^{91,92}, Maxime Tarabichi^{1,91}, Matthew W Fittall⁹¹, Jan O Korbel^{7,8}, Peter J Campbell^{1,2} and Peter Van Loo^{91,92}

Germline genetic determinants of the somatic mutation landscape

Sebastian M Waszak⁸, Bin Zhu⁹⁶, Bernardo Rodriguez-Martin^{42,43,44}, Esa Pitkänen⁸, Tobias Rausch⁸, Yilong Li¹, Natalie Saini⁹⁷, Leszek J Klimczak⁹⁸, Joachim Weischenfeldt^{8,99,100}, Nikos Sidiropoulos¹⁰⁰, Ludmil B Alexandrov^{1,101}, Francesc Muiyas^{47,48,49}, Raquel Rabionet^{47,49,102}, Georgia Escaramis^{47,103,104}, Adrian Baez-Ortega⁵⁵, Mattia Bosio^{40,47,49}, Aliaksei Z Holik⁴⁷, Hana Susak^{47,49}, Eva G Alvarez^{42,43,44}, Alicia L Bruzos^{42,43,44}, Javier Temes^{42,43}, Aparna Prasad⁴⁹, Nina Habermann⁸, Serap Erkek⁸, Lara Urban^{7,8}, Claudia Calabrese^{7,8}, Benjamin Raeder⁸, Eoghan Harrington¹⁰⁵, Simon Mayes¹⁰⁶, Daniel Turner¹⁰⁶, Sissel Juul¹⁰⁵, Steven A Roberts¹⁰⁷, Lei Song⁹⁶, Roelof Koster¹⁰⁸, Lisa Mirabello⁹⁶, Xing Hua⁹⁶, Tomas J Tanskanen¹⁰⁹, Marta Tojo⁴⁴, David C Wedge^{1,65,66}, Jorge Zamora^{1,42,43,44}, Jieming Chen^{64,110}, Lauri A Aaltonen¹¹¹, Gunnar Rätsch^{112,113,114,115,116,117}, Roland F Schwarz^{7,118,119,120}, Atul J Butte¹²¹, Alvis Brazma⁷, Peter J Campbell^{1,2}, Stephen J Chanock⁹⁶, Nilanjan Chatterjee^{122,123,123}, Oliver Stegle^{7,8,124}, Olivier Harismendy¹²⁵, G Steven Bova¹²⁶, Dmitry A Gordenin⁹⁷, Jose MC Tubio^{42,43,44}, Douglas F Easton^{82,83}, Xavier Estivill^{47,84} and Jan O Korbel^{7,8}

Replicative Immortality

David Haan⁹, Lina Sieverling^{127,128}, Lars Feuerbach¹²⁷, Lincoln D Stein^{12,13} and Joshua M Stuart⁹

Ethical considerations of genomic cloud computing

Don Chalmers¹²⁹, Yann Joly¹³⁰, Bartha Knoppers¹³⁰, Fruzsina Molnár-Gábor¹³¹, Jan O Korbel^{7,8}, Mark Phillips¹³⁰ and Adrian Thorogood and David Townend¹³⁰

Box 1: Online resources for data access, visualisation, exploration and analysis

Mary Goldman¹³², Junjun Zhang¹⁵, Nuno A Fonseca^{7,133}, Qian Xiang¹³⁴, Brian Craft¹³², Elena Piñeiro-Yáñez¹³⁵, Alfonso Muñoz⁷, Robert Petryszak⁷, Anja Füllgrabe⁷, Fatima Al-Shahrour¹³⁵, Maria Keays⁷, David Haussler^{132,136}, John Weinstein^{137,138}, Wolfgang Huber⁸, Alfonso Valencia^{40,76}, Irene Papatheodorou⁷, Jingchun Zhu¹³², Brian O'Connor^{15,37}, Lincoln D Stein^{12,13}, Alvis Brazma⁷, Vincent Ferretti^{15,86} and Miguel Vazquez^{40,41}

Methods 1.1 Validation Process

L Jonathan Dursi^{12,25}, Christina K Yung¹⁵, Matthew H Bailey^{26,27}, Gordon Saksena³, Keiran M Raine¹, Ivo Buchhalter^{28,29,30}, Kortine Kleinheinz^{28,30}, Matthias Schlesner^{28,31}, Yu Fan³², David Torrents^{40,76}, Matthias Bieg^{139,140}, Paul C Boutros^{12,18,20,21}, Ken Chen¹⁴¹, Zechen Chong¹⁴², Kristian Cibulskis³, Oliver Drechsel^{47,49}, Roland Eils^{28,30,143,144}, Robert S Fulton^{26,27,35}, Josep Gelpi^{40,145}, Mark Gerstein^{63,64,69}, Santiago Gonzalez^{7,8}, Gad Getz^{3,4,5,6}, Ivo G Gut^{49,74}, Faraz Hach^{146,147}, Michael Heindold^{28,30}, Taobo Hu¹⁴⁸, Vincent Huang¹², Barbara Hutter^{140,149,150}, Hyung-Lae Kim⁵⁶, Natalie Jäger²⁸, Jongsun Jung¹⁵¹, Sushant Kumar^{63,64}, Yogesh Kumar¹⁴⁸, Christopher Lalansingh¹², Ignaty Leshchiner³, Ivica Letunic⁶², Dimitri Livitz³, Eric Z Ma¹⁴⁸, Yosef Maruvka^{3,19,152}, R Jay Mashl^{27,57}, Michael D McLellan^{26,27,35}, Ana Milovanovic⁴⁰, Morten Muhlig Nielsen¹⁵³, Brian O'Connor^{15,37}, Stephan Ossowski^{47,48,49}, Nagarajan Paramasivam^{28,140}, Jakob Skou Pedersen^{153,154}, Marc D Perry^{14,15}, Montserrat Puiggròs⁴⁰, Romina Royo⁴⁰, Esther Rheinbay^{3,6,19}, S Cenk Sahinalp^{147,155,156},

Cancer is driven by genetic change, and the advent of massively parallel sequencing has enabled

Iman Sarrafi^{147,156}, Chip Stewart³, Miranda D Stobbe^{49,74}, Grace Tiao³, Jeremiah A Wala^{3,6,157}, Jiayin Wang^{27,58,158}, Wenyi Wang³², Sebastian M Waszak⁸, Joachim Weischenfeldt^{8,99,100}, Michael Wendl^{27,159,160}, Johannes Werner^{28,161}, Zhenggang Wu¹⁴⁸, Hong Xue¹⁴⁸, Sergei Yakneen⁸, Takafumi N Yamaguchi¹², Kai Ye^{58,59}, Venkata Yellapantula^{67,68}, Junjun Zhang¹⁵, David A Wheeler^{33,34}, Li Ding^{26,27,35} and Jared T Simpson^{12,36}

Methods 1.2 Processing of Validation Data

Christina K Yung¹⁵, Brian D O'Connor^{15,37}, Sergei Yakneen⁸, Junjun Zhang¹⁵, Kyle Ellrott³⁸, Kortine Kleinheinz^{28,30}, Naoki Miyoshi³⁹, Keiran M Raine¹, Romina Royo⁴⁰, Gordon Saksena³, Matthias Schlesner^{28,31}, Solomon I Shorser¹², Miguel Vazquez^{40,41}, Joachim Weischenfeldt^{8,99,100}, Denis Yuen¹², Adam P Butler¹, Brandi N Davis-Dusenbery¹⁶², Roland Eils^{28,30,143,144}, Vincent Ferretti^{15,86}, Robert L Grossman¹⁶³, Olivier Harismendy¹²⁵, Youngwook Kim^{164,165}, Hidewaki Nakagawa⁸¹, Steven J Newhouse⁷, David Torrents^{40,76} and Lincoln D Stein^{12,13}

Methods 2. Whole Genome Sequencing Somatic Variant Calling

Junjun Zhang¹⁵, Christina K Yung¹⁵ and Solomon I Shorser¹²

Methods 2.1 Whole Genome Alignment

Keiran M Raine¹, Junjun Zhang¹⁵ and Brian O'Connor^{15,37}

Methods 2.2.1 DKFZ Pipeline

Kortine Kleinheinz^{28,30}, Tobias Rausch⁸, Jan O Korbel^{7,8}, Ivo Buchhalter^{28,29,30}, Michael C Heinold^{28,30}, Barbara Hutter^{140,149,150}, Natalie Jäger²⁸, Nagarajan Paramasivam^{28,140} and Matthias Schlesner^{28,31}

Methods 2.2.2 EMBL Pipeline

Joachim Weischenfeldt^{8,99,100}, Tobias Rausch⁸

Methods 2.2.3 Sanger Pipeline

Keiran M Raine¹, Jonathan Hinton¹, David R Jones¹, Andrew Menzies¹ and Lucy Stebbings¹

Methods 2.2.4 Broad Pipeline

Gordon Saksena³, Dimitri Livitz³, Esther Rheinbay^{3,6,19}, Julian M Hess^{3,152}, Ignaty Leshchiner³, Chip Stewart³, Grace Tiao³, Jeremiah A Wala^{3,6,157}, Amaro Taylor-Weiner⁹⁰, Mara Rosenberg^{3,19}, Andrew J Dunford³, Manaswi Gupta³, Marcin Imielinski^{166,167}, Matthew Meyerson^{3,6,157}, Rameen Beroukhi^{3,6,168} and Gad Getz^{3,4,5,6}

Methods 2.2.5 MuSE Pipeline

Yu Fan³² and Wenyi Wang³²

Methods 2.3 Consensus Somatic SNV/Indel Annotation

Andrew Menzies¹, Matthias Schlesner^{28,31}, Jüri Reimand^{12,18}, Priyanka Dhingra^{71,73} and Ekta Khurana^{70,71,72,73}

Methods 2.4.1 Somatic SNV and indel Merging

L Jonathan Dursi^{12,25}, Christina K Yung¹⁵, Matthew H Bailey^{26,27}, Gordon Saksena³, Keiran M Raine¹, Ivo Buchhalter^{28,29,30}, Kortine Kleinheinz^{28,30}, Matthias Schlesner^{28,31}, Yu Fan³², David Torrents^{40,76}, Matthias Bieg^{139,140}, Paul C Boutros^{12,18,20,21}, Ken Chen¹⁴¹, Zechen Chong¹⁴², Kristian Cibulskis³, Oliver Drechsel^{47,49}, Roland Eils^{28,30,143,144}, Robert S Fulton^{26,27,35}, Josep Gelpi^{40,145}, Mark Gerstein^{63,64,69}, Santiago Gonzalez^{7,8}, Gad Getz^{3,4,5,6}, Ivo G Gut^{49,74}, Faraz Hach^{146,147}, Michael Heinold^{28,30}, Taobo Hu¹⁴⁸, Vincent Huang¹², Barbara Hutter^{140,149,150}, Hyung-Lae Kim⁵⁶, Natalie Jäger²⁸, Jongsun Jung¹⁵¹, Sushant Kumar^{63,64}, Yogesh Kumar¹⁴⁸, Christopher Lalansingh¹², Ignaty Leshchiner³, Ivica Letunic⁶², Dimitri Livitz³, Eric Z Ma¹⁴⁸, Yosef Maruvka^{3,19,152}, R Jay Mashl^{27,57}, Michael D McLellan^{26,27,35}, Ana Milovanovic⁴⁰, Morten Muhlig Nielsen¹⁵³, Brian O'Connor^{15,37}, Stephan Ossowski^{47,48,49}, Nagarajan Paramasivam^{28,140}, Jakob Skou Pedersen^{153,154}, Marc D Perry^{14,15}, Montserrat Puiggròs⁴⁰, Romina Royo⁴⁰, Esther Rheinbay^{3,6,19}, S Cenik Sahinalp^{147,155,156}, Iman Sarrafi^{147,156}, Chip Stewart³, Miranda D Stobbe^{49,74}, Grace Tiao³, Jeremiah A Wala^{3,6,157}, Jiayin Wang^{27,58,158}, Wenyi Wang³², Sebastian M Waszak⁸, Joachim Weischenfeldt^{8,99,100}, Michael Wendl^{27,159,160}, Johannes Werner^{28,161}, Zhenggang Wu¹⁴⁸, Hong Xue¹⁴⁸, Sergei Yakneen⁸, Takafumi N Yamaguchi¹², Kai Ye^{58,59}, Venkata Yellapantula^{67,68}, Junjun Zhang¹⁵, David A Wheeler^{33,34}, Li Ding^{26,27,35} and Jared T Simpson^{12,36}

Methods 2.4.2 Somatic SV Merging

Joachim Weischenfeldt^{8,99,100}, Francesco Favero¹⁶⁹ and Yilong Li¹

Methods 2.4.3 Somatic Copy Number Alteration Merging

Stefan Dentre^{1,65,91}, Jeff Wintersinger^{170,171,172} and Ignaty Leshchiner³

Methods 2.5.3 Oxidative Artefact Filtration

Dimitri Livitz³, Ignaty Leshchiner³, Chip Stewart³, Esther Rheinbay^{3,6,19}, Gordon Saksena³ and Gad Getz^{3,4,5,6}

Methods 2.5.4 Strand Bias Filtration

Matthias Bieg^{139,140}, Ivo Buchhalter^{28,29,30}, Johannes Werner^{28,161} and Matthias Schlesner^{28,31}

Methods 2.6 miniBAM generation

Jeremiah Wala^{3,6,157}, Gordon Saksena³, Rameen Beroukhi^{3,6,168} and Gad Getz^{3,4,5,6}

Methods 3. Germline Variant Identification from WGS

Tobias Rausch⁸, Grace Tiao³, Sebastian M Waszak⁸, Bernardo Rodriguez-Martin^{42,43,44}, Suyash Shringarpure⁴⁵, Dai-Ying Wu⁴⁶, Sergei Yakneen⁸, German M Demidov^{47,48,49}, Olivier Delaneau^{50,51,52}, Shuto Hayashi³⁹, Seiya Imoto^{39,39}, Nina Habermann⁸, Ayellet V Segre^{3,53}, Erik Garrison¹, Andy Cafferkey⁷, Eva G Alvarez^{42,43,44}, Alicia L Bruzos^{42,43,44}, Jorge Zamora^{1,42,43,44}, José María Heredia-Genestar⁵⁴, Francesc Muiyas^{47,48,49}, Oliver Drechsel^{47,49}, L Jonathan Dursi^{12,25}, Adrian Baez-Ortega⁵⁵, Hyung-Lae Kim⁵⁶, Matthew H Bailey^{26,27}, R Jay Mashl^{27,57}, Kai Ye^{58,59}, Ivo Buchhalter^{28,29,30}, Vasilisa Rudneva⁸, Ji Wan Park¹⁷³, Eun Pyo Hong¹⁷³, Seong Gu Heo¹⁷³, Anthony DiBiase⁶⁰, Kuan-lin Huang^{27,61}, Ivica Letunic⁶², Michael D McLellan^{26,27,35}, Steven J Newhouse⁷, Matthias Schlesner^{28,31}, Tal Shmaya⁴⁶, Sushant Kumar^{63,64}, David C Wedge^{1,65,66}, Mark H Wright⁴⁵, Venkata D Yellapantula^{67,68}, Mark Gerstein^{63,64,69}, Ekta Khurana^{70,71,72,73}, Tomas Marques-

systematic documentation of this variation at whole genome scale¹⁻³. We report the integrative

Bonet^{74,75,76,77}, Arcadi Navarro^{74,75,76}, Carlos D Bustamante^{45,78}, Jared T Simpson^{12,36}, Li Ding^{26,27,35}, Reiner Siebert^{79,80}, Hidewaki Nakagawa⁸¹, Douglas F Easton^{82,83}, Stephan Ossowski^{47,48,49}, Jose MC Tubio^{42,43,44}, Gad Getz^{3,4,5,6}, Francisco M De La Vega^{45,46,78} and Xavier Estivill and Jan O Korbel^{47,84}

Methods 4. RNA-Seq analysis

Nuno A Fonseca^{7,133}, André Kahles, Kjong-Van Lehmann^{112,114,115,174,175}, Lara Urban^{7,8}, Cameron M Soulette³⁷, Yuichi Shiraiishi³⁹, Fenglin Liu^{176,177}, Yao He¹⁷⁶, Deniz Demircio lu^{178,179}, Natalie R Davidson^{112,114,115,117,174}, Claudia Calabrese^{7,8}, Junjun Zhang¹⁵, Marc D Perry^{14,15}, Qian Xiang¹³⁴, Liliana Greger⁷, Siliang Li^{180,181}, Dongbing Liu^{180,181}, Stefan G Stark^{115,174,182,183}, Fan Zhang¹⁷⁶, Samirkumar B Amin^{184,185,186}, Peter Bailey¹⁸⁷, Aurélien Chateigner¹⁵, Isidro Cortés-Ciriano^{93,94,95}, Brian Craft¹³², Serap Erkek⁸, Milana Frenkel-Morgenstern¹⁸⁸, Mary Goldman¹³², Katherine A Hoadley^{23,24}, Yong Hou^{180,181}, Matthew R Huska¹¹⁸, Ekta Khurana^{70,71,72,73}, Helena Kilpinen¹⁸⁹, Jan O Korbel^{7,8}, Fabien C Lamaze¹², Chang Li^{180,181}, Xiaobo Li^{180,181}, Xinyue Li¹⁸⁰, Xingmin Liu^{180,181}, Maximilian G Marin³⁷, Julia Markowski¹¹⁸, Tannistha Nandi¹⁹⁰, Morten Muhlig Nielsen¹⁵³, Akinyemi I Ojesina^{191,192,193}, Qiang Pan-Hammarström^{180,194}, Peter J Park^{94,95}, Chandra Sekhar Pedamallu^{3,6,168}, Jakob Pedersen^{153,154}, Reiner Siebert^{79,80}, Hong Su^{180,181}, Patrick Tan^{190,195,196,197}, Bin Tean Teh^{195,196,197,198,199}, Jian Wang¹⁸⁰, Sebastian M Waszak⁸, Heng Xiong^{180,181}, Sergei Yakneen⁸, Chen Ye^{180,181}, Christina Yung¹⁵, Xiuqing Zhang¹⁸⁰, Liangtao Zheng¹⁷⁶, Jingchun Zhu¹³², Shida Zhu^{180,181}, Philip Awadalla^{12,13}, Chad J Creighton²⁰⁰, Matthew Meyerson^{3,6,157}, BF Francis Ouellette^{16,17}, Kui Wu^{180,181}, Huanming Yang¹⁸⁰, Jonathan Göke^{178,201}, Roland F Schwarz^{7,118,119,120}, Oliver Stegle^{7,8,124}, Zemin Zhang^{176,202}, Alvis Brazma⁷, Gunnar Rätsch^{112,113,114,115,116,117} and Angela N Brooks^{3,37,157}

Methods 5. Clustering of tumour genomes based on telomere maintenance-related features

David Haan⁹, Lincoln D Stein^{12,13} and Joshua M Stuart⁹

Methods 6. Clustered mutational processes in PCAWG

Jonas Demeulemeester^{91,92}, Maxime Tarabichi^{1,91}, Matthew W Fittall⁹¹, Peter J Campbell^{1,2}, Jan O Korbel^{7,8} and Peter Van Loo^{91,92}

Methods 7. Tumours without detected driver mutations

Esther Rheinbay^{3,6,19}, Amaro Taylor-Weiner⁹⁰, Radhakrishnan Sabarinathan^{87,88,89}, Peter J Campbell^{1,2} and Gad Getz^{3,4,5,6}

Methods 8. Panorama of driver mutations in human cancer

Radhakrishnan Sabarinathan^{87,88,89}, Oriol Pich^{87,89}, Inigo Martincorena¹, Carlota Rubio-Perez^{87,89,203}, Malene Juul¹⁵³, Jeremiah Wala^{3,6,157}, Steven Schumacher^{3,204}, Ofer Shapira^{3,157}, Nikos Sidiropoulos¹⁰⁰, Sebastian M Waszak⁸, David Tamborero^{87,89}, Loris Mularoni^{87,89}, Esther Rheinbay^{3,6,19}, Henrik Hornshøj¹⁵³, Jordi Deu-Pons^{89,205}, Ferran Muiños^{87,89}, Johanna Bertl^{153,206}, Qianyun Guo¹⁵⁴, Chad J Creighton²⁰⁰, Joachim Weischenfeldt^{8,99,100}, Jan O Korbel^{7,8}, Gad Getz^{3,4,5,6}, Peter J Campbell^{1,2}, Jakob Pedersen^{153,154}, Rameen Beroukhi^{3,6,168} and Abel Gonzalez-Perez^{87,89,207}

Notes 1. Pilot-63 benchmarking, variant consensus development and validation

L Jonathan Dursi^{12,25}, Christina K Yung¹⁵, Matthew H Bailey^{26,27}, Gordon Saksena³, Keiran M Raine¹, Ivo Buchhalter^{28,29,30}, Kortine Kleinheinz^{28,30}, Matthias Schlesner^{28,31}, Yu Fan³², David Torrents^{40,76}, Matthias Bieg^{139,140}, Paul C Boutros^{12,18,20,21}, Ken Chen¹⁴¹, Zechen Chong¹⁴², Kristian Cibulskis³, Oliver Drechsel^{47,49}, Roland Eils^{28,30,143,144}, Robert S Fulton^{26,27,35}, Josep Gelpi^{40,145}, Mark Gerstein^{63,64,69}, Santiago Gonzalez^{7,8}, Gad Getz^{3,4,5,6}, Ivo G Gut^{49,74}, Faraz Hach^{146,147}, Michael Heinold^{28,30}, Taobo Hu¹⁴⁸, Vincent Huang¹², Barbara Hutter^{140,149,150}, Hyung-Lae Kim⁵⁶, Natalie Jäger²⁸, Jongsun Jung¹⁵¹, Sushant Kumar^{63,64}, Yogesh Kumar¹⁴⁸, Christopher Lalansingh¹², Ignaty Leshchiner³, Ivica Letunic⁶², Dimitri Livitz³, Eric Z Ma¹⁴⁸, Yosef Maruvka^{3,19,152}, R Jay Mashl^{27,57}, Michael D McLellan^{26,27,35}, Ana Milovanovic⁴⁰, Morten Muhlig Nielsen¹⁵³, Brian O'Connor^{15,37}, Stephan Ossowski^{47,48,49}, Nagarajan Paramasivam^{28,140}, Jakob Skou Pedersen^{153,154}, Marc D Perry^{14,15}, Montserrat Puiggròs⁴⁰, Romina Royo⁴⁰, Esther Rheinbay^{3,6,19}, S Cenk Sahinalp^{147,155,156}, Iman Sarrafi^{147,156}, Chip Stewart³, Miranda D Stobbe^{49,74}, Grace Tiao³, Jeremiah A Wala^{3,6,157}, Jiayin Wang^{27,58,158}, Wenyi Wang³², Sebastian M Waszak⁸, Joachim Weischenfeldt^{8,99,100}, Michael Wendl^{27,159,160}, Johannes Werner^{28,161}, Zhenggang Wu¹⁴⁸, Hong Xue¹⁴⁸, Sergei Yakneen⁸, Takafumi N Yamaguchi¹², Kai Ye^{58,59}, Venkata Yellapantula^{67,68}, Junjun Zhang¹⁵, David A Wheeler^{33,34}, Li Ding^{26,27,35} and Jared T Simpson^{12,36}

Notes 4. Production somatic variant calling on the PCAWG Compute Cloud

Christina K Yung¹⁵, Brian D O'Connor^{15,37}, Sergei Yakneen⁸, Junjun Zhang¹⁵, Kyle Ellrott³⁸, Kortine Kleinheinz^{28,30}, Naoki Miyoshi³⁹, Keiran M Raine¹, Romina Royo⁴⁰, Gordon Saksena³, Matthias Schlesner^{28,31}, Solomon I Shorser¹², Miguel Vazquez^{40,41}, Joachim Weischenfeldt^{8,99,100}, Denis Yuen¹², Adam P Butler¹, Brandi N Davis-Dusenbery¹⁶², Roland Eils^{28,30,143,144}, Vincent Ferretti^{15,86}, Robert L Grossman¹⁶³, Olivier Harismendy¹²⁵, Youngwook Kim^{164,165}, Hidewaki Nakagawa⁸¹, Steven J Newhouse⁷, David Torrents^{40,76} and Lincoln D Stein^{12,13}

Notes 5. PCAWG data portals

Mary Goldman¹³², Junjun Zhang¹⁵, Nuno A Fonseca^{7,133}, Isidro Cortés-Ciriano^{93,94,95}, Qian Xiang¹³⁴, Brian Craft¹³², Elena Piñero-Yáñez¹³⁵, Brian D O'Connor^{15,37}, Wojciech Bazant⁷, Elisabet Barrera⁷, Alfonso Muñoz⁷, Robert Petryszak⁷, Anja Füllgrabe⁷, Fatima Al-Shahrouh¹³⁵, Maria Keays⁷, David Haussler^{132,136}, John Weinstein^{137,138}, Wolfgang Huber⁸, Alfonso Valencia^{40,76}, Irene Papatheodorou⁷, Jingchun Zhu¹³², Vincent Ferretti^{15,86} and Miguel Vazquez^{40,41}

ICGC/TCGA Pan-Cancer Analysis of Whole Genomes Working Groups

Steering committee

Peter J Campbell^{1,2}, Gad Getz^{3,4,5,6}, Jan O Korbel^{7,8}, Lincoln D Stein^{12,13} and Joshua M Stuart⁹

Executive committee

Sultan T Al-Sedairy²⁰⁸, Axel Aretz²⁰⁹, Cindy Bell²¹⁰, Miguel Betancourt²¹¹, Christiane Buchholz²¹², Fabien Calvo²¹³, Christine Chomienne²¹⁴, Michael Dunn²¹⁵, Stuart Edmonds²¹⁶, Eric Green²¹⁷, Shailja Gupta²¹⁸, Carolyn M Hutter²¹⁷, Karine Jegalian²¹⁹,

analysis of >2,600 whole cancer genomes and their matching normal tissues across 38 tumour

Jennifer L Jennings^{10,11}, Nic Jones²²⁰, Hyung-Lae Kim⁵⁶, Youyong Lu^{221,222,223}, Hitoshi Nakagama²²⁴, Gerd Nettekoven²²⁵, Laura Planko²²⁵, David Scott²²⁰, Tatsuhiro Shibata^{226,227}, Kiyo Shimizu²²⁸, Lincoln D Stein^{12,13}, Michael Rudolf Stratton¹, Takashi Yugawa²²⁸, Giampaolo Tortora^{229,230}, K VijayRaghavan²¹⁸, Huanming Yang¹⁸⁰ and Jean C Zenkhusen²³¹

Ethics and legal working group

Yann Joly¹³⁰, Fruzsina Molnár-Gábor¹³¹, Mark Phillips¹³⁰, Adrian Thorogood¹³⁰, David Townend²³², Don Chalmers¹²⁹ and Bartha M Knoppers¹³⁰

Technical working group

Brice Aminou¹⁵, Javier Bartolome⁴⁰, Keith A Boroevich^{81,233}, Rich Boyce⁷, Alvis Brazma⁷, Angela N Brooks^{3,37,157}, Alex Buchanan³⁸, Ivo Buchhalter^{28,29,30}, Adam P Butler¹, Niall J Byrne¹⁵, Andy Cafferkey⁷, Peter J Campbell^{1,2}, Zhaohong Chen²³⁴, Sunghoon Cho²³⁵, Wan Choi²³⁶, Peter Clapham¹, Brandi N Davis-Dusenbery¹⁶², Francisco M De La Vega^{45,46,78}, Jonas Demeulemeester^{91,92}, Michelle T Dow²³⁴, Lewis Jonathan Dursi^{12,25}, Juergen Eils^{143,144}, Roland Eils^{28,30,143,144}, Kyle Ellrott³⁸, Claudiu Farcas²³⁴, Nodirjon Fayzullaev¹⁵, Vincent Ferretti^{15,86}, Paul Flicek⁷, Nuno A Fonseca^{7,133}, Josep Li Gelpi^{40,145}, Gad Getz^{3,4,5,6}, Robert L Grossman¹⁶³, Olivier Harismendy¹²⁵, Allison P Heath²³⁷, Michael C Heindold^{28,30}, Julian M Hess^{3,152}, Oliver Hofmann²³⁸, Jongwhi H Hong²³⁹, Thomas J Hudson^{240,241}, Barbara Hutter^{140,149,150}, Carolyn M Hutter²¹⁷, Daniel Hübschmann^{30,120,143,242,243}, Seiya Imoto^{39,39}, Sinisa Ivkovic²⁴⁴, Seung-Hyup Jeon²³⁶, Wei Jiao¹², Jongsun Jung¹⁵¹, Rolf Kabbe²⁸, Andre Kahles^{112,113,114,115,175}, Jules NA Kerssemakers²⁸, Hyung-Lae Kim⁵⁶, Hyunghwan Kim²³⁶, Jihoon Kim²⁴⁵, Youngwook Kim^{164,165}, Kortine Kleinheinz^{28,30}, Jan O Korbel^{7,8}, Michael Koscher²⁴⁶, Antonios Koures²³⁴, Milena Kovacevic²⁴⁴, Chris Lawerenz¹⁴⁴, Ignaty Leshchiner³, Jia Liu²⁴⁷, Dimitri Livitz³, George L Mihaiescu¹⁵, Sanja Mijalkovic²⁴⁴, Ana Mijalkovic Mijalkovic-Lazic²⁴⁴, Satoru Miyano³⁹, Naoki Miyoshi³⁹, Hardeep K Nahal-Bose¹⁵, Hidewaki Nakagawa⁸¹, Mia Nastic²⁴⁴, Steven J Newhouse⁷, Jonathan Nicholson¹, David Ocana⁷, Kazuhiro Ohi³⁹, Lucila Ohno-Machado²³⁴, Larsson Omberg⁸⁵, BF Francis Ouellette^{16,17}, Nagarajan Paramasivam^{28,140}, Marc D Perry^{14,15}, Todd D Pihl²⁴⁸, Manuel Prinz²⁸, Montserrat Puiggròs⁴⁰, Petar Radovic²⁴⁴, Keiran M Raine¹, Esther Rheinbay^{3,6,19}, Mara Rosenberg^{3,19}, Romina Royo⁴⁰, Gunnar Rätsch^{112,113,114,115,116,117}, Gordon Saksena³, Matthias Schlesner^{28,31}, Solomon I Shorser¹², Charles Short⁷, Heidi J Sofia²¹⁷, Jonathan Spring¹⁶³, Adam J Struck³⁸, Grace Tiao³, Nebojsa Tijanic²⁴⁴, David Torrents^{40,76}, Peter Van Loo^{91,92}, Miguel Vazquez^{40,41}, David Vicente⁴⁰, Jeremiah A Wala^{3,6,157}, Zhining Wang²³¹, Sebastian M Waszak⁸, Joachim Weischenfeldt^{8,99,100}, Johannes Werner^{28,161}, Ashley Williams²³⁴, Youngchoon Woo²³⁶, Adam J Wright¹², Qian Xiang¹³⁴, Liming Yang²³¹, Denis Yuen¹², Brian D O'Connor^{15,37}, Lincoln D Stein^{12,13}, Sergei Yakneen⁸, Christina K Yung¹⁵ and Junjun Zhang¹⁵

Annotations working group

Angela N Brooks^{3,37,157}, Ivo Buchhalter^{28,29,30}, Peter J Campbell^{1,2}, Priyanka Dhingra^{71,73}, Lars Feuerbach¹²⁷, Mark Gerstein^{63,64,69}, Gad Getz^{3,4,5,6}, Mark P Hamilton²⁴⁹, Henrik Hornshøj¹⁵³, Todd A Johnson²³³, Andre Kahles^{112,113,114,115,175}, Abdullah Kahraman^{250,251,252}, Manolis Kellis^{3,253}, Jan O Korbel^{7,8}, Morten Muhlig Nielsen¹⁵³, Jakob Skou Pedersen^{153,154}, Paz Polak^{3,4,6}, Jüri Reimand^{12,18}, Esther Rheinbay^{3,6,19}, Nicola D Roberts¹, Gunnar Rätsch^{112,113,114,115,116,117}, Richard Sallari³, Nasa Sinnott-Armstrong^{3,45}, Alfonso Valencia^{40,76}, Miguel Vazquez^{40,41}, Sebastian M Waszak⁸, Joachim Weischenfeldt^{8,99,100}, Christian von Mering^{252,254} and Ekta Khurana^{70,71,72,73}

Quality control working group

Sergi Beltran^{49,74}, Ivo Buchhalter^{28,29,30}, Peter J Campbell^{1,2}, Roland Eils^{28,30,143,144}, Daniela S Gerhard²⁵⁵, Gad Getz^{3,4,5,6}, Marta Gut^{49,74}, Barbara Hutter^{140,149,150}, Daniel Hübschmann^{30,120,143,242,243}, Kortine Kleinheinz^{28,30}, Jan O Korbel^{7,8}, Dimitri Livitz³, Marc D Perry^{14,15}, Keiran M Raine¹, Esther Rheinbay^{3,6,19}, Mara Rosenberg^{3,19}, Gordon Saksena³, Matthias Schlesner^{28,31}, Miranda D Stobbe^{49,74}, Jean-Rémi Trotta⁷⁴, Johannes Werner^{28,161}, Justin P Whalley⁷⁴ and Ivo G Gut^{49,74}

Novel somatic mutation calling methods

Matthew H Bailey^{26,27}, Beifang Niu²⁵⁶, Matthias Bieg^{139,140}, Paul C Boutros^{12,18,20,21}, Ivo Buchhalter^{28,29,30}, Adam P Butler¹, Ken Chen¹⁴¹, Zechen Chong¹⁴², Oliver Drexel^{47,49}, Lewis Jonathan Dursi^{12,25}, Roland Eils^{28,30,143,144}, Kyle Ellrott³⁸, Shadielle MG Espirito¹², Yu Fan³², Robert S Fulton^{26,27,35}, Shengjie Gao¹⁸⁰, Josep Li Gelpi^{40,145}, Mark Gerstein^{63,64,69}, Gad Getz^{3,4,5,6}, Santiago Gonzalez^{7,8}, Ivo G Gut^{49,74}, Faraz Hach^{146,147}, Michael C Heindold^{28,30}, Julian M Hess^{3,152}, Jonathan Hinton¹, Taobo Hu¹⁴⁸, Vincent Huang¹², Yi Huang^{158,257}, Barbara Hutter^{140,149,150}, David R Jones¹, Jongsun Jung¹⁵¹, Natalie Jäger²⁸, Hyung-Lae Kim⁵⁶, Kortine Kleinheinz^{28,30}, Sushant Kumar^{63,64}, Yogesh Kumar¹⁴⁸, Christopher M Lalansingh¹², Ignaty Leshchiner³, Ivica Letunic⁶², Dimitri Livitz³, Eric Z Ma¹⁴⁸, Yosef E Maruvka^{3,19,152}, R Jay Mashl^{27,57}, Michael D McLellan^{26,27,35}, Andrew Menzies¹, Ana Milovanovic⁴⁰, Morten Muhlig Nielsen¹⁵³, Stephan Ossowski^{47,48,49}, Nagarajan Paramasivam^{28,140}, Jakob Skou Pedersen^{153,154}, Marc D Perry^{14,15}, Montserrat Puiggròs⁴⁰, Keiran M Raine¹, Esther Rheinbay^{3,6,19}, Romina Royo⁴⁰, S Cenik Sahinalp^{147,155,156}, Gordon Saksena³, Iman Sarrafi^{147,156}, Matthias Schlesner^{28,31}, Lucy Stebbings¹, Chip Stewart³, Miranda D Stobbe^{49,74}, Jon W Teague¹, Grace Tiao³, David Torrents^{40,76}, Jeremiah A Wala^{3,6,157}, Jiayin Wang^{27,58,158}, Wenyi Wang³², Sebastian M Waszak⁸, Joachim Weischenfeldt^{8,99,100}, Michael C Wendl^{27,159,160}, Johannes Werner^{28,161}, David A Wheeler^{33,34}, Zhenggang Wu¹⁴⁸, Hong Xue¹⁴⁸, Sergei Yakneen⁸, Takafumi N Yamaguchi¹², Kai Ye^{58,59}, Venkata D Yellapantula^{67,68}, Christina K Yung¹⁵, Junjun Zhang¹⁵, Li Ding^{26,27,35} and Jared T Simpson^{12,36}

Drivers and functional interpretation

Federico Abascal¹, Samirkumar B Amin^{184,185,186}, Gary D Bader¹³, Pratiti Bandopadhyay^{3,258,259}, Jonathan Barenboim¹², Rameen Beroukhi^{3,6,168}, Johanna Bertl^{153,206}, Keith A Boroevich^{81,233}, Søren Brunak^{260,261}, Peter J Campbell^{1,2}, Joana Carlevaro-Fita^{262,263,264}, Dimple Chakravarty^{265,266}, Calvin Wing Yiu Chan^{28,128}, Ken Chen¹⁴¹, Jung Kyoon Choi²⁶⁷, Jordi Deu-Pons^{89,205}, Priyanka Dhingra^{71,73}, Klev Diamanti²⁶⁸, Lars Feuerbach¹²⁷, J Lynn Fink^{40,269}, Nuno A Fonseca^{7,133}, Joan Figola²⁰⁵, Carlo Gambacorti-Passerini²⁷⁰, Dale W Garsed²⁷¹, Qianyun Guo¹⁵⁴, Ivo G Gut^{49,74}, David Haan⁹, Mark P Hamilton²⁴⁹, Nicholas J Haradhvala^{3,19}, Arif O Harmanci^{64,272}, Mohamed Helmy¹⁷¹, Carl Herrmann^{28,30,273}, Julian M

types, by the ICGC/TCGA Pan-Cancer Analysis of Whole Genomes (PCAWG) consortium. We

Hess^{3,152}, Asger Hobolth^{154,206}, Ermin Hodzic¹⁵⁶, Chen Hong^{127,128}, Henrik Hornshøj¹⁵³, Keren Isaev^{12,18}, Jose MG Izarzugaza²⁶⁰, Rory Johnson^{263,274}, Todd A Johnson²³³, Malene Juul¹⁵³, Randi Istrup Juul¹⁵³, Andre Kahles^{112,113,114,115,175}, Abdullah Kahraman^{250,251,252}, Manolis Kellis^{3,253}, Ekta Khurana^{70,71,72,73}, Jaegil Kim³, Jong K Kim²⁷⁵, Youngwook Kim^{164,165}, Jan Komorowski^{268,276}, Jan O Korbel^{7,8}, Sushant Kumar^{63,64}, Andrés Lanzós^{263,264,274}, Erik Larsson¹¹², Donghoon Lee⁶⁴, Kjong-Van Lehmann^{112,114,115,174,175}, Shantao Li⁶⁴, Xiaotong Li⁶⁴, Ziao Lin^{3,277}, Eric Minwei Liu^{71,73,278}, Lucas Lochovsky^{63,64,186}, Shaoke Lou^{63,64}, Tobias Madsen¹⁵³, Kathleen Marchal^{279,280}, Iñigo Martincorena¹, Alexander Martinez-Fundichely^{71,72,73}, Yosef E Maruvka^{3,19,152}, Patrick D McGillivray⁶³, William Meyerson^{64,281}, Ferran Muiños^{87,89}, Loris Mularoni^{87,89}, Hidewaki Nakagawa⁸¹, Morten Muhlig Nielsen¹⁵³, Marta Paczkowska¹², Keunchil Park^{282,283}, Kiejung Park²⁸⁴, Tirso Pons²⁸⁵, Sergio Pulido-Tamayo^{279,280}, Jüri Reimand^{12,18}, Iker Reyes-Salazar⁸⁷, Matthew A Reyna²⁸⁶, Esther Rheinbay^{3,6,19}, Mark A Rubin^{274,287,288,289,290}, Carlota Rubio-Perez^{87,89,203}, S Cenk Sahinalp^{147,155,156}, Gordon Saksena³, Leonidas Salichos^{63,64}, Chris Sander^{112,157,291,292}, Steven E Schumacher^{3,204}, Mark Shackleton²⁷¹, Ofer Shapira^{3,157}, Ciyue Shen^{292,293}, Raunak Shrestha¹⁴⁷, Shimin Shuai^{12,13}, Nikos Sidiropoulos¹⁰⁰, Lina Sieverling^{127,128}, Nasa Sinnott-Armstrong^{3,45}, Lincoln D Stein^{12,13}, David Tamborero^{87,89}, Grace Tiao³, Tatsuhiko Tsunoda^{233,294,295,296}, Husen M Umer^{268,297}, Liis Uusküla-Reimand^{298,299}, Alfonso Valencia^{40,76}, Miguel Vazquez^{40,41}, Lieven PC Verbeke^{280,300}, Claes Wadelius³⁰¹, Lina Wadi¹², Jiayin Wang^{27,58,158}, Jonathan Warrell^{63,64}, Sebastian M Waszak⁸, Joachim Weischenfeldt^{8,99,100}, Guanming Wu³⁰², Jun Yu³⁰³, Jing Zhang⁶⁴, Xuanping Zhang^{158,304}, Yan Zhang^{64,305,306}, Zhongming Zhao³⁰⁷, Lihua Zou³⁰⁸, Christian von Mering^{252,254}, Mark Gerstein^{63,64,69}, Gad Getz^{3,4,5,6}, Michael S Lawrence^{3,19,233}, Jakob Skou Pedersen^{153,154}, Benjamin J Raphael²⁸⁶, Joshua M Stuart⁹ and David A Wheeler^{33,34}

Integration of transcriptome and genome

Samirkumar B Amin^{184,185,186}, Philip Awadalla^{12,13}, Peter J Bailey¹⁸⁷, Claudia Calabrese^{7,8}, Aurélien Chateigner¹⁵, Isidro Cortés-Ciriano^{93,94,95}, Brian Craft¹³², David Craft^{3,309}, Chad J Creighton²⁰⁰, Natalie R Davidson^{112,114,115,117,174}, Deniz Demircio lu^{178,179}, Serap Erkek⁸, Nuno A Fonseca^{7,133}, Milana Frenkel-Morgenstern¹⁸⁸, Mary J Goldman¹³², Liliana Greger⁷, Jonathan Göke^{178,201}, Yao He¹⁷⁶, Katherine A Hoadley^{23,24}, Yong Hou^{180,181}, Matthew R Huska¹¹⁸, Andre Kahles^{112,113,114,115,175}, Ekta Khurana^{70,71,72,73}, Helena Kilpinen¹⁸⁹, Jan O Korbel^{7,8}, Fabien C Lamaze¹², Kjong-Van Lehmann^{112,114,115,174,175}, Chang Li^{180,181}, Siliang Li^{180,181}, Xiaobo Li^{180,181}, Xinyue Li¹⁸⁰, Dongbing Liu^{180,181}, Fenglin Liu^{176,177}, Xingmin Liu^{180,181}, Maximillian G Marin³⁷, Julia Markowski¹¹⁸, Matthew Meyerson^{3,6,157}, Tannistha Nandi¹⁹⁰, Morten Muhlig Nielsen¹⁵³, Akinyemi I Ojesina^{191,192,193}, BF Francis Ouellette^{16,17}, Qiang Pan-Hammarström^{180,194}, Peter J Park^{94,95}, Chandra Sekhar Pedamallu^{3,6,168}, Jakob Skou Pedersen^{153,154}, Marc D Perry^{14,15}, Roland F Schwarz^{7,118,119,120}, Yuichi Shiraiishi³⁹, Reiner Siebert^{79,80}, Cameron M Soulette³⁷, Stefan G Stark^{115,174,182,183}, Oliver Stegle^{7,8,124}, Hong Su^{180,181}, Patrick Tan^{190,195,196,197}, Bin Tean Teh^{195,196,197,198,199}, Lara Urban^{7,8}, Jian Wang¹⁸⁰, Sebastian M Waszak⁸, Kui Wu^{180,181}, Qian Xiang¹³⁴, Heng Xiong^{180,181}, Sergei Yakneen⁸, Huanming Yang¹⁸⁰, Chen Ye^{180,181}, Christina K Yung¹⁵, Fan Zhang¹⁷⁶, Junjun Zhang¹⁵, Xiuqing Zhang¹⁸⁰, Zemin Zhang^{176,202}, Liangtao Zheng¹⁷⁶, Jingchun Zhu¹³², Shida Zhu^{180,181}, Alvis Brazma⁷, Angela N Brooks^{3,37,157} and Gunnar Rättsch^{112,113,114,115,116,117}

Integration of epigenome and genome

Hiroyuki Aburatani³¹⁰, Hans Binder^{311,312}, Huy Q Dinh³¹³, Lars Feuerbach¹²⁷, Shengjie Gao¹⁸⁰, Ivo G Gut^{49,74}, Simon C Heath^{49,74}, Steve Hoffmann^{311,312,314,315}, Charles David Imbusch¹²⁷, Ekta Khurana^{70,71,72,73}, Helene Kretzmer^{312,315}, Peter W Laird³¹⁶, Jose I Martin-Subero^{76,317}, Genta Nagae^{310,318}, Paz Polak^{3,4,6}, Hui Shen³¹⁹, Reiner Siebert^{79,80}, Nasa Sinnott-Armstrong^{3,45}, Miranda D Stobbe^{49,74}, Qi Wang²⁴⁶, Dieter Weichenhan³²⁰, Sergei Yakneen⁸, Wanding Zhou³¹⁹, Benjamin P Berman^{313,321,322}, Benedikt Brors^{127,150,323} and Christoph Plass³²⁰

Patterns of structural variations, signatures, genomic correlations, retrotransposons, mobile elements

Kadir C Akdemir¹⁴¹, Eva G Alvarez^{42,43,44}, Adrian Baez-Ortega⁵⁵, Paul C Boutros^{12,18,20,21}, David D L Bowtell²⁷¹, Benedikt Brors^{127,150,323}, Kathleen H Burns^{324,325}, John Busanovich^{3,326}, Kin Chan³²⁷, Ken Chen¹⁴¹, Isidro Cortés-Ciriano^{93,94,95}, Ana Dueso-Barroso⁴⁰, Andrew J Dunford³, Paul A Edwards^{328,329}, Xavier Estivill^{47,84}, Dariush Etemadmoghadam²⁷¹, Lars Feuerbach¹²⁷, J Lynn Fink^{40,269}, Milana Frenkel-Morgenstern¹⁸⁸, Dale W Garsed²⁷¹, Mark Gerstein^{63,64,69}, Dmitry A Gordenin⁹⁷, David Haan⁹, James E Haber³³⁰, Julian M Hess^{3,152}, Barbara Hutter^{140,149,150}, Marcin Imielinski^{166,167}, David TW Jones^{331,332}, Young Seok Ju^{1,267}, Marat D Kazanov^{333,334,335}, Leszek J Klimczak⁹⁸, Youngil Koh^{336,337}, Jan O Korbel^{7,8}, Kiran Kumar³, Eunjung Alice Lee³³⁸, Jake June-Koo Lee^{94,95}, Yilong Li¹, Andy G Lynch^{328,329,339}, Geoff Macintyre³²⁸, Florian Markowetz^{328,329}, Iñigo Martincorena¹, Alexander Martinez-Fundichely^{71,72,73}, Matthew Meyerson^{3,6,157}, Satoru Miyano³⁹, Hidewaki Nakagawa⁸¹, Fabio CP Navarro⁶³, Stephan Ossowski^{47,48,49}, Peter J Park^{94,95}, John V Pearson^{340,341}, Montserrat Puiggròs⁴⁰, Karsten Rippe¹²⁰, Nicola D Roberts¹, Steven A Roberts¹⁰⁷, Bernardo Rodriguez-Martin^{42,43,44}, Steven E Schumacher^{3,204}, Ralph Scully³⁴², Mark Shackleton²⁷¹, Nikos Sidiropoulos¹⁰⁰, Lina Sieverling^{127,128}, Chip Stewart³, David Torrents^{40,76}, Jose MC Tubio^{42,43,44}, Izar Villasante⁴⁰, Nicola Waddell^{340,341}, Jeremiah A Wala^{3,6,157}, Joachim Weischenfeldt^{8,99,100}, Lixing Yang³⁴³, Xiaotong Yao^{166,344}, Sung-Soo Yoon³³⁷, Jorge Zamora^{1,42,43,44}, Cheng-Zhong Zhang^{3,6,157}, Rameen Beroukhi^{3,6,168} and Peter J Campbell^{1,2}

Mutation signatures and processes

Ludmil B Alexandrov^{1,101}, Erik N Bergstrom³⁴⁵, Arnoud Boot^{196,346}, Paul C Boutros^{12,18,20,21}, Kin Chan³²⁷, Kyle Covington³⁴, Akihiro Fujimoto⁸¹, Gad Getz^{3,4,5,6}, Dmitry A Gordenin⁹⁷, Nicholas J Haradhvala^{3,19}, Mi Ni Huang^{196,346}, S. M. Ashiqul Islam¹⁰¹, Marat D Kazanov^{333,334,335}, Jaegil Kim³, Leszek J Klimczak⁹⁸, Michael S Lawrence^{3,19,233}, Iñigo Martincorena¹, John R McPherson^{196,346}, Sandro Morganello¹, Ville Mustonen^{347,348,349}, Hidewaki Nakagawa⁸¹, Alvin Wei Tian Ng³⁵⁰, Paz Polak^{3,4,6}, Stephenie D Prokopec¹², Steven A Roberts¹⁰⁷, Radhakrishnan Sabarinathan^{87,88,89}, Natalie Saini⁹⁷, Tatsuhiko Shibata^{226,227}, Yuichi Shiraiishi³⁹, Ignacio Vázquez-García^{1,67,354,355}, Yang Wu^{196,346}, Fouad Yousif¹², Willie Yu³⁵⁶, Steven G Rozen^{196,197,346}, Michael Rudolf Stratton¹ and Bin Tean Teh^{195,196,197,198,199}

describe the generation of the PCAWG resource, facilitated by international data sharing using

Germline cancer genome

Ludmil B Alexandrov^{1,101}, Eva G Alvarez^{42,43,44}, Adrian Baez-Ortega⁵⁵, Matthew H Bailey^{26,27}, Mattia Bosio^{40,47,49}, G Steven Bova¹²⁶, Alvis Brazma⁷, Alicia L Bruzos^{42,43,44}, Ivo Buchhalter^{28,29,30}, Carlos D Bustamante^{45,78}, Atul J Butte¹²¹, Andy Cafferkey⁷, Claudia Calabrese^{7,8}, Peter J Campbell^{1,2}, Stephen J Chanock⁹⁶, Nilanjan Chatterjee^{122,123,123}, Jieming Chen^{64,110}, Francisco M De La Vega^{45,46,78}, Olivier Delaneau^{50,51,52}, German M Demidov^{47,48,49}, Anthony DiBiase⁶⁰, Li Ding^{26,27,35}, Oliver Drechsel^{47,49}, Lewis Jonathan Dursi^{12,25}, Douglas F Easton^{82,83}, Serap Erkek⁸, Georgia Escaramis^{47,103,104}, Erik Garrison¹, Mark Gerstein^{63,64,69}, Gad Getz^{3,4,5,6}, Dmitry A Gordenin⁹⁷, Nina Habermann⁸, Olivier Harismendy¹²⁵, Eoghan Harrington¹⁰⁵, Shuto Hayashi³⁹, Seong Gu Heo¹⁷³, José María Heredia-Genestar⁵⁴, Aliaksei Z Holik⁴⁷, Eun Pyo Hong¹⁷³, Xing Hua⁹⁶, Kuan-lin Huang^{27,61}, Seiya Imoto^{39,39}, Sissel Juul¹⁰⁵, Ekta Khurana^{70,71,72,73}, Hyung-Lae Kim⁵⁶, Youngwook Kim^{164,165}, Leszek J Klimczak⁹⁸, Roelof Koster¹⁰⁸, Sushant Kumar^{63,64}, Ivica Letunic⁶², Yilong Li¹, Tomas Marques-Bonet^{74,75,76,77}, R Jay Mashl^{27,57}, Simon Mayes¹⁰⁶, Michael D McLellan^{26,27,35}, Lisa Mirabello⁹⁶, Francesc Muias^{47,48,49}, Hidewaki Nakagawa⁸¹, Arcadi Navarro^{74,75,76}, Steven J Newhouse⁷, Stephan Ossowski^{47,48,49}, Ji Wan Park¹⁷³, Esa Pitkänen⁸, Aparna Prasad⁴⁹, Raquel Rabionet^{47,49,102}, Benjamin Raeder⁸, Tobias Rausch⁸, Steven A Roberts¹⁰⁷, Bernardo Rodriguez-Martin^{42,43,44}, Vasilisa A Rudneva⁸, Gunnar Rättsch^{112,113,114,115,116,117}, Natalie Saini⁹⁷, Matthias Schlesner^{28,31}, Roland F Schwarz^{7,118,119,120}, Ayellet V Segre^{3,53}, Tal Shmaya⁴⁶, Suyash S Shringarpure⁴⁵, Nikos Sidiropoulos¹⁰⁰, Reiner Siebert^{79,80}, Jared T Simpson^{12,36}, Lei Song⁹⁶, Oliver Stegle^{7,8,124}, Hana Susak^{47,49}, Tomas J Tanskanen¹⁰⁹, Grace Tiao³, Marta Tojo⁴⁴, Jose MC Tubio^{42,43,44}, Daniel J Turner¹⁰⁶, Lara Urban^{7,8}, Sebastian M Waszak⁸, David C Wedge^{1,65,66}, Joachim Weischenfeldt^{8,99,100}, David A Wheeler^{33,34}, Mark H Wright⁴⁵, Dai-Ying Wu⁴⁶, Tian Xia³⁵⁷, Sergei Yakneen⁸, Kai Ye^{58,59}, Venkata D Yellapantula^{67,68}, Jorge Zamora^{1,42,43,44}, Bin Zhu⁹⁶, Xavier Estivill^{47,84} and Jan O Korbel^{7,8}

Tumour subtypes and clinical translation

Fatima Al-Shahrour¹³⁵, Gurnit Atwal^{12,13,172}, Peter J Bailey¹⁸⁷, Paul C Boutros^{12,18,20,21}, Peter J Campbell^{1,2}, David K Chang^{187,358}, Susanna L Cooke¹⁸⁷, Vikram Deshpande¹⁹, Bishoy M Faltas¹¹⁷, William C Faquin¹⁹, Gad Getz^{3,4,5,6}, Syed Haider¹², Wei Jiao¹², Vera B Kaiser³⁵⁹, Rosa Karli³⁶⁰, Mamoru Kato³⁶¹, Kirsten Kübler^{3,6,19}, Alexander J Lazar²², Constance H Li^{12,18}, David N Louis¹⁹, Adam Margolin³⁸, Sancha Martin^{1,362}, Hardeep K Nahal-Bose¹⁵, G Petur Nielsen¹⁹, Serena Nik-Zainal^{1,351,352,353}, Larsson Omberg⁸⁵, Christine P'ng¹², Marc D Perry^{14,15}, Paz Polak^{3,4,6}, Esther Rheinbay^{3,6,19}, Mark A Rubin^{274,287,288,289,290}, Colin A Semple³⁵⁹, Dennis C Sgroi¹⁹, Tatsuhiro Shibata^{226,227}, Reiner Siebert^{79,80}, Jaclyn Smith³⁸, Miranda D Stobbe^{49,74}, Ren X Sun¹², Kevin Thai¹⁵, Derek W Wright^{363,364}, Chin-Lee Wu¹⁹, Ke Yuan^{328,362,365}, Junjun Zhang¹⁵, Andrew V Biankin^{187,358,366,367}, Levi Garraway¹⁵⁷, Sean M Grimmond³⁶⁸, Katherine A Hoadley^{23,24} and Lincoln D Stein^{12,13}

Evolution and heterogeneity

David J Adams¹, Pavana Anur³⁶⁹, Rameen Beroukhi^{3,6,168}, Paul C Boutros^{12,18,20,21}, David D L Bowtell²⁷¹, Peter J Campbell^{1,2}, Shaolong Cao³², Elizabeth L Christie²⁷¹, Marek Cmero^{370,371,372}, Yupeng Cun³⁷³, Kevin J Dawson¹, Jonas Demeulemeester^{91,92}, Stefan C D'Entro^{1,65,91}, Amit G Deshwar³⁷⁴, Nilgun Donmez^{147,156}, Ruben M Drews³²⁸, Roland Eils^{28,30,143,144}, Yu Fan³², Matthew W Fittall⁹¹, Dale W Garsed²⁷¹, Moritz Gerstung^{7,8}, Gad Getz^{3,4,5,6}, Santiago Gonzalez^{7,8}, Gavin Ha³, Kerstin Haase⁹¹, Marcin Imielinski^{166,167}, Lara Jerman^{8,375}, Yuan Ji^{376,377}, Clemency Jolly⁹¹, Kortine Kleinheinz^{28,30}, Juhee Lee³⁷⁸, Henry Lee-Six¹, Ignaty Leshchiner³, Dimitri Livitz³, Geoff Macintyre³²⁸, Saleem Malik^{147,156}, Florian Markowetz^{328,329}, Iñigo Martincorena¹, Thomas J Mitchell^{1,329,379}, Quaid D Morris^{172,380}, Ville Mustonen^{347,348,349}, Layla Oesper³⁸¹, Martin Peifer³⁷³, Myron Peto³⁸², Benjamin J Raphael²⁸⁶, Daniel Rosebrock³, Yulia Rubanova^{36,172}, S Cenk Sahinalp^{147,155,156}, Adriana Salcedo¹², Matthias Schlesner^{28,31}, Steven E Schumacher^{3,204}, Subhjit Sengupta³⁸³, Ruian Shi³⁸⁰, Seung Jun Shin¹⁸³, Oliver Spiro³, Lincoln D Stein^{12,13}, Maxime Tarabichi^{1,91}, Shankar Vembu^{380,384}, Ignacio Vázquez-García^{1,67,354,355}, Wenyi Wang³², David A Wheeler^{33,34}, Jeffrey A Wintersinger^{170,171,172}, Tsun-Po Yang³⁷³, Xiaotong Yao^{166,344}, Kaixian Yu³⁸⁵, Ke Yuan^{328,362,365}, Hongtu Zhu^{386,387}, Paul T Spellman³⁸⁸, Peter Van Loo^{91,92} and David C Wedge^{1,65,66}

Portals, visualisation and software infrastructure

Fatima Al-Shahrour¹³⁵, Elisabet Barrera⁷, Wojciech Bazant⁷, Alvis Brazma⁷, Isidro Cortés-Ciriano^{93,94,95}, Brian Craft¹³², David Craft^{3,309}, Vincent Ferretti^{15,86}, Nuno A Fonseca^{7,133}, Anja Füllgrabe⁷, Mary J Goldman¹³², Wolfgang Huber⁸, Maria Keays⁷, Alfonso Muñoz⁷, Brian D O'Connor^{15,37}, Irene Papatheodorou⁷, Robert Petryszak⁷, Elena Piñero-Yañez¹³⁵, Alfonso Valencia^{40,76}, John N Weinstein^{137,138}, Qian Xiang¹³⁴, Junjun Zhang¹⁵, David Haussler^{132,136}, Miguel Vazquez^{40,41} and Jingchun Zhu¹³²

Mitochondrial variants and HLA/immunogenicity

Peter J Campbell^{1,2}, Yiwen Chen³², Chad J Creighton²⁰⁰, Li Ding^{26,27,35}, Akihiro Fujimoto⁸¹, Masashi Fujita⁸¹, Gad Getz^{3,4,5,6}, Leng Han³⁰⁴, Takanori Hasegawa³⁹, Shuto Hayashi³⁹, Seiya Imoto^{39,39}, Young Seok Ju^{1,267}, Hyung-Lae Kim⁵⁶, Youngwook Kim^{164,165}, Youngil Koh^{336,337}, Mitsuhiro Komura³⁹, Jun Li³², Iñigo Martincorena¹, Satoru Miyano³⁹, Shinichi Mizuno³⁸⁹, Keunchil Park^{282,283}, Eigo Shimizu³⁹, Yumeng Wang^{32,390}, John N Weinstein^{137,138}, Yanxun Xu³⁹¹, Rui Yamaguchi³⁹, Fan Yang³⁸⁰, Yang Yang³⁰⁴, Christopher J Yoon²⁶⁷, Sung-Soo Yoon³³⁷, Yuan Yuan³², Fan Zhang¹⁷⁶, Zemin Zhang^{176,202}, Han Liang³² and Hidewaki Nakagawa⁸¹

Pathogens

Malik Alawi^{392,393}, Ivan Borozan¹², Daniel S Brewer^{394,395}, Colin S Cooper^{395,396,397}, Nikita Desai¹⁵, Roland Eils^{28,30,143,144}, Vincent Ferretti^{15,86}, Adam Grundhoff^{392,398}, Murat Iskar³⁹⁹, Kortine Kleinheinz^{28,30}, Hidewaki Nakagawa⁸¹, Akinyemi I Ojesina^{191,192,193}, Chandra Sekhar Pedamallu^{3,6,168}, Matthias Schlesner^{28,31}, Xiaoping Su⁴⁰⁰, Marc Zaparka³⁹⁹ and Peter Lichter^{149,399}

Providers of tumour sequencing data

compute clouds. Cancer genomes contained 4-5 driver mutations on average when combining

Tumour Specific Providers – Australia (Ovarian cancer)

Kathryn Alsop²⁷¹, Australian Ovarian Cancer Study Group^{340,401,402}, Timothy JC Bruxner²⁶⁹, Angelika N Christ²⁶⁹, Elizabeth L Christie²⁷¹, Stephen M Corder⁴⁰³, Prue A Cowin⁴⁰¹, Ronny Drapkin⁴⁰⁴, Dariush Etemadmoghadam²⁷¹, Sian Fereday⁴⁰¹, Dale W Garsed²⁷¹, Joshy George¹⁸⁶, Sean M Grimmond³⁶⁸, Anne Hamilton⁴⁰¹, Oliver Holmes^{340,341}, Jillian A Hung^{405,406}, Karin S Kassahn^{269,407}, Stephen H Kazakoff^{340,341}, Catherine J Kennedy^{408,409}, Conrad R Leonard^{340,341}, Linda Miles²⁷¹, David K Miller^{269,358,410}, Gisela Mir Arnau⁴⁰¹, Chris Mitchell⁴⁰¹, Felicity Newell^{340,341}, Katia Nones^{340,341}, Ann-Marie Patch^{340,341}, John V Pearson^{340,341}, Michael C Quinn^{340,341}, Mark Shackleton²⁷¹, Darrin F Taylor²⁶⁹, Heather Thorne⁴⁰¹, Nadia Traficante⁴⁰¹, Ravikiran Veduru⁴⁰¹, Nick M Waddell³⁴¹, Nicola Waddell^{340,341}, Paul M Waring⁴¹¹, Scott Wood^{340,341}, Qinying Xu^{340,341}, Anna deFazio^{412,413,414} and David D L Bowtell²⁷¹

Tumour Specific Providers – Australia (Pancreatic cancer)

Matthew J Anderson²⁶⁹, Davide Antonello⁴¹⁵, Andrew P Barbour^{416,417}, Claudio Bassi⁴¹⁵, Samantha Bersani⁴¹⁸, Timothy JC Bruxner²⁶⁹, Ivana Cataldo^{418,419}, David K Chang^{187,358}, Lorraine A Chantrill^{358,420}, Yoke-Eng Chiew⁴¹², Angela Chou^{358,421}, Angelika N Christ²⁶⁹, Sara Cingarlini²²⁹, Nicole Cloonan⁴²², Vincenzo Corbo^{419,423}, Maria Vittoria Davi⁴²⁴, Fraser R Duthie^{187,425}, J Lynn Fink^{40,269}, Anthony J Gill^{358,421}, Janet S Graham^{187,426}, Ivon Harliwong²⁶⁹, Oliver Holmes^{340,341}, Nigel B Jamieson^{187,367,427}, Amber L Johns^{358,410}, Karin S Kassahn^{269,407}, Stephen H Kazakoff^{340,341}, James G Kench^{358,421,428}, Luca Landoni⁴¹⁵, Rita T Lawlor⁴¹⁹, Conrad R Leonard^{340,341}, Andrea Mafficini⁴¹⁹, Neil D Merrett^{415,429}, David K Miller^{269,358,410}, Marco Miotto⁴¹⁵, Elizabeth A Musgrove¹⁸⁷, Adnan M Nagrial³⁵⁸, Felicity Newell^{340,341}, Katia Nones^{340,341}, Karin A Oien^{411,430}, Marina Pajic³⁵⁸, Ann-Marie Patch^{340,341}, John V Pearson^{340,341}, Mark Pinese⁴³¹, Michael C Quinn^{340,341}, Alan J Robertson²⁶⁹, Ilse Rooman³⁵⁸, Borislav C Rusev⁴¹⁹, Jaswinder S Samra^{415,421}, Maria Scardoni⁴¹⁸, Christopher J Scarlett^{358,432}, Aldo Scarpa⁴¹⁹, Elisabetta Sereni⁴¹⁵, Katarzyna O Sikora⁴¹⁹, Michele Simbolo⁴²³, Morgan L Taschuk¹⁵, Christopher W Toon³⁵⁸, Giampaolo Tortora^{229,230}, Caterina Vicentini⁴¹⁹, Nick M Waddell³⁴¹, Nicola Waddell^{340,341}, Scott Wood^{340,341}, Jianmin Wu³⁵⁸, Qinying Xu^{340,341}, Nikolajs Zeps^{433,434}, Andrew V Biankin^{187,358,366,367} and Sean M Grimmond³⁶⁸

Tumour Specific Providers – Australia (Skin cancer)

Lauri A Aaltonen¹¹¹, Andreas Behren⁴³⁵, Hazel Burke⁴³⁶, Jonathan Cebon⁴³⁵, Rebecca A Dagg⁴³⁷, Ricardo De Paoli-Iseppi⁴³⁸, Ken Dutton-Regester³⁴⁰, Matthew A Field⁴³⁹, Anna Fitzgerald⁴⁴⁰, Sean M Grimmond³⁶⁸, Peter Hersey⁴³⁶, Oliver Holmes^{340,341}, Valerie Jakrot⁴³⁶, Peter A Johansson³⁴⁰, Hojabr Kakavand⁴³⁸, Stephen H Kazakoff^{340,341}, Richard F Kefford⁴⁴¹, Loretta MS Lau⁴⁴², Conrad R Leonard^{340,341}, Georgina V Long⁴⁴³, Felicity Newell^{340,341}, Katia Nones^{340,341}, Ann-Marie Patch^{340,341}, John V Pearson^{340,341}, Hilda A Pickett⁴⁴², Antonia L Pritchard³⁴⁰, Gulietta M Pupo⁴⁴⁴, Robyn PM Saw⁴⁴³, Sarah-Jane Schramm⁴⁴⁵, Mark Shackleton²⁷¹, Catherine A Shang⁴⁴⁰, Ping Shang⁴⁴³, Andrew J Spillane⁴⁴³, Jonathan R Stretch⁴⁴³, Varsha Tembe⁴⁴⁵, John F Thompson⁴⁴³, Ricardo E Vilain⁴⁴⁶, Nick M Waddell³⁴¹, Nicola Waddell^{340,341}, James S Wilmott⁴⁴³, Scott Wood^{340,341}, Qinying Xu^{340,341}, Jean Y Yang⁴⁴⁷, Nicholas K Hayward^{340,436}, Graham J Mann^{448,449} and Richard A Scolyer^{413,443,446,450}

Tumour Specific Providers – Canada (Pancreatic cancer)

John Bartlett^{451,452}, Prashant Bavi⁴⁵³, Ivan Borozan¹², Dianne E Chadwick⁴⁵⁴, Michelle Chan-Seng-Yue⁴⁵³, Sean Cleary^{453,455}, Ashton A Connor^{455,456}, Karolina Czajka²⁴¹, Robert E Denroche⁴⁵³, Neesha C Dhani⁴⁵⁷, Jenna Eagles²⁴¹, Vincent Ferretti^{15,86}, Steven Gallinger^{453,455,456}, Robert C Grant^{453,456}, David Hedley⁴⁵⁷, Michael A Hollingsworth⁴⁵⁸, Gun Ho Jang⁴⁵³, Jeremy Johns²⁴¹, Sangeetha Kalimuthu⁴⁵³, Sheng-Ben Liang⁴⁵⁹, Ilinca Lungu^{453,460}, Xuemei Luo¹², Faridah Mbabaali²⁴¹, Treasa A McPherson⁴⁵⁶, Jessica K Miller²⁴¹, Malcolm J Moore⁴⁵⁷, Faiyaz Notta^{453,461}, Danielle Pasternack²⁴¹, Gloria M Petersen⁴⁶², Michael H A Roehrl^{18,453,463,464,465}, Michelle Sam²⁴¹, Iris Selander⁴⁵⁶, Stefano Serra⁴¹¹, Sagedeh Shahabi⁴⁵⁹, Morgan L Taschuk¹⁵, Sarah P Thayer⁴⁵⁸, Lee E Timms²⁴¹, Gavin W Wilson^{12,453}, Julie M Wilson⁴⁵³, Bradley G Wouters⁴⁶⁶, Thomas J Hudson^{240,241}, John D McPherson^{241,453,467} and Lincoln D Stein^{12,13}

Tumour Specific Providers – Canada (Prostate cancer)

Timothy A Beck^{15,468}, Vinayak Bhandari¹², Colin C Collins¹⁴⁷, Shadrielle MG Espiritu¹², Neil E Fleshner⁴⁶⁹, Natalie S Fox¹², Michael Fraser¹², Syed Haider¹², Lawrence E Heisler⁴⁷⁰, Vincent Huang¹², Emilie Lalonde¹², Julie Livingstone¹², John D McPherson^{241,453,467}, Alice Meng⁴⁷¹, Veronica Y Sabelnykova¹², Adriana Salcedo¹², Yu-Jia Shiah¹², Theodoros Van der Kwast⁴⁷², Takafumi N Yamaguchi¹², Paul C Boutros^{12,18,20,21} and Robert G Bristow^{18,473,474,475,476}

Tumour Specific Providers – China (Gastric cancer)

Shuai Ding⁴⁷⁷, Daiming Fan⁴⁷⁸, Yong Hou^{180,181}, Yi Huang^{158,257}, Lin Li¹⁸⁰, Siliang Li^{180,181}, Dongbing Liu^{180,181}, Xingmin Liu^{180,181}, Yongzhan Nie^{478,479}, Hong Su^{180,181}, Jian Wang¹⁸⁰, Kui Wu^{180,181}, Xiao Xiao¹⁵⁸, Rui Xing^{222,480}, Shanlin Yang⁴⁷⁷, Yingyan Yu⁴⁸¹, Xiuqing Zhang¹⁸⁰, Yong Zhou¹⁸⁰, Shida Zhu^{180,181}, Youyong Lu^{221,222,223} and Huanming Yang¹⁸⁰

Tumour Specific Providers – EU: France (Renal cancer)

Rosamonde E Banks⁴⁸², Guillaume Bourque^{483,484}, Alvis Brazma⁷, Paul Brennan⁴⁸⁵, Louis Letourneau⁴⁸⁶, Yasser Riazalhosseini⁴⁸⁴, Ghislaine Scelo⁴⁸⁵, Naveen Vasudev⁴⁸⁷, Juris Viksna⁴⁸⁸, Mark Lathrop⁴⁸⁴ and Jörg Tost⁴⁸⁹

Tumour Specific Providers – EU: United Kingdom (Breast cancer)

Sung-Min Ahn⁴⁹⁰, Ludmil B Alexandrov^{1,101}, Samuel Aparicio⁴⁹¹, Laurent Arnould⁴⁹², MR Aure⁴⁹³, Shriram G Bhosle¹, E Birney⁷, Ake Borg⁴⁹⁴, S Boyault⁴⁹⁵, AB Brinkman⁴⁹⁶, JE Brock⁴⁹⁷, A Broeks⁴⁹⁸, Adam P Butler¹, AL Børresen-Dale⁴⁹³, C Caldas^{499,500}, Peter J Campbell^{1,2}, Suet-Feung Chin^{499,500}, Helen Davies^{1,351,352}, C Desmedt^{501,502}, L Dirix⁵⁰³, S Dronov¹, Anna Ehinger⁵⁰⁴, JE Eyfjord⁵⁰⁵, A Fatima²⁰⁴, JA Foekens⁵⁰⁶, PA Futreal⁵⁰⁷, Øystein Garred^{508,509}, Moritz Gerstung^{7,8}, Dilip D Giri⁵¹⁰, D Glodzik¹, Dorte Grabau⁵¹¹, Holmfridur Hilmarsdottir⁵⁰⁵, GK Hooijer⁵¹², Jocelyne Jacquemier⁵¹³, SJ Jang⁵¹⁴, Jon G Jonasson⁵⁰⁵, Jos Jonkers⁵¹⁵, HY Kim⁵¹³, Tari A King^{516,517}, Stian Knappskog^{1,518,518}, G Kong⁵¹³, S Krishnamurthy⁵¹⁹, SR

coding and non-coding genomic elements, but ~5% of cases had no drivers identified, suggesting

Lakhani⁵²⁰, Anita Langerød⁴⁹³, Denis Larsimont⁵²¹, HJ Lee⁵¹⁴, JY Lee⁵²², Ming Ta Michael Lee⁵⁰⁷, Yilong Li¹, Ole Christian Lingjærde⁵²³, Gaetan MacGrogan⁵²⁴, JWM Martens⁵⁰⁶, Sancha Martin^{1,362}, Iñigo Martincorena¹, Andrew Menzies¹, Sandro Morganello¹, Ville Mustonen^{347,348,349}, Serena Nik-Zainal^{1,351,352,353}, Sarah O'Meara¹, I Pauporte²¹⁴, Sarah Pinder⁵²⁵, X Pivot⁵²⁶, Elena Provenzano⁵²⁷, CA Purdie⁵²⁸, Keiran M Raine¹, M Ramakrishna¹, K Ramakrishnan¹, Jorge Reis-Filho⁵¹⁰, AL Richardson²⁰⁴, M Ringnér⁴⁹⁴, Javier Bartolomé Rodríguez⁴⁰, FG Rodríguez-González²⁶¹, G Romieu⁵²⁹, Roberto Salgado⁴¹¹, Torill Sauer⁵²³, R Shepherd¹, AM Sieuwerts⁵⁰⁶, PT Simpson⁵²⁰, M Smid⁵⁰⁶, C Sotiriou²³⁴, PN Span⁵³⁰, Lucy Stebbings¹, Ólafur Andri Stefánsson⁵³¹, Alasdair Stenhouse⁵³², HG Stunnenberg^{181,533}, Fred Sweep⁵³⁴, BK Tan⁵³⁵, Jon W Teague¹, Gilles Thomas⁵³⁶, AM Thompson⁵³², S Tommasi⁵³⁷, I Treilleux^{538,539}, Andrew Tutt²⁰⁴, NT Ueno³⁸⁷, S Van Laere⁵⁰³, Peter Van Loo^{91,92}, GG Van den Eynden⁵⁰³, P Vermeulen⁵⁰³, Alain Viari⁴¹⁹, A Vincent-Salomon⁵³³, David C Wedge^{1,65,66}, Bernice Huimin Wong⁵⁴⁰, Lucy Yates¹, X Zou¹, CHM van Deurzen⁵⁴¹, MJ van de Vijver⁴¹¹, L van't Veer⁵⁴² and Michael Rudolf Stratton¹

Tumour Specific Providers – Germany (Malignant lymphoma)

Ole Ammerpohl^{543,544}, Sietse Aukema^{545,546}, Anke K Bergmann⁵⁴⁷, Stephan H Bernhart^{311,312,315}, Hans Binder^{311,312}, Arndt Borkhardt⁵⁴⁸, Christoph Borst⁵⁴⁹, Benedikt Brors^{127,150,323}, Birgit Burkhardt⁵⁵⁰, Alexander Claviez⁵⁵¹, Roland Eils^{28,30,143,144}, Maria Elisabeth Goebler⁵⁵², Andrea Haake⁵⁴³, Siegfried Haas⁵⁴⁹, Martin Hansmann⁵⁵³, Jessica I Hoell⁵⁴⁸, Steve Hoffmann^{311,312,314,315}, Michael Hummel⁵⁵⁴, Daniel Hübschmann^{30,120,143,242,243}, Dennis Karsch⁵⁵⁵, Wolfram Klapper⁵⁴⁵, Kortine Kleinheinz^{28,30}, Michael Kneba⁵⁵⁵, Jan O Korbel^{7,8}, Helene Kretzmer^{312,315}, Markus Kreuz⁵⁵⁶, Dieter Kube⁵⁵⁷, Ralf Küppers⁵⁵⁸, Chris Lawerenz¹⁴⁴, Dido Lenze⁵⁵⁴, Peter Lichter^{149,399}, Markus Loeffler⁵⁵⁶, Cristina López^{80,543}, Luisa Mantovani-Löffler⁵⁵⁹, Peter Möller⁵⁶⁰, German Ott⁵⁶¹, Bernhard Radlwimmer³⁹⁹, Julia Richter^{543,545}, Marius Rohde⁵⁶², Philip C Rosenstiel⁵⁶³, Andreas Rosenwald⁵⁶⁴, Markus B Schilhabel⁵⁶³, Matthias Schlesner^{28,31}, Stefan Schreiber⁵⁶⁵, Peter F Stadler^{311,312,315}, Peter Staib⁵⁶⁶, Stephan Stilgenbauer⁵⁶⁷, Stephanie Sungalee⁸, Monika Szczepanowski⁵⁴⁵, Umut H Toprak^{30,568}, Lorenz HP Trümper⁵⁵⁷, Rabea Wagener^{80,543}, Thorsten Zenz¹⁵⁰ and Reiner Siebert^{79,80}

Tumour Specific Providers – Germany (Paediatric Brain cancer)

Ivo Buchhalter^{28,29,30}, Juergen Eils^{143,144}, Roland Eils^{28,30,143,144}, Volker Hovestadt³⁹⁹, Barbara Hutter^{140,149,150}, David TW Jones^{331,332}, Natalie Jäger²⁸, Christof von Kalle¹²⁰, Marcel Kool^{246,331}, Jan O Korbel^{7,8}, Andrey Korshunov²⁴⁶, Pablo Landgraf^{569,570}, Chris Lawerenz¹⁴⁴, Hans Lehrach⁵⁷¹, Paul A Northcott⁵⁷², Stefan M Pfister^{246,331,573}, Bernhard Radlwimmer³⁹⁹, Guido Reifenberger⁵⁷⁰, Matthias Schlesner^{28,31}, Hans-Jörg Warnatz⁵⁷¹, Joachim Weischenfeldt^{8,99,100}, Stephan Wolf⁵⁷⁴, Marie-Laure Yaspo⁵⁷¹, Marc Zapatka³⁹⁹ and Peter Lichter^{149,399}

Tumour Specific Providers – Germany (Prostate cancer)

Yassen Assenov⁵⁷⁵, Benedikt Brors^{127,150,323}, Juergen Eils^{143,144}, Roland Eils^{28,30,143,144}, Lars Feuerbach¹²⁷, Clarissa Gerhauser³²⁰, Jan O Korbel^{7,8}, Chris Lawerenz¹⁴⁴, Hans Lehrach⁵⁷¹, Sarah Minner⁵⁷⁶, Christoph Plass³²⁰, Thorsten Schlomm^{99,577}, Nikos Sidiropoulos¹⁰⁰, Ronald Simon⁵⁷⁸, Hans-Jörg Warnatz⁵⁷¹, Dieter Weichenhan³²⁰, Joachim Weischenfeldt^{8,99,100}, Marie-Laure Yaspo⁵⁷¹, Guido Sauter⁵⁷⁸ and Holger Sültmann^{150,579}

Tumour Specific Providers – India (Oral cancer)

Nidhan K Biswas⁵⁸⁰, Luca Landoni⁴¹⁵, Arindam Maitra⁵⁸⁰, Partha P Majumder⁵⁸⁰ and Rajiv Sarin⁵⁸¹

Tumour Specific Providers – Italy (Pancreatic cancer)

Davide Antonello⁴¹⁵, Stefano Barbi⁴²³, Claudio Bassi⁴¹⁵, Samantha Bersani⁴¹⁸, Giada Bonizzato⁴¹⁹, Cinzia Cantù⁴¹⁹, Ivana Cataldo^{418,419}, Sara Cingarlini²²⁹, Vincenzo Corbo^{419,423}, Maria Vittoria Davi⁴²⁴, Angelo P Dei Tos⁵⁸², Matteo Fassan⁵⁸³, Sonia Grimaldi⁴¹⁹, Luca Landoni⁴¹⁵, Rita T Lawlor⁴¹⁹, Claudio Luchini⁴¹⁸, Andrea Mafficini⁴¹⁹, Giuseppe Malleo⁴¹⁵, Giovanni Marchegiani⁴¹⁵, Michele Milella²²⁹, Marco Miotto⁴¹⁵, Salvatore Paiella⁴¹⁵, Antonio Pea⁴¹⁵, Paolo Pederzoli⁴¹⁵, Borislav C Rusev⁴¹⁹, Andrea Ruzzenente⁴¹⁵, Roberto Salvia⁴¹⁵, Maria Scardonì⁴¹⁸, Elisabetta Sereni⁴¹⁵, Michele Simbolo⁴²³, Nicola Sperandio⁴¹⁹, Giampaolo Tortora^{229,230}, Caterina Vicentini⁴¹⁹ and Aldo Scarpa⁴¹⁹

Tumour Specific Providers – Japan (Biliary tract cancer)

Yasuhiro Arai²²⁶, Natsuko Hama²²⁶, Nobuyoshi Hiraoka⁵⁸⁴, Fumie Hosoda^{226,226}, Mamoru Kato³⁶¹, Hiromi Nakamura²²⁶, Hidenori Ojima⁵⁸⁵, Takuji Okusaka⁵⁸⁶, Yasushi Totoki²²⁶, Tomoko Urushidate²²⁷ and Tatsuhiro Shibata^{226,227}

Tumour Specific Providers – Japan (Gastric cancer)

Yasuhiro Arai²²⁶, Masashi Fukayama⁵⁸⁷, Natsuko Hama²²⁶, Fumie Hosoda^{226,226}, Shumpei Ishikawa⁵⁸⁸, Hitoshi Katai⁵⁸⁹, Mamoru Kato³⁶¹, Hiroto Katoh⁵⁸⁸, Daisuke Komura⁵⁸⁸, Genta Nagae^{310,318}, Hiromi Nakamura²²⁶, Hirofumi Rokutan³⁶¹, Mihoko Saito-Adachi³⁶¹, Akihiro Suzuki^{310,590}, Hirokazu Taniguchi⁵⁹¹, Kenji Tatsuno³¹⁰, Yasushi Totoki²²⁶, Tetsuo Ushiku⁵⁸⁷, Shinichi Yachida^{226,592}, Shogo Yamamoto³¹⁰, Hiroyuki Aburatani³¹⁰ and Tatsuhiro Shibata^{226,227}

Tumour Specific Providers – Japan (Liver cancer)

Hiroyuki Aburatani³¹⁰, Hiroshi Aikata⁵⁹³, Koji Arihiro⁵⁹³, Shun-ichi Ariizumi⁵⁹⁴, Keith A Borojevich^{81,233}, Kazuaki Chayama⁵⁹³, Akihiro Fujimoto⁸¹, Masashi Fujita⁸¹, Mayuko Furuta⁸¹, Kunihito Gotoh⁵⁹⁵, Natsuko Hama²²⁶, Takanori Hasegawa³⁹, Shinya Hayami⁵⁹⁶, Shuto Hayashi³⁹, Satoshi Hirano⁵⁹⁷, Seiya Imoto^{39,39}, Mamoru Kato³⁶¹, Yoshiiku Kawakami⁵⁹³, Kazuhiro Maejima⁸¹, Satoru Miyano³⁹, Genta Nagae^{310,318}, Hiromi Nakamura²²⁶, Toru Nakamura⁵⁹⁷, Kaoru Nakano⁸¹, Hideki Ohdan⁵⁹³, Aya Sasaki-Oku⁸¹, Yuichi Shiraishi³⁹, Hiroko Tanaka³⁹, Yasushi Totoki²²⁶, Tatsuhiro Tsunoda^{233,294,295,296}, Masaki Ueno⁵⁹⁶, Rui Yamaguchi³⁹, Masakazu Yamamoto⁵⁹⁴, Hiroki Yamaue⁵⁹⁶, Hidewaki Nakagawa⁸¹ and Tatsuhiro Shibata^{226,227}

Tumour Specific Providers – Singapore (Biliary tract cancer)

Su Pin Choo⁵⁹⁸, Ioana Cutcutache^{196,346}, Narong Khuntikeo^{415,599}, John R McPherson^{196,346}, Choon Kiat Ong⁶⁰⁰, Chawalit Pairojkul⁴¹¹, Irinel Popescu⁶⁰¹, Steven G Rozen^{196,197,346}, Patrick Tan^{190,195,196,197} and Bin Tean Teh^{195,196,197,198,199}

Tumour Specific Providers – South Korea (Blood cancer)

Keun Soo Ahn⁶⁰², Hyung-Lae Kim⁵⁶, Youngil Koh^{336,337} and Sung-Soo Yoon³³⁷

that cancer driver discovery is not yet complete. Chromothripsis is frequently an early event in

Tumour Specific Providers – Spain (Chronic Lymphocytic Leukaemia)

Marta Aymerich⁶⁰³, Josep Ll Gelpi^{40,145}, Ivo G Gut^{49,74}, Marta Gut^{49,74}, Armando Lopez-Guillermo⁶⁰⁴, Carlos López-Otín⁶⁰⁵, Xose S Puente⁶⁰⁵, Romina Royo⁴⁰, David Torrents^{40,76} and Elias Campo^{606,607}

Tumour Specific Providers – United Kingdom (Bone cancer)

Fernanda Amary⁶⁰⁸, Daniel Baumhoer⁶⁰⁹, Sam Behjati¹, Bodil Bjerkehagen^{609,610}, PA Futreal⁵⁰⁷, Ola Myklebost⁵¹⁸, Nischalan Pillay⁶¹¹, Patrick Tarpey⁶¹², Roberto Tirabosco⁶¹³, Olga Zaikova⁶¹⁴, Peter J Campbell^{1,2} and Adrienne M Flanagan⁶¹⁵

Tumour Specific Providers – United Kingdom (Chronic myeloid disorders)

Jacqueline Boulton⁶¹⁶, David T Bowen¹, Adam P Butler¹, Mario Cazzola⁶¹⁷, Carlo Gambacorti-Passerini²⁷⁰, Anthony R Green³²⁹, Eva Hellstrom-Lindberg⁶¹⁸, Luca Malcovati⁶¹⁷, Sancha Martin^{1,362}, Jyoti Nangalia⁶¹⁹, Elli Papaemmanuil¹, Paresh Vyas^{340,620} and Peter J Campbell^{1,2}

Tumour Specific Providers – United Kingdom (Oesophageal cancer)

Yeng Ang⁶²¹, Hugh Barr⁶²², Duncan Beardsmore⁶²³, Matthew Eldridge³²⁸, James Gossage⁶²⁴, Nicola Grehan³⁵², George B Hanna⁶²⁵, Stephen J Hayes^{626,627}, Ted R Hupp⁶²⁸, David Khoo⁶²⁹, Jesper Lagergren^{618,630}, Laurence B Lovat¹⁸⁹, Shona MacRae¹³⁷, Maria O'Donovan³⁵², J Robert O'Neill⁶³¹, Simon L Parsons⁶³², Shaun R Preston⁶³³, Sonia Puig⁶³⁴, Tom Roques⁶³⁵, Grant Sanders²⁴, Sharmila Sothi⁶³⁶, Simon Tavare³²⁸, Olga Tucker⁶³⁷, Richard Turkington⁶³⁸, Timothy J Underwood⁶³⁹, Ian Welch⁶⁴⁰ and Rebecca C Fitzgerald³⁵²

Tumour Specific Providers – United Kingdom (Prostate cancer)

Daniel M Berney⁶⁴¹, Johann S De Bono³⁹⁶, G Steven Bova¹²⁶, Daniel S Brewer^{394,395}, Adam P Butler¹, Declan Cahill⁶⁴², Niedzica Camacho³⁹⁶, Nening M Dennis⁶⁴², Tim Dudderidge^{642,643}, Sandra E Edwards³⁹⁶, Cyril Fisher⁶⁴², Christopher S Foster^{644,645}, Mohammed Ghori¹, Pelvender Gill⁶²⁰, Vincent J Gnanapragasam^{379,646}, Gunes Gundem²⁷⁸, Freddie C Hamdy⁶⁴⁷, Steve Hawkins³²⁸, Steven Hazell⁶⁴², William Howat³⁷⁹, William B Isaacs⁶⁴⁸, Katalin Karaszi⁶²⁰, Jonathan D Kay¹⁸⁹, Vincent Khoo⁶⁴², Zsafia Kote-Jarai³⁹⁶, Barbara Kremeyer¹, Pardeep Kumar⁶⁴², Adam Lambert⁶²⁰, Daniel A Leongamornlert^{1,396}, Naomi Livni⁶⁴², Yong-Jie Lu^{641,649}, Hayley J Luxton¹⁸⁹, Andy G Lynch^{328,329,339}, Luke Marsden⁶²⁰, Charlie E Massie³²⁸, Lucy Matthews³⁹⁶, Erik Mayer^{642,650}, Ultan McDermott¹, Sue Merson³⁹⁶, Thomas J Mitchell^{1,329,379}, David E Neal^{328,379}, Anthony Ng⁶⁵¹, David Nicol⁶⁴², Christopher Ogden⁶⁴², Edward W Rowe⁶⁴², Nimish C Shah³⁷⁹, Jon W Teague¹, Sarah Thomas⁶⁴², Alan Thompson⁶⁴², Peter Van Loo^{91,92}, Clare Verrill^{620,652}, Tapio Visakorpi¹²⁶, Anne Y Warren^{379,653}, David C Wedge^{1,65,66}, Hayley C Whitaker¹⁸⁹, Jorge Zamora^{1,42,43,44}, Hongwei Zhang⁶⁴⁹, Nicholas van As⁶⁴², Colin S Cooper^{395,396,397} and Rosalind A Eeles^{396,642}

Tumour Specific Providers – United States (TCGA)

Adam Abeshouse²⁷⁸, Nishant Agrawal¹⁶³, Rehan Akbani^{352,654}, Hikmat Al-Ahmadie²⁷⁸, Monique Albert⁴⁵², Kenneth Aldape^{400,655}, Adrian Ally⁶⁵⁶, Yeng Ang⁶²¹, Elizabeth L Appelbaum^{27,189}, Joshua Armenia⁶⁵⁷, Sylvia Asa^{632,658}, J Todd Auman⁶⁵⁹, Matthew H Bailey^{26,27}, Miruna Balasundaram⁶⁵⁶, Saianand Balu²⁴, Jill Barnholtz-Sloan^{660,661}, Hugh Barr⁶²², John Bartlett^{451,452}, Oliver F Bathe^{662,663}, Stephen B Baylin^{123,643}, Duncan Beardsmore⁶²³, Christopher Benz⁶⁶⁴, Andrew Berchuck⁶⁶⁵, Benjamin P Berman^{313,321,322}, Rameen Beroukhi^{3,6,168}, Mario Berrios⁶⁶⁶, Darell Bigner⁶⁶⁷, Michael Birrer¹⁹, Tom Bodenheimer²⁴, Lori Boice⁶³⁴, Moiz S Bootwalla⁶⁶⁶, Marcus Bosenberg⁶⁶⁸, Reanne Bowlby⁶⁵⁶, Jeffrey Boyd⁶⁶⁹, Russell R Broadus⁴⁰⁰, Malcolm Brock⁶⁷⁰, Denise Brooks⁶⁵⁶, Susan Bullman^{3,168}, Samantha J Caesar-Johnson²³¹, Thomas E Carey⁶⁷¹, Rebecca Carlsen⁶⁵⁶, Robert Cerfolio⁶⁷², Vishal S Chandan⁶⁷³, Hsiao-Wei Chen^{621,657}, Andrew D Cherniack^{3,3,157,168}, Jeremy Chien⁶⁷⁴, Juok Cho³, Eric Chuah⁶⁵⁶, Carrie Cibulskis³, Kristian Cibulskis³, Leslie Cope⁶⁷⁵, Matthew G Cordes^{27,635}, Kyle Covington³⁴, Erin Curley⁶⁷⁶, Bogdan Czerniak^{400,629}, Ludmila Danilova⁶⁷⁵, Ian J Davis⁶⁷⁷, Timothy Defreitas³, John A Demchok²³¹, Noreen Dhalla⁶⁵⁶, Rajiv Dhir⁶⁷⁸, Li Ding^{26,27,35}, Harsha Vardhan Doddapaneni³⁴, Adel El-Naggar^{400,629}, Ina Felau²³¹, Martin L Ferguson⁶⁷⁹, Gaetano Finocchiaro⁶⁸⁰, Kwun M Fong⁶⁸¹, Scott Frazer³, William Friedman⁶⁸², Catrina C Fronick^{27,635}, Lucinda A Fulton²⁷, Robert S Fulton^{26,27,35}, Stacey B Gabriel³, Jianjiong Gao⁶⁵⁷, Nils Gehlenborg^{3,683}, Jeffrey E Gershenwald^{684,685}, Gad Getz^{3,4,5,6}, Ronald Ghossein⁵¹⁰, Nasra H Giama⁶⁸⁶, Richard A Gibbs³⁴, Carmen Gomez⁶⁸⁷, James Gossage⁶²⁴, Ramaswamy Govindan²⁶, Nicola Grehan³⁵², George B Hanna⁶²⁵, D Neil Hayes^{24,688,689}, Stephen J Hayes^{626,627}, Apurva M Hegde^{137,138}, David I Heiman³, Zachary Heins²⁷⁸, Austin J Heppner²⁴, Katherine A Hoadley^{23,24}, Andrea Holbrook⁶⁶⁶, Robert A Holt⁶⁵⁶, Alan P Hoyle²⁴, Ralph H Hruban^{675,675}, Jianhong Hu³⁴, Mei Huang⁶³⁴, David Huntsman⁶⁹⁰, Ted R Hupp⁶²⁸, Jason Huse²⁷⁸, Christine A Iacobuzio-Donahue⁵¹⁰, Michael Ittmann^{691,692}, Joy C Jayaseelan³⁴, Stuart R Jefferys²⁴, Corbin D Jones⁶⁹³, Steven JM Jones⁶⁹⁴, Hartmut Juhl⁶⁹⁵, Koo Jeong Kang⁶⁹⁶, Beth Karlan⁶⁹⁷, Katayoon Kasaian⁶⁹⁴, Electron Kebebew^{698,699}, David Khoo⁶²⁹, Hark Kyun Kim⁷⁰⁰, Jaegil Kim³, Tari A King^{516,517}, Viktoriya Korchina³⁴, Ritika Kundra^{621,657}, Jesper Lagergren^{618,630}, Phillip H Lai⁶⁶⁶, Peter W Laird³¹⁶, Eric Lander³, Michael S Lawrence^{3,19,233}, Alexander J Lazar²², Xuan Le⁷⁰¹, Darlene Lee⁶⁵⁶, Douglas A Levine^{278,702}, Lora Lewis³⁴, Tim Ley⁷⁰³, Haiyan Irene Li⁶⁵⁶, Pei Lin³, W M Linehan⁷⁰⁴, Eric Minwei Liu^{71,73,278}, Fei Fei Liu³⁸⁰, Laurence B Lovat¹⁸⁹, Yiling Lu¹³⁸, Lisa Lype⁷⁰⁵, Yussanne Ma⁶⁵⁶, Shona MacRae¹³⁷, Dennis T Maglinte^{666,706}, Elaine R Mardis^{27,669,707}, Jeffrey Marks^{415,708}, Marco A Marra⁶⁵⁶, Thomas J Matthew³⁷, Michael Mayo⁶⁵⁶, Karen McCune⁷⁰⁹, Michael D McLellan^{26,27,35}, Samuel R Meier³, Shaowu Meng²⁴, Matthew Meyerson^{3,6,157}, Piotr A Mieczkowski²³, Tom Mikkelsen⁷¹⁰, Christopher A Miller²⁷, Gordon B Mills⁷¹¹, Richard A Moore⁶⁵⁶, Carl Morrison^{411,712}, Lisle E Mose²⁴, Catherine D Moser⁶⁸⁶, Andrew J Mungall⁶⁵⁶, Karen Mungall⁶⁵⁶, David Mutch⁷¹³, Donna M Muzny⁷¹⁴, Jerome Myers⁷¹⁵, Yulia Newton³⁷, Michael S Noble³, Peter O'Donnell⁷¹⁶, Brian Patrick O'Neill⁷¹⁷, Angelica Ochoa²⁷⁸, Akinyemi I Ojesina^{191,192,193}, Joong-Won Park⁷¹⁸, Joel S Parker⁷¹⁹, Simon L Parsons⁶³², Harvey Pass⁷²⁰, Alessandro Pastore¹¹², Chandra Sekhar Pedamallu^{3,6,168}, Nathan A Pennell⁷²¹, Charles M Perou⁷²², Gloria M Petersen⁴⁶², Nicholas Petrelli⁷²³, Olga Potapova⁷²⁴, Shaun R Preston⁶³³, Sonia Puig⁶³⁴, Janet S Rader⁷²⁵, Suresh Ramalingam⁷²⁶, W Kimryn Rathmell⁷²⁷, Victor Reuter⁵¹⁰, Sheila M Reynolds⁷⁰⁵, Matthew Ringel⁷²⁸, Jeffrey Roach⁷²⁹, Lewis R Roberts⁶⁸⁶, A Gordon Robertson⁶⁵⁶, Tom Roques⁶³⁵, Mark A Rubin^{274,287,288,289,290}, Sara Sadeghi⁶⁵⁶, Gordon Saksena³,

tumour evolution: in acral melanoma, for example, these clustered events precede most somatic

Charles Saller⁷³⁰, Francisco Sanchez-Vega^{621,657}, Chris Sander^{112,157,291,292}, Grant Sanders²⁴, Dirk Schadendorf^{149,731}, Jacqueline E Schein⁶⁵⁶, Heather K Schmidt²⁷, Nikolaus Schultz⁶⁵⁷, Steven E Schumacher^{3,204}, Richard A Scolyer^{413,443,446,450}, Raja Seethala⁷³², Yasin Senbabaoglu¹¹², Troy Shelton⁶⁷⁶, Yan Shi²⁴, Juliann Shih^{3,168}, Ilya Shmulevich⁷⁰⁵, Craig Shriver⁷³³, Sabina Signoretti^{168,263,734}, Janae V Simons²⁴, Samuel Singer^{415,735}, Payal Sipahimalani⁶⁵⁶, Tara J Skelly²³, Karen Smith-McCune⁷⁰⁹, Nicholas D Socci¹¹², Heidi J Sofia²¹⁷, Matthew G Soloway⁷¹⁹, Anil K Sood⁷³⁶, Sharmila Sothi⁶³⁶, Angela Tam⁶⁵⁶, Donghui Tan²³, Roy Tarnuzzer²³¹, Nina Thiessen⁶⁵⁶, R Houston Thompson⁷³⁷, Leigh B Thorne⁶³⁴, Ming Tsao^{632,658}, Olga Tucker⁶³⁷, Richard Turkington⁶³⁸, Christopher Umbricht^{324,623,738}, Timothy J Underwood⁶³⁹, David J Van Den Berg⁶⁶⁶, Erwin G Van Meir⁷³⁹, Umadevi Veluvolu²³, Douglas Voet³, Jiayin Wang^{27,58,158}, Linghua Wang³⁴, Zhining Wang²³¹, Paul Weinberger⁷⁴⁰, John N Weinstein^{137,138}, Daniel J Weisenberger⁶⁶⁶, Ian Welch⁶⁴⁰, David A Wheeler^{33,34}, Dennis Wigle⁷⁴¹, Matthew D Wilkerson²³, Richard K Wilson^{27,742}, Boris Winterhoff⁷⁴³, Maciej Wiznerowicz^{744,745}, Tina Wong^{27,656}, Winghing Wong⁷⁴⁶, Liu Xi³⁴, Liming Yang²³¹, Christina Yau⁶⁶⁴, Venkata D Yellapantula^{67,68}, Hailei Zhang³, Hongxin Zhang⁶⁵⁷, Jiashan Zhang²³¹, Carolyn M Hutter²¹⁷ and Jean C Zenklusen²³¹

Author Affiliations

1. Wellcome Sanger Institute, Wellcome Genome Campus, Hinxton, Cambridge, CB10 1SA, UK.
2. Department of Haematology, University of Cambridge, Cambridge CB2 2XY, UK.
3. Broad Institute of MIT and Harvard, Cambridge, MA 02142, USA.
4. Center for Cancer Research, Massachusetts General Hospital, Boston, MA 02129, USA.
5. Department of Pathology, Massachusetts General Hospital, Boston, MA 02115, USA.
6. Harvard Medical School, Boston, MA 02115, USA.
7. European Molecular Biology Laboratory, European Bioinformatics Institute (EMBL-EBI), Wellcome Genome Campus, Hinxton, Cambridge, CB10 1SD, UK.
8. Genome Biology Unit, European Molecular Biology Laboratory (EMBL), Heidelberg 69117, Germany.
9. Biomolecular Engineering Department, University of California Santa Cruz, Santa Cruz, CA 95064, USA.
10. Adaptive Oncology Initiative, Ontario Institute for Cancer Research, Toronto, ON M5G 0A3, Canada.
11. International Cancer Genome Consortium (ICGC)/ICGC Accelerating Research in Genomic Oncology (ARGO) Secretariat, Toronto, ON M5G 0A3, Canada.
12. Computational Biology Program, Ontario Institute for Cancer Research, Toronto, ON M5G 0A3, Canada.
13. Department of Molecular Genetics, University of Toronto, Toronto, ON M5S 1A8, Canada.
14. Department of Radiation Oncology, University of California San Francisco, San Francisco, CA 94518, USA.
15. Genome Informatics Program, Ontario Institute for Cancer Research, Toronto, ON M5G 0A3, Canada.
16. Department of Cell and Systems Biology, University of Toronto, Toronto, ON M5S 3G5, Canada.
17. Genome Informatics, Ontario Institute for Cancer Research, Toronto, ON M5G 2C4, Canada.
18. Department of Medical Biophysics, University of Toronto, Toronto, ON M5S 1A8, Canada.
19. Massachusetts General Hospital, Boston, MA 02114, USA.
20. Department of Pharmacology, University of Toronto, Toronto, ON M5S 1A8, Canada.
21. University of California Los Angeles, Los Angeles, CA 90095, USA.
22. Departments of Pathology, Genomic Medicine and Translational Molecular Pathology, The University of Texas MD Anderson Cancer Center, Houston, TX 77030, USA.
23. Department of Genetics, University of North Carolina at Chapel Hill, Chapel Hill, NC 27599, USA.
24. Lineberger Comprehensive Cancer Center, University of North Carolina at Chapel Hill, Chapel Hill, NC 27599, USA.
25. The Hospital for Sick Children, Toronto, ON M5G 0A4, Canada.
26. Alvin J. Siteman Cancer Center, Washington University School of Medicine, St Louis, MO 63110, USA.
27. The McDonnell Genome Institute at Washington University, St Louis, MO 63108, USA.
28. Division of Theoretical Bioinformatics, German Cancer Research Center (DKFZ), Heidelberg 69120, Germany.
29. Heidelberg Center for Personalized Oncology (DKFZ-HIPO), German Cancer Research Center, Heidelberg 69120, Germany.
30. Institute of Pharmacy and Molecular Biotechnology and BioQuant, Heidelberg University, Heidelberg 69120, Germany.
31. Bioinformatics and Omics Data Analytics, German Cancer Research Center (DKFZ), Heidelberg 69120, Germany.
32. Department of Bioinformatics and Computational Biology, The University of Texas MD Anderson Cancer Center, Houston, TX 77030, USA.
33. Department of Molecular and Human Genetics, Baylor College of Medicine, Houston, TX 77030, USA.
34. Human Genome Sequencing Center, Baylor College of Medicine, Houston, TX 77030, USA.
35. Department of Genetics, Department of Medicine, Washington University in St Louis, St Louis, MO 63110, USA.
36. Department of Computer Science, University of Toronto, Toronto, ON M5S 1A8, Canada.
37. University of California Santa Cruz, Santa Cruz, CA 95064, USA.
38. Oregon Health & Science University, Portland, OR 97239, USA.
39. The Institute of Medical Science, The University of Tokyo, Tokyo 108-8639, Japan.
40. Barcelona Supercomputing Center (BSC), Barcelona 08034, Spain.
41. Department of Clinical and Molecular Medicine, Faculty of Medicine and Health Sciences, Norwegian University of Science and Technology, Trondheim 7030, Norway.
42. Centre for Research in Molecular Medicine and Chronic Diseases (CiMUS), Universidade de Santiago de Compostela, Santiago de Compostela 15706, Spain.

point mutations and affect several cancer genes simultaneously. Cancers with abnormal telomere

-
43. Department of Zoology, Genetics and Physical Anthropology, (CiMUS), Universidade de Santiago de Compostela, Santiago de Compostela 15706, Spain.
 44. The Biomedical Research Centre (CINBIO), Universidade de Vigo, Vigo 36310, Spain.
 45. Department of Genetics, Stanford University School of Medicine, Stanford, CA 94305, USA.
 46. Anai Systems, Inc, Carlsbad, CA 92013, USA.
 47. Centre for Genomic Regulation (CRG), The Barcelona Institute of Science and Technology, Barcelona 08003, Spain.
 48. Institute of Medical Genetics and Applied Genomics, University of Tübingen, Tübingen 72076, Germany.
 49. Universitat Pompeu Fabra (UPF), Barcelona 08003, Spain.
 50. Department of Computational Biology, University of Lausanne, Lausanne 1015, Switzerland.
 51. Department of Genetic Medicine and Development, University of Geneva Medical School, Geneva CH 1211, Switzerland.
 52. Swiss Institute of Bioinformatics, University of Geneva, Geneva CH 1211, Switzerland.
 53. Department of Ophthalmology and Ocular Genomics Institute, Massachusetts Eye and Ear, Harvard Medical School, Boston, MA 02114, USA.
 54. Institute of Evolutionary Biology (UPF-CSIC), Department of Experimental and Health Sciences, Universitat Pompeu Fabra, Barcelona 08003, Spain.
 55. Transmissible Cancer Group, Department of Veterinary Medicine, University of Cambridge, Cambridge CB3 0ES, UK.
 56. Department of Biochemistry, College of Medicine, Ewha Womans University, Seoul 07895, South Korea.
 57. Division of Oncology, Washington University School of Medicine, St Louis, MO 63110, USA.
 58. School of Electronic and Information Engineering, Xi'an Jiaotong University, Xi'an 710048, China.
 59. The First Affiliated Hospital, Xi'an Jiaotong University, Xi'an 710049, China.
 60. Independent Consultant, Wellesley 02481, USA.
 61. Icahn School of Medicine at Mount Sinai, New York, NY 10029, USA.
 62. Biobyte solutions GmbH, Heidelberg 69126, Germany.
 63. Department of Molecular Biophysics and Biochemistry, Yale University, New Haven, CT 06520, USA.
 64. Program in Computational Biology and Bioinformatics, Yale University, New Haven, CT 06520, USA.
 65. Big Data Institute, Li Ka Shing Centre, University of Oxford, Oxford OX3 7LF, UK.
 66. Oxford NIHR Biomedical Research Centre, University of Oxford, Oxford OX4 2PG, UK.
 67. Department of Epidemiology and Biostatistics, Memorial Sloan Kettering Cancer Center, New York, NY 10065, USA.
 68. The McDonnell Genome Institute at Washington University, Department of Genetics, Department of Medicine, Siteman Cancer Center, Washington University in St Louis, St Louis, MO 63108, USA.
 69. Department of Computer Science, Yale University, New Haven, CT 06520, USA.
 70. Controlled Department and Institution, New York, NY 10065, USA.
 71. Department of Physiology and Biophysics, Weill Cornell Medicine, New York, NY 10065, USA.
 72. Englander Institute for Precision Medicine, Weill Cornell Medicine, New York, NY 10065, USA.
 73. Institute for Computational Biomedicine, Weill Cornell Medicine, New York, NY 10021, USA.
 74. CNAG-CRG, Centre for Genomic Regulation (CRG), Barcelona Institute of Science and Technology (BIST), Barcelona 08028, Spain.
 75. Department of Experimental and Health Sciences, Institute of Evolutionary Biology (UPF-CSIC), Universitat Pompeu Fabra, Barcelona 08003, Spain.
 76. Institució Catalana de Recerca i Estudis Avançats (ICREA), Barcelona 08010, Spain.
 77. Institut Català de Paleontologia Miquel Crusafont, Universitat Autònoma de Barcelona, Barcelona 08193, Spain.
 78. Department of Biomedical Data Science, Stanford University School of Medicine, Stanford, CA 94305, USA.
 79. Human Genetics, University of Kiel, Kiel 24118, Germany.
 80. Institute of Human Genetics, Ulm University and Ulm University Medical Center, Ulm 89081, Germany.
 81. RIKEN Center for Integrative Medical Sciences, Yokohama, Kanagawa 230-0045, Japan.
 82. Centre for Cancer Genetic Epidemiology, Department of Oncology, University of Cambridge, Cambridge CB1 8RN, UK.
 83. Centre for Cancer Genetic Epidemiology, Department of Public Health and Primary Care, University of Cambridge, Cambridge CB1 8RN, UK.
 84. Quantitative Genomics Laboratories (qGenomics), Barcelona 08950, Spain.
 85. Sage Bionetworks, Seattle, WA 98109, USA.
 86. Department of Biochemistry and Molecular Medicine, University of Montreal, Montreal, QC H3C 3J7, Canada.
 87. Institute for Research in Biomedicine (IRB Barcelona), Barcelona 08028, Spain.
 88. National Centre for Biological Sciences, Tata Institute of Fundamental Research, Bangalore 560065, India.
 89. Research Program on Biomedical Informatics, Universitat Pompeu Fabra, Barcelona 08002, Spain.
 90. Broad Institute of MIT and Harvard, Cambridge, MA 02124, USA.
 91. The Francis Crick Institute, London NW1 1AT, UK.
 92. University of Leuven, Leuven B-3000, Belgium.
 93. Centre for Molecular Science Informatics, Department of Chemistry, University of Cambridge, Cambridge CB2 1EW, UK.
 94. Department of Biomedical Informatics, Harvard Medical School, Boston, MA 02115, USA.
 95. Ludwig Center at Harvard Medical School, Boston, MA 02115, USA.

maintenance often originate in tissues with low replicative activity, with several different

-
96. Division of Cancer Epidemiology and Genetics, National Cancer Institute, National Institutes of Health, Bethesda, MD 20892, USA.
97. Genome Integrity and Structural Biology Laboratory, National Institute of Environmental Health Sciences (NIEHS), Durham, NC 27709, USA.
98. Integrative Bioinformatics Support Group, National Institute of Environmental Health Sciences (NIEHS), Durham, NC 27709, USA.
99. Department of Urology, Charité Universitätsmedizin Berlin, Berlin 10117, Germany.
100. Finsen Laboratory and Biotech Research & Innovation Centre (BRIC), University of Copenhagen, Copenhagen 2200, Denmark.
101. Department of Cellular and Molecular Medicine and Department of Bioengineering and Moores Cancer Center, University of California San Diego, La Jolla, CA 92093, USA.
102. Department of Genetics, Microbiology and Statistics, University of Barcelona, IRSJD, IBUB, Barcelona 08028, Spain.
103. CIBER Epidemiología y Salud Pública (CIBERESP), Madrid 28029, Spain.
104. Research Group on Statistics, Econometrics and Health (GRECS), UdG, Barcelona 8041, Spain.
105. Oxford Nanopore Technologies, New York, NY 10013, USA.
106. Applications Department, Oxford Nanopore Technologies, Oxford OX4 4DQ, UK.
107. School of Molecular Biosciences and Center for Reproductive Biology, Washington State University, Pullman, WA 99164, USA.
108. Laboratory of Translational Genomics, Division of Cancer Epidemiology and Genetics, National Cancer Institute, National Institutes of Health, Bethesda, MD 20892, USA.
109. Department of Medical and Clinical Genetics, Genome-Scale Biology Research Program, University of Helsinki, Helsinki 00100, Finland.
110. Integrated Graduate Program in Physical and Engineering Biology, Yale University, New Haven, CT 06520, USA.
111. Applied Tumor Genomics Research Program, Research Programs Unit, University of Helsinki, Helsinki 00290, Finland.
112. Computational Biology Center, Memorial Sloan Kettering Cancer Center, New York, NY 10065, USA.
113. Department of Biology, ETH Zurich, Zürich 8093, Switzerland.
114. Department of Computer Science, ETH Zurich, Zurich 8092, Switzerland.
115. SIB Swiss Institute of Bioinformatics, Lausanne 1015, Switzerland.
116. University Hospital Zurich, Zurich 8091, Switzerland.
117. Weill Cornell Medical College, New York, NY 10065, USA.
118. Berlin Institute for Medical Systems Biology, Max Delbrück Center for Molecular Medicine, Berlin 13125, Germany.
119. German Cancer Consortium (DKTK), Partner site Berlin.
120. German Cancer Research Center (DKFZ), Heidelberg 69120, Germany.
121. Bakar Computational Health Sciences Institute and Department of Pediatrics, University of California, San Francisco, CA 94158-2549, USA.
122. Department of Biostatistics, Bloomberg School of Public Health, Johns Hopkins University, Baltimore, MD 21205, USA.
123. Department of Oncology, The Johns Hopkins School of Medicine, The Sidney Kimmel Comprehensive Cancer Center at Johns Hopkins University, Baltimore, MD 21230, USA.
124. Division of Computational Genomics and Systems Genetics, German Cancer Research Center (DKFZ), Heidelberg 69120, Germany.
125. Division of Biomedical Informatics, Department of Medicine, & Moores Cancer Center, UC San Diego School of Medicine, San Diego, CA 92093, USA.
126. Faculty of Medicine and Health Technology, Tampere University and Tays Cancer Center, Tampere University Hospital, Tampere FI-33014, Finland.
127. Division of Applied Bioinformatics, German Cancer Research Center (DKFZ), Heidelberg 69120, Germany.
128. Faculty of Biosciences, Heidelberg University, Heidelberg 69120, Germany.
129. Centre for Law and Genetics, University of Tasmania, Sandy Bay Campus, Hobart, TAS 7001, Australia.
130. Centre of Genomics and Policy, McGill University and Génome Québec Innovation Centre, Montreal, QC H3A 1A4, Canada.
131. Heidelberg Academy of Sciences and Humanities, Heidelberg 69120, Germany.
132. UC Santa Cruz Genomics Institute, University of California Santa Cruz, Santa Cruz, CA 95064, USA.
133. CIBIO/InBIO - Research Center in Biodiversity and Genetic Resources, Universidade do Porto, Vairão 4485-601, Portugal.
134. Ontario Institute for Cancer Research, Toronto, ON M5G 0A3, Canada.
135. Bioinformatics Unit, Spanish National Cancer Research Centre (CNIO), Madrid 28029, Spain.
136. Howard Hughes Medical Institute, University of California Santa Cruz, Santa Cruz, CA 95065, USA.
137. Cancer Unit, MRC University of Cambridge, Cambridge CB2 0XZ, UK.
138. Department of Bioinformatics and Computational Biology and Department of Systems Biology, The University of Texas MD Anderson Cancer Center, Houston, TX 77030, USA.
139. Center for Digital Health, Berlin Institute of Health and Charité - Universitätsmedizin Berlin, Berlin 10117, Germany.
140. Heidelberg Center for Personalized Oncology (DKFZ-HIPO), German Cancer Research Center (DKFZ), Heidelberg 69120, Germany.
141. University of Texas MD Anderson Cancer Center, Houston, TX 77030, USA.
142. Department of Genetics and Informatics Institute, University of Alabama at Birmingham, Birmingham, AL 35294, USA.
143. Heidelberg University, Heidelberg 69120, Germany.

mechanisms of escaping critical telomere attrition. Common and rare germline variants affect

-
144. New BIH Digital Health Center, Berlin Institute of Health (BIH) and Charité - Universitätsmedizin Berlin, Berlin 10117, Germany.
 145. Department Biochemistry and Molecular Biomedicine, University of Barcelona, Barcelona 08028, Spain.
 146. Department of Urologic Sciences, University of British Columbia, Vancouver, BC V5Z 1M9, Canada.
 147. Vancouver Prostate Centre, Vancouver, BC V6H 3Z6, Canada.
 148. Division of Life Science and Applied Genomics Center, Hong Kong University of Science and Technology, Clear Water Bay, Hong Kong, China.
 149. German Cancer Consortium (DKTK), Heidelberg 69120, Germany.
 150. National Center for Tumor Diseases (NCT) Heidelberg, Heidelberg 69120, Germany.
 151. Genome Integration Data Center, Syntekabio, Inc, Daejeon, 34025, South Korea.
 152. Massachusetts General Hospital Center for Cancer Research, Charlestown, MA 02129, USA.
 153. Department of Molecular Medicine (MOMA), Aarhus University Hospital, Aarhus N 8200, Denmark.
 154. Bioinformatics Research Centre (BiRC), Aarhus University, Aarhus 8000, Denmark.
 155. Indiana University, Bloomington, IN 47405, USA.
 156. Simon Fraser University, Burnaby, BC V5A 1S6, Canada.
 157. Dana-Farber Cancer Institute, Boston, MA 02215, USA.
 158. School of Computer Science and Technology, Xi'an Jiaotong University, Xi'an 710048, China.
 159. Department of Genetics, Washington University School of Medicine, St Louis, MO 63110, USA.
 160. Department of Mathematics, Washington University in St Louis, St Louis, MO 63130, USA.
 161. Department of Biological Oceanography, Leibniz Institute of Baltic Sea Research, Rostock 18119, Germany.
 162. Seven Bridges Genomics, Charlestown, MA 02129, USA.
 163. University of Chicago, Chicago, IL 60637, USA.
 164. Department of Health Sciences and Technology, Sungkyunkwan University School of Medicine, Seoul 06351, South Korea.
 165. Samsung Genome Institute, Seoul 06351, South Korea.
 166. New York Genome Center, New York, NY 10013, USA.
 167. Weill Cornell Medicine, New York, NY 10065, USA.
 168. Department of Medical Oncology, Dana-Farber Cancer Institute, Boston, MA 02115, USA.
 169. Rigshospitalet, Copenhagen 2200, Denmark.
 170. Department of Computer Science, University of Toronto, Toronto, ON M5S 2E4, Canada.
 171. The Donnelly Centre, University of Toronto, Toronto, ON M5S 3E1, Canada.
 172. Vector Institute, Toronto, ON M5G 0A3, Canada.
 173. Department of Medical Genetics, College of Medicine, Hallym University, Chuncheon 24252, South Korea.
 174. Department of Biology, ETH Zurich, Wolfgang-Pauli-Strasse 27, 8093 Zürich, Switzerland.
 175. University Hospital Zurich, Zurich, 8091, Switzerland.
 176. Peking University, Beijing 100871, China.
 177. School of Life Sciences, Peking University, Beijing 100180, China.
 178. Computational and Systems Biology, Genome Institute of Singapore, Singapore 138672, Singapore.
 179. School of Computing, National University of Singapore, Singapore 117417, Singapore.
 180. BGI-Shenzhen, Shenzhen 518083, China.
 181. China National GeneBank-Shenzhen, Shenzhen 518083, China.
 182. Computational & Systems Biology Program, Memorial Sloan Kettering Cancer Center, New York, NY 10065, USA.
 183. Korea University, Seoul 02481, South Korea.
 184. Department of Genomic Medicine, The University of Texas MD Anderson Cancer Center, Houston, TX 77030, USA.
 185. Quantitative & Computational Biosciences Graduate Program, Baylor College of Medicine, Houston, TX 77030, USA.
 186. The Jackson Laboratory for Genomic Medicine, Farmington, CT 06032, USA.
 187. Wolfson Wohl Cancer Research Centre, Institute of Cancer Sciences, University of Glasgow, Bearsden, Glasgow G61 1QH, UK.
 188. The Azrieli Faculty of Medicine, Bar-Ilan University, Safed 13195, Israel.
 189. University College London, London WC1E 6BT, UK.
 190. Genome Institute of Singapore, Singapore 138672, Singapore.
 191. Department of Epidemiology, University of Alabama at Birmingham, Birmingham, AL 35294, USA.
 192. HudsonAlpha Institute for Biotechnology, Huntsville, AL 35806, USA.
 193. O'Neal Comprehensive Cancer Center, University of Alabama at Birmingham, Birmingham, AL 35294, USA.
 194. Department of Biosciences and Nutrition, Karolinska Institutet, Stockholm 14183, Sweden.
 195. Cancer Science Institute of Singapore, National University of Singapore, Singapore 169609, Singapore.
 196. Programme in Cancer & Stem Cell Biology, Duke-NUS Medical School, Singapore 169857, Singapore.
 197. SingHealth, Duke-NUS Institute of Precision Medicine, National Heart Centre Singapore, Singapore 169609, Singapore.
 198. Institute of Molecular and Cell Biology, Singapore 169609, Singapore.
 199. Laboratory of Cancer Epigenome, Division of Medical Science, National Cancer Centre Singapore, Singapore 169610, Singapore.
 200. Department of Medicine, Baylor College of Medicine, Houston, TX 77030, USA.
 201. National Cancer Centre Singapore, Singapore 169610, Singapore.

patterns of somatic mutation, including point mutations, structural variants and somatic

-
202. BIOCIC, ICG and College of Life Sciences, Peking University, Beijing 100871, China.
203. Vall d'Hebron Institute of Oncology: VHIO, Barcelona 08035, Spain.
204. Department of Cancer Biology, Dana-Farber Cancer Institute, Boston, MA 02215, USA.
205. Institute for Research in Biomedicine (IRB Barcelona), The Barcelona Institute of Science and Technology, Barcelona 8003, Spain.
206. Department of Mathematics, Aarhus University, Aarhus 8000, Denmark.
207. Institut Hospital del Mar d'Investigacions Mèdiques (IMIM), Barcelona 08003, Spain.
208. King Faisal Specialist Hospital and Research Centre, Al Maather, Riyadh 12713, Saudi Arabia.
209. DLR Project Management Agency, Bonn 53227, Germany.
210. Genome Canada, Ottawa, ON K2P 1P1, Canada.
211. Instituto Carlos Slim de la Salud, Mexico City, Mexico.
212. Federal Ministry of Education and Research, Berlin 10117, Germany.
213. Institut Gustave Roussy, Villejuif 94805, France.
214. Institut National du Cancer (INCA), Boulogne-Billancourt 92100, France.
215. The Wellcome Trust, London NW1 2BE, UK.
216. Prostate Cancer Canada, Toronto, ON M5C 1M1, Canada.
217. National Human Genome Research Institute, National Institutes of Health, Bethesda, MD 20892, USA.
218. Department of Biotechnology, Ministry of Science & Technology, Government of India, New Delhi, Delhi 110003, India.
219. Science Writer, Garrett Park, MD 20896, USA.
220. Cancer Research UK, London EC1V 4AD, UK.
221. Chinese Cancer Genome Consortium, Shenzhen 518083, China.
222. Laboratory of Molecular Oncology, Key Laboratory of Carcinogenesis and Translational Research (Ministry of Education), Peking University Cancer Hospital & Institute, Beijing 100142, China.
223. Peking University Cancer Hospital & Institute, Key Laboratory of Carcinogenesis and Translational Research (Ministry of Education), Peking University Cancer Hospital & Institute, Beijing 100142, China.
224. National Cancer Center, Tokyo 104-0045, Japan.
225. German Cancer Aid, Bonn 53113, Germany.
226. Division of Cancer Genomics, National Cancer Center Research Institute, National Cancer Center, Tokyo 104-0045, Japan.
227. Laboratory of Molecular Medicine, Human Genome Center, The Institute of Medical Science, The University of Tokyo, Minato-ku, Tokyo 108-8639, Japan.
228. Japan Agency for Medical Research and Development, Chiyoda-ku, Tokyo 100-0004, Japan.
229. Medical Oncology, University and Hospital Trust of Verona, Verona 37134, Italy.
230. University of Verona, Verona 37129, Italy.
231. National Cancer Institute, National Institutes of Health, Bethesda, MD 20892, USA.
232. CAPHRI Research School, Maastricht University, Maastricht, ER 6200MD, The Netherlands.
233. Laboratory for Medical Science Mathematics, RIKEN Center for Integrative Medical Sciences, Yokohama, Kanagawa 230-0045, Japan.
234. University of California San Diego, San Diego, CA 92093, USA.
235. PDXen Biosystems Inc, Seoul 4900, South Korea.
236. Electronics and Telecommunications Research Institute, Daejeon 34129, South Korea.
237. Children's Hospital of Philadelphia, Philadelphia, PA 19146, USA.
238. University of Melbourne Centre for Cancer Research, Melbourne, VIC 3010, Australia.
239. Syntekabio Inc, Daejeon 34025, South Korea.
240. AbbVie, North Chicago, IL 60064, USA.
241. Genomics Research Program, Ontario Institute for Cancer Research, Toronto, ON M5G 0A3, Canada.
242. Department of Pediatric Immunology, Hematology and Oncology, University Hospital, Heidelberg 69120, Germany.
243. Heidelberg Institute for Stem Cell Technology and Experimental Medicine (HI-STEM), Heidelberg 69120, Germany.
244. Seven Bridges, Charlestown, MA 02129, USA.
245. Health Sciences Department of Biomedical Informatics, University of California San Diego, La Jolla, CA 92093, USA.
246. Functional and Structural Genomics, German Cancer Research Center (DKFZ), Heidelberg 69120, Germany.
247. Leidos Biomedical Research, Inc, McLean, VA 22102, USA.
248. CSRA Incorporated, Fairfax, VA 22042, USA.
249. Department of Internal Medicine, Stanford University, Stanford, CA 94305, USA.
250. Clinical Bioinformatics, Swiss Institute of Bioinformatics, Geneva 1202, Switzerland.
251. Institute for Pathology and Molecular Pathology, University Hospital Zurich, Zurich 8091, Switzerland.
252. Institute of Molecular Life Sciences, University of Zurich, Zurich 8057, Switzerland.
253. MIT Computer Science and Artificial Intelligence Laboratory, Massachusetts Institute of Technology, Cambridge, MA 02139, USA.
254. Institute of Molecular Life Sciences and Swiss Institute of Bioinformatics, University of Zurich, Zurich 8057, Switzerland.
255. Office of Cancer Genomics, National Cancer Institute, National Institutes of Health, Bethesda, MD 20892, USA.
256. Computer Network Information Center, Chinese Academy of Sciences, Beijing 100190, China.

retrotransposition. PCAWG found few non-coding mutations that drive cancer beyond those in the

-
257. Genepplus-Shenzhen, Shenzhen 518122, China.
258. Dana-Farber/Boston Children's Cancer and Blood Disorders Center, Boston, MA 02215, USA.
259. Department of Pediatrics, Harvard Medical School, Boston, MA 02115, USA.
260. Technical University of Denmark, Lyngby 2800, Denmark.
261. University of Copenhagen, Copenhagen 2200, Denmark.
262. Department for BioMedical Research, University of Bern, Bern 3008, Switzerland.
263. Department of Medical Oncology, Inselspital, University Hospital and University of Bern, Bern 3010, Switzerland.
264. Graduate School for Cellular and Biomedical Sciences, University of Bern, Bern 3012, Switzerland.
265. Department of Genitourinary Medical Oncology - Research, Division of Cancer Medicine, The University of Texas MD Anderson Cancer Center, Houston, TX 77030, USA.
266. Department of Urology, Icahn School of Medicine at Mount Sinai, New York, NY 10029, USA.
267. Korea Advanced Institute of Science and Technology, Daejeon 34141, South Korea.
268. Science for Life Laboratory, Department of Cell and Molecular Biology, Uppsala University, Uppsala SE-75124, Sweden.
269. Queensland Centre for Medical Genomics, Institute for Molecular Bioscience, The University of Queensland, St Lucia, Brisbane, QLD 4072, Australia.
270. University of Milano Bicocca, Monza 20052, Italy.
271. Sir Peter MacCallum Department of Oncology, Peter MacCallum Cancer Centre, University of Melbourne, Melbourne, VIC 3000, Australia.
272. Center for Precision Health, School of Biomedical Informatics, The University of Texas Health Science Center, Houston, TX 77030, USA.
273. Health Data Science Unit, University Clinics, Heidelberg 69120, Germany.
274. Department for Biomedical Research, University of Bern, Bern 3008, Switzerland.
275. Research Core Center, National Cancer Centre Korea, Goyang-si 410-769, South Korea.
276. Institute of Computer Science, Polish Academy of Sciences, Warszawa 01-248, Poland.
277. Harvard University, Cambridge, MA 02138, USA.
278. Memorial Sloan Kettering Cancer Center, New York, NY 10065, USA.
279. Department of Information Technology, Ghent University, Ghent B-9000, Belgium.
280. Department of Plant Biotechnology and Bioinformatics, Ghent University, Ghent B-9000, Belgium.
281. Yale School of Medicine, Yale University, New Haven, CT 06520, USA.
282. Division of Hematology-Oncology, Samsung Medical Center, Sungkyunkwan University School of Medicine, Seoul 06351, South Korea.
283. Samsung Advanced Institute for Health Sciences and Technology, Sungkyunkwan University School of Medicine, Seoul 06351, South Korea.
284. Cheonan Industry-Academic Collaboration Foundation, Sangmyung University, Cheonan 31066, South Korea.
285. Spanish National Cancer Research Centre, Madrid 28029, Spain.
286. Department of Computer Science, Princeton University, Princeton, NJ 08540, USA.
287. Bern Center for Precision Medicine, University Hospital of Bern, University of Bern, Bern 3008, Switzerland.
288. Englander Institute for Precision Medicine, Weill Cornell Medicine and New York Presbyterian Hospital, New York, NY 10021, USA.
289. Meyer Cancer Center, Weill Cornell Medicine, New York, NY 10065, USA.
290. Pathology and Laboratory, Weill Cornell Medical College, New York, NY 10021, USA.
291. cBio Center, Dana-Farber Cancer Institute, Harvard Medical School, Boston, MA 02115, USA.
292. Department of Cell Biology, Harvard Medical School, Boston, MA 02115, USA.
293. cBio Center, Dana-Farber Cancer Institute, Boston, MA 02215, USA.
294. CREST, Japan Science and Technology Agency, Tokyo 113-0033, Japan.
295. Department of Medical Science Mathematics, Medical Research Institute, Tokyo Medical and Dental University, Bunkyo-ku, Tokyo 113-8510, Japan.
296. Laboratory for Medical Science Mathematics, Department of Biological Sciences, Graduate School of Science, The University of Tokyo, Bunkyo-ku, Tokyo 113-0033, Japan.
297. Science for Life Laboratory, Department of Oncology-Pathology, Karolinska Institutet, Stockholm 17121, Sweden.
298. Department of Gene Technology, Tallinn University of Technology, Tallinn 12616, Estonia.
299. Genetics & Genome Biology Program, SickKids Research Institute, The Hospital for Sick Children, Toronto, ON M5G 1X8, Canada.
300. Department of Information Technology, Ghent University, Interuniversitair Micro-Electronica Centrum (IMEC), Ghent B-9000, Belgium.
301. Science for Life Laboratory, Department of Immunology, Genetics and Pathology, Uppsala University, Uppsala SE-75108, Sweden.
302. Oregon Health & Sciences University, Portland, OR 97239, USA.
303. Department of Medicine and Therapeutics, The Chinese University of Hong Kong, Shatin, NT, Hong Kong, China.
304. The University of Texas Health Science Center at Houston, Houston, TX 77030, USA.
305. Department of Biomedical Informatics, College of Medicine, The Ohio State University, Columbus, OH 43210, USA.

TERT promoter⁴; identified new signatures of mutational processes causing base substitutions,

-
306. The Ohio State University Comprehensive Cancer Center (OSUCCC – James), Columbus, OH 43210, USA.
307. The University of Texas School of Biomedical Informatics (SBMI) at Houston, Houston, TX 77030, USA.
308. Department of Biochemistry and Molecular Genetics, Feinberg School of Medicine, Northwestern University, Chicago, IL 60637, USA.
309. Physics Division, Optimization and Systems Biology Lab, Massachusetts General Hospital, Boston, MA 02114, USA.
310. Genome Science Division, Research Center for Advanced Science and Technology, The University of Tokyo, Tokyo 153-8904, Japan.
311. Bioinformatics Group, Department of Computer Science, University of Leipzig, Leipzig 04109, Germany.
312. Interdisciplinary Center for Bioinformatics, University of Leipzig, Leipzig 04109, Germany.
313. Center for Bioinformatics and Functional Genomics, Cedars-Sinai Medical Center, Los Angeles, CA 90048, USA.
314. Computational Biology, Leibniz Institute on Aging - Fritz Lipmann Institute (FLI), Jena 07745, Germany.
315. Transcriptome Bioinformatics, LIFE Research Center for Civilization Diseases, University of Leipzig, Leipzig 04109, Germany.
316. Center for Epigenetics, Van Andel Research Institute, Grand Rapids, MI 49503, USA.
317. Institut d'Investigacions Biomèdiques August Pi i Sunyer (IDIBAPS), Barcelona 08036, Spain.
318. Research Center for Advanced Science and Technology, The University of Tokyo, Minato-ku, Tokyo 108-8639, Japan.
319. Van Andel Research Institute, Grand Rapids, MI 49503, USA.
320. Cancer Epigenomics, German Cancer Research Center (DKFZ), Heidelberg 69120, Germany.
321. Department of Biomedical Sciences, Cedars-Sinai Medical Center, Los Angeles, CA 90048, USA.
322. The Hebrew University Faculty of Medicine, Jerusalem 91120, Israel.
323. German Cancer Consortium (DKTK), German Cancer Research Center (DKFZ), Heidelberg 69120, Germany.
324. Department of Pathology, Johns Hopkins University School of Medicine, Baltimore, MD 21205, USA.
325. McKusick-Nathans Institute of Genetic Medicine, Sidney Kimmel Comprehensive Cancer Center, Johns Hopkins University School of Medicine, Baltimore, MD 21205, USA.
326. Foundation Medicine, Inc, Cambridge, MA 02141, USA.
327. University of Ottawa Faculty of Medicine, Department of Biochemistry, Microbiology and Immunology, Ottawa, ON K1H 8M5, Canada.
328. Cancer Research UK Cambridge Institute, University of Cambridge, Cambridge CB2 0RE, UK.
329. University of Cambridge, Cambridge CB2 1TN, UK.
330. Brandeis University, Waltham, MA 02254, USA.
331. Hopp Children's Cancer Center (KiTZ), Heidelberg 69120, Germany.
332. Pediatric Glioma Research Group, German Cancer Research Center (DKFZ), Heidelberg 69120, Germany.
333. A.A. Kharkevich Institute of Information Transmission Problems, Moscow 127051, Russia.
334. Oncology and Immunology, Dmitry Rogachev National Research Center of Pediatric Hematology, Moscow 117997, Russia.
335. Skolkovo Institute of Science and Technology, Moscow 121205, Russia.
336. Center For Medical Innovation, Seoul National University Hospital, Seoul 03080, South Korea.
337. Department of Internal Medicine, Seoul National University Hospital, Seoul 03080, South Korea.
338. Division of Genetics and Genomics, Boston Children's Hospital, Harvard Medical School, Boston, MA 02115, USA.
339. School of Medicine/School of Mathematics and Statistics, University of St Andrews, St Andrews, Fife KY16 9SS, UK.
340. Department of Genetics and Computational Biology, QIMR Berghofer Medical Research Institute, Brisbane, QLD 4006, Australia.
341. Institute for Molecular Bioscience, University of Queensland, St Lucia, Brisbane, QLD 4072, Australia.
342. Cancer Research Institute, Beth Israel Deaconess Medical Center, Boston, MA 02215, USA.
343. Ben May Department for Cancer Research, Department of Human Genetics, The University of Chicago, Chicago, IL 60637, USA.
344. Tri-Institutional PhD Program in Computational Biology and Medicine, Weill Cornell Medicine, New York, NY 10065, USA.
345. Department of Cellular and Molecular Medicine and Department of Bioengineering and Moores Cancer Center, University of California, San Diego, La Jolla, CA 92093, USA.
346. Centre for Computational Biology, Duke-NUS Medical School, Singapore 169857, Singapore.
347. Department of Computer Science, University of Helsinki, Helsinki 00014, Finland.
348. Institute of Biotechnology, University of Helsinki, Helsinki 00014, Finland.
349. Organismal and Evolutionary Biology Research Programme, University of Helsinki, Helsinki 00014, Finland.
350. Programme in Cancer & Stem Cell Biology, Centre for Computational Biology, Duke-NUS Medical School, Singapore 169857, Singapore.
351. Academic Department of Medical Genetics, University of Cambridge, Addenbrooke's Hospital, Cambridge CB2 0QQ, UK.
352. MRC Cancer Unit, University of Cambridge, Cambridge CB2 0XZ, UK.
353. The University of Cambridge School of Clinical Medicine, Cambridge CB2 0SP, UK.
354. Department of Applied Mathematics and Theoretical Physics, Centre for Mathematical Sciences, University of Cambridge, Cambridge CB3 0WA, UK.
355. Department of Statistics, Columbia University, New York, NY 10027, USA.
356. Duke-NUS Medical School, Singapore 169857, Singapore.

indels and structural variation^{5,6}; analysed timings and patterns of tumour evolution⁷; described

-
357. School of Electronic Information and Communications, Huazhong University of Science and Technology, Wuhan, Hubei 430074, China.
358. The Kinghorn Cancer Centre, Cancer Division, Garvan Institute of Medical Research, University of NSW, Sydney, NSW 2010, Australia.
359. MRC Human Genetics Unit, MRC IGMM, University of Edinburgh, Edinburgh EH4 2XU, UK.
360. Bioinformatics Group, Division of Molecular Biology, Department of Biology, Faculty of Science, University of Zagreb, Zagreb 10000, Croatia.
361. Department of Bioinformatics, Division of Cancer Genomics, National Cancer Center Research Institute, National Cancer Center, Tokyo 104-0045, Japan.
362. University of Glasgow, Glasgow G61 1BD, UK.
363. MRC-University of Glasgow Centre for Virus Research, Glasgow G61 1QH, UK.
364. Wolfson Wohl Cancer Research Centre, Institute of Cancer Sciences, University of Glasgow, Bearsden, Glasgow G61 1BD, UK.
365. School of Computing Science, University of Glasgow, Glasgow G12 8RZ, UK.
366. South Western Sydney Clinical School, Faculty of Medicine, University of NSW, Liverpool, NSW 2170, Australia.
367. West of Scotland Pancreatic Unit, Glasgow Royal Infirmary, Glasgow G31 2ER, UK.
368. University of Melbourne Centre for Cancer Research, Melbourne, VIC 3052, Australia.
369. Molecular and Medical Genetics, Oregon Health and Science University, Portland, OR 97201, USA.
370. Department of Surgery, University of Melbourne, Parkville, VIC 3010, Australia.
371. The Murdoch Children's Research Institute, Royal Children's Hospital, Parkville, VIC 3052, Australia.
372. Walter + Eliza Hall Institute, Parkville, VIC 3052, Australia.
373. University of Cologne, Cologne 50931, Germany.
374. The Edward S. Rogers Sr. Department of Electrical and Computer Engineering, University of Toronto, Toronto, ON M5S 3G4, Canada.
375. University of Ljubljana, Ljubljana 1000, Slovenia.
376. Department of Public Health Sciences, The University of Chicago, Chicago, IL 60637, USA.
377. Research Institute, NorthShore University HealthSystem, Evanston, IL 60201, USA.
378. Department of Statistics, University of California Santa Cruz, Santa Cruz, CA 95064, USA.
379. Cambridge University Hospitals NHS Foundation Trust, Cambridge CB2 0QQ, UK.
380. University of Toronto, Toronto, ON M5G 2M9, Canada.
381. Department of Computer Science, Carleton College, Northfield, MN 55057, USA.
382. Molecular and Medical Genetics, Oregon Health & Science University, Portland, OR 97239, USA.
383. Center for Psychiatric Genetics, NorthShore University HealthSystem, Evanston, IL 60201, USA.
384. Argmix Consulting, North Vancouver, BC V7M 2J5, Canada.
385. Department of Biostatistics, The University of Texas MD Anderson Cancer Center, Houston, TX 77030, USA.
386. Department of Biostatistics, University of North Carolina at Chapel Hill, Chapel Hill, NC 27599, USA.
387. The University of Texas MD Anderson Cancer Center, Houston, TX 77030, USA.
388. Molecular and Medical Genetics, Knight Cancer Institute, Oregon Health & Science University, Portland, OR 97219, USA.
389. Department of Health Sciences, Faculty of Medical Sciences, Kyushu University, Fukuoka 812-8582, Japan.
390. Baylor College of Medicine, Houston, TX 77030, USA.
391. Department of Applied Mathematics and Statistics, Johns Hopkins University, Baltimore, MD 21218, USA.
392. Heinrich Pette Institute, Leibniz Institute for Experimental Virology, Hamburg 20251, Germany.
393. University Medical Center Hamburg-Eppendorf, Bioinformatics Core, Hamburg 20246, Germany.
394. Earlham Institute, Norwich NR4 7UZ, UK.
395. Norwich Medical School, University of East Anglia, Norwich NR4 7TJ, UK.
396. The Institute of Cancer Research, London SW7 3RP, UK.
397. University of East Anglia, Norwich NR4 7TJ, UK.
398. German Center for Infection Research (DZIF), Partner Site Hamburg-Borstel-Lübeck-Riems, Hamburg, Germany.
399. Division of Molecular Genetics, German Cancer Research Center (DKFZ), Heidelberg 69120, Germany.
400. Department of Pathology, The University of Texas MD Anderson Cancer Center, Houston, TX 77030, USA.
401. Peter MacCallum Cancer Centre, University of Melbourne, Melbourne, VIC 3000, Australia.
402. QIMR Berghofer Medical Research Institute, Brisbane, QLD 4006, Australia.
403. Victorian Institute of Forensic Medicine, Southbank, VIC 3006, Australia.
404. University of Pennsylvania, Philadelphia, PA 19104, USA.
405. Centre for Cancer Research, The Westmead Institute for Medical Research, Sydney, NSW 2145, Australia.
406. Department of Gynaecological Oncology, Westmead Hospital, Sydney, NSW 2145, Australia.
407. Genetics and Molecular Pathology, SA Pathology, Adelaide, SA 5000, Australia.
408. Centre for Cancer Research, The Westmead Institute for Medical Research, The University of Sydney, Sydney, NSW 2145, Australia.
409. Department of Gynaecological Oncology, Westmead Hospital, Sydney, NSW 2006, Australia.
410. Garvan Institute of Medical Research, Darlinghurst, NSW 2010 Australia.
411. Department of Clinical Pathology, University of Melbourne, Melbourne, VIC 3052, Australia.

the diverse transcriptional consequences of somatic mutation on splicing, expression levels, fusion

-
412. Centre for Cancer Research, The Westmead Institute for Medical Research, and Department of Gynaecological Oncology, Westmead Hospital, Sydney, NSW 2145, Australia.
413. The University of Sydney, Sydney, NSW 2006, Australia.
414. The Westmead Institute for Medical Research. The University of Sydney. The Department of Gynaecological Oncology, Westmead Hospital, Westmead, NSW 2145, Australia.
415. Department of Surgery, Pancreas Institute, University and Hospital Trust of Verona, Verona 37134, Italy.
416. Department of Surgery, Princess Alexandra Hospital, Woolloongabba QLD 4102, Australia.
417. Surgical Oncology Group, Diamantina Institute, The University of Queensland, Woolloongabba, Brisbane, QLD 4102, Australia.
418. Department of Diagnostics and Public Health, University and Hospital Trust of Verona, Verona 37134, Italy.
419. ARC-Net Centre for Applied Research on Cancer, University and Hospital Trust of Verona, Verona 37134, Italy.
420. Illawarra Shoalhaven Local Health District L3 Illawarra Cancer Care Centre, Wollongong Hospital, Wollongong NSW 2500, Australia.
421. University of Sydney, Sydney, NSW 2006, Australia.
422. School of Biological Sciences, The University of Auckland, Auckland 1010, New Zealand.
423. Department of Pathology and Diagnostics, University and Hospital Trust of Verona, Verona 37134, Italy.
424. Department of Medicine, Section of Endocrinology, University and Hospital Trust of Verona, Verona 37134, Italy.
425. Department of Pathology, Queen Elizabeth University Hospital, Glasgow G51 4TF, UK.
426. Department of Medical Oncology, Beatson West of Scotland Cancer Centre, Glasgow G12 0YN, UK.
427. Academic Unit of Surgery, School of Medicine, College of Medical, Veterinary and Life Sciences, University of Glasgow, Glasgow Royal Infirmary, Glasgow G4 0SF, UK.
428. Tissue Pathology and Diagnostic Oncology, Royal Prince Alfred Hospital, Camperdown, NSW 2050, Australia.
429. Discipline of Surgery, Western Sydney University, Penrith, NSW 2751, Australia.
430. Institute of Cancer Sciences, College of Medical Veterinary and Life Sciences, University of Glasgow, Glasgow G12 8QQ, UK.
431. The Kinghorn Cancer Centre, Cancer Division, Garvan Institute of Medical Research, University of NSW, Sydney, NSW 2109, Australia.
432. School of Environmental and Life Sciences, Faculty of Science, The University of Newcastle, Ourimbah, NSW 2258, Australia.
433. Eastern Clinical School, Monash University, Melbourne, VIC 3128, Australia.
434. Epworth HealthCare, Richmond, VIC 3121, Australia.
435. Olivia Newton-John Cancer Research Institute, La Trobe University, Heidelberg, VIC 3084, Australia.
436. Melanoma Institute Australia, The University of Sydney, Wollstonecraft NSW 2065, Australia.
437. Children's Hospital at Westmead, The University of Sydney, Westmead, NSW 2145, Australia.
438. Melanoma Institute Australia, The University of Sydney, Sydney, NSW 2065, Australia.
439. Australian Institute of Tropical Health and Medicine, James Cook University, Douglas, QLD 4814, Australia.
440. Bioplatforms Australia, North Ryde, NSW 2109, Australia.
441. Melanoma Institute Australia, Macquarie University, Wollstonecraft NSW, 2109, Australia.
442. Children's Medical Research Institute, Westmead, NSW 2145 Australia.
443. Melanoma Institute Australia, The University of Sydney, Wollstonecraft 2065, NSW, Australia.
444. Centre for Cancer Research, The Westmead Millennium Institute for Medical Research, University of Sydney, Westmead Hospital, Westmead, NSW 2145, Australia.
445. Centre for Cancer Research, Westmead Institute for Medical Research, Westmead, NSW 2145, Australia.
446. Discipline of Pathology, Sydney Medical School, The University of Sydney, Sydney, NSW 2065, Australia.
447. School of Mathematics and Statistics, The University of Sydney, Sydney, NSW 2006 Australia.
448. Melanoma Institute Australia, The University of Sydney, Wollstonecraft, NSW 2065, Australia.
449. Westmead Institute for Medical Research, University of Sydney, Westmead, NSW 2145 Australia.
450. Royal Prince Alfred Hospital, Sydney, NSW 2050, Australia.
451. Diagnostic Development, Ontario Institute for Cancer Research, Toronto, ON M5G 0A3, Canada.
452. Ontario Tumour Bank, Ontario Institute for Cancer Research, Toronto, ON M5G 0A3, Canada.
453. PanCuRx Translational Research Initiative, Ontario Institute for Cancer Research, Toronto, ON M5G 0A3, Canada.
454. BioSpecimen Sciences Program, University Health Network, Toronto, ON M5G 2C4, Canada, Toronto, ON M5G 2C4, Canada.
455. Hepatobiliary/Pancreatic Surgical Oncology Program, University Health Network, Toronto, ON M5G 2C4, Canada.
456. Lunenfeld-Tanenbaum Research Institute, Mount Sinai Hospital, Toronto, ON M5G 1X5, Canada.
457. Division of Medical Oncology, Princess Margaret Cancer Centre, Toronto, ON M5G 2M9, Canada.
458. University of Nebraska Medical Center, Omaha, NE 68198-6880, USA.
459. BioSpecimen Sciences Program, University Health Network, Toronto, ON M5G 2C4, Canada.
460. Transformative Pathology, Ontario Institute for Cancer Research, Toronto, ON M5G 0A3, Canada.
461. University Health Network, Princess Margaret Cancer Centre, Toronto, ON M5G 1L7, Canada.
462. Department of Health Sciences Research, Mayo Clinic, Rochester, MN 55905, USA.
463. BioSpecimen Sciences, Laboratory Medicine (Toronto), Medical Biophysics, PanCuRX, Toronto, ON M5S 1A8, Canada.
464. Department of Laboratory Medicine and Pathobiology, University of Toronto, Toronto, ON M5S 1A8, Canada.
465. Department of Pathology, Human Oncology and Pathogenesis Program, Memorial Sloan Kettering Cancer Center, New York, NY 10053, USA.

genes and promoter activity^{8,9}; and evaluated a range of more specialised features of cancer

-
466. Department of Medical Biophysics, University of Toronto, Toronto, ON M5G 1L7, Canada.
467. Department of Biochemistry and Molecular Medicine, University California at Davis, Sacramento, CA 95817, USA.
468. Human Longevity Inc, San Diego, CA 92121, USA.
469. Department of Surgical Oncology, Princess Margaret Cancer Centre, Toronto, ON M5G 2M9, Canada.
470. Genome Informatics Program, Ontario Institute for Cancer Research, Toronto, ON M5G 2C4, Canada.
471. STTARR Innovation Facility, Princess Margaret Cancer Centre, Toronto, ON M5G 1L7, Canada.
472. Department of Pathology, Toronto General Hospital, Toronto, ON M5G 2C4, Canada.
473. CRUK Manchester Institute and Centre, Manchester M20 4GJ, UK.
474. Department of Radiation Oncology, University of Toronto, Toronto, ON M5S 1A8, Canada.
475. Manchester Cancer Research Centre, Cancer Division, FBMH, University of Manchester, Manchester M20 4GJ, UK.
476. Radiation Medicine Program, Princess Margaret Cancer Centre, Toronto, ON M5G 2M9, Canada.
477. Hefei University of Technology, Anhui 230009, China.
478. State Key Laboratory of Cancer Biology, and Xijing Hospital of Digestive Diseases, Fourth Military Medical University, Shaanxi 710032, China.
479. Fourth Military Medical University, Shaanxi 710032, China.
480. Laboratory of Molecular Oncology, Key Laboratory of Carcinogenesis and Translational Research (Ministry of Education), Peking University Cancer Hospital & Institute, Beijing, 100142, China.
481. Department of Surgery, Ruijin Hospital, Shanghai Jiaotong University School of Medicine, Shanghai 200025, China.
482. Leeds Institute of Medical Research, University of Leeds, St James's University Hospital, Leeds LS9 7TF, UK.
483. Canadian Center for Computational Genomics, McGill University, Montreal, QC H3A 0G1, Canada.
484. Department of Human Genetics, McGill University, Montreal, QC H3A 1B1, Canada.
485. International Agency for Research on Cancer, Lyon 69008, France.
486. McGill University and Genome Quebec Innovation Centre, Montreal, QC H3A 0G1, Canada.
487. Leeds Institute of Medical Research @ St James's, University of Leeds, St James's University Hospital, Leeds LS9 7TF, UK.
488. Institute of Mathematics and Computer Science, University of Latvia, Riga LV 1459, Latvia.
489. Centre National de Génotypage, CEA - Institut de Génomique, Evry 91000, France.
490. Department of Oncology, Gil Medical Center, Gachon University, Incheon 405-760, South Korea.
491. Department of Molecular Oncology, BC Cancer Agency, Vancouver, BC V5Z 1L3, Canada.
492. Los Alamos National Laboratory, Los Alamos, NM 87545, USA.
493. Department of Genetics, Institute for Cancer Research, Oslo University Hospital, The Norwegian Radium Hospital, Oslo O310, Norway.
494. Lund University, Lund 223 62, Sweden.
495. Translational Research Lab, Centre Léon Bérard, Lyon 69373, France.
496. Department of Molecular Biology, Faculty of Science, Radboud Institute for Molecular Life Sciences, Radboud University, Nijmegen 6500 HB, The Netherlands.
497. Department of Pathology, Brigham and Women's Hospital, Harvard Medical School, Boston, MA 02115, USA.
498. Department of Molecular Pathology, The Netherlands Cancer Institute, Amsterdam 1066 CX, The Netherlands.
499. Cancer Research UK Cambridge Institute, University of Cambridge, Li Ka Shing Centre, Cambridge CB2 0RE, UK.
500. Department of Oncology, University of Cambridge, Cambridge CB2 1TN, UK.
501. Breast Cancer Translational Research Laboratory JC Heuson, Institut Jules Bordet, Brussels 1000, Belgium.
502. Laboratory for Translational Breast Cancer Research, Department of Oncology, KU Leuven, Leuven 3000, Belgium.
503. Translational Cancer Research Unit, GZA Hospitals St.-Augustinus, Center for Oncological Research, Faculty of Medicine and Health Sciences, University of Antwerp, Antwerp 2000, Belgium.
504. Department of Gynecology & Obstetrics, Department of Clinical Sciences, Skåne University Hospital, Lund University, Lund SE-221 85, Sweden.
505. Icelandic Cancer Registry, Icelandic Cancer Society, Reykjavik 125, Iceland.
506. Department of Medical Oncology, Josephine Nefkens Institute and Cancer Genomics Centre, Erasmus Medical Center, Rotterdam 3015 CN, The Netherlands.
507. National Genotyping Center, Institute of Biomedical Sciences, Academia Sinica, Taipei 115, Taiwan.
508. Department of Pathology, Oslo University Hospital Ullevål, Oslo 0450, Norway.
509. Faculty of Medicine and Institute of Clinical Medicine, University of Oslo, Oslo NO-0316, Norway.
510. Department of Pathology, Memorial Sloan Kettering Cancer Center, New York, NY 10065, USA.
511. Department of Pathology, Skåne University Hospital, Lund University, Lund SE-221 85, Sweden.
512. Department of Pathology, Academic Medical Center, Amsterdam 1105 AZ, The Netherlands.
513. Department of Pathology, College of Medicine, Hanyang University, Seoul 133-791, South Korea.
514. Department of Pathology, Asan Medical Center, College of Medicine, Ulsan University, Songpa-gu, Seoul 05505, South Korea.
515. The Netherlands Cancer Institute, Amsterdam 1066 CX, The Netherlands.
516. Department of Surgery, Brigham and Women's Hospital, Dana-Farber Cancer Institute, Boston, MA 02115, USA.
517. Department of Surgery, Memorial Sloan-Kettering Cancer Center, New York, NY 10065, USA.
518. Department of Clinical Science, University of Bergen, Bergen 5020, Norway.

genomes^{8,10–18}.

-
519. Morgan Welch Inflammatory Breast Cancer Research Program and Clinic, The University of Texas MD Anderson Cancer Center, Houston, TX 77030, USA.
520. The University of Queensland Centre for Clinical Research, The Royal Brisbane & Women's Hospital, Herston, QLD 4029, Australia.
521. Department of Pathology, Institut Jules Bordet, Brussels 1000, Belgium.
522. Institute for Bioengineering and Biopharmaceutical Research (IBBR), Hanyang University, Seoul 133-791, South Korea.
523. University of Oslo, Oslo 0316, Norway.
524. Institut Bergonié, Bordeaux 33076, France.
525. Department of Research Oncology, Guy's Hospital, King's Health Partners AHSC, King's College London School of Medicine, London SE1 9RT, UK.
526. University Hospital of Minjoo, INSERM UMR 1098, Besançon 25000, France.
527. Cambridge Breast Unit, Addenbrooke's Hospital, Cambridge University Hospital NHS Foundation Trust and NIHR Cambridge Biomedical Research Centre, Cambridge CB2 2QQ, UK.
528. East of Scotland Breast Service, Ninewells Hospital, Aberdeen AB25 2XF, UK.
529. Oncologie Sénologie, ICM Institut Régional du Cancer, Montpellier 34298, France.
530. Department of Radiation Oncology, Radboud University Nijmegen Medical Centre, Nijmegen 6525 GA, The Netherlands.
531. University of Iceland, Reykjavik 101, Iceland.
532. Dundee Cancer Centre, Ninewells Hospital, Dundee DD2 1SY, UK.
533. Institut Curie, INSERM Unit 830, Paris 75248, France.
534. Department of Laboratory Medicine, Radboud University Nijmegen Medical Centre, Nijmegen 6525 GA, The Netherlands.
535. Department of General Surgery, Singapore General Hospital, Singapore 169608, Singapore.
536. Universite Lyon, INCa-Synergie, Centre Léon Bérard, Lyon 69008, France.
537. Giovanni Paolo II / I.R.C.C.S. Cancer Institute, Bari BA 70124, Italy.
538. Department of Biopathology, Centre Léon Bérard, Lyon 69008, France.
539. Université Claude Bernard Lyon 1, Villeurbanne 69100, France.
540. NCCS-VARI Translational Research Laboratory, National Cancer Centre Singapore, Singapore 169610, Singapore.
541. Department of Pathology, Erasmus Medical Center Rotterdam, Rotterdam 3015 GD, The Netherlands.
542. Division of Molecular Carcinogenesis, The Netherlands Cancer Institute, Amsterdam 1066 CX, The Netherlands.
543. Institute of Human Genetics, Christian-Albrechts-University, Kiel 24118, Germany.
544. Institute of Human Genetics, Ulm University and Ulm University Medical Center of Ulm, Ulm 89081, Germany.
545. Hematopathology Section, Institute of Pathology, Christian-Albrechts-University, Kiel 24118, Germany.
546. Institute of Human Genetics, University of Ulm and University Hospital of Ulm, Ulm 89081, Germany.
547. Department of Human Genetics, Hannover Medical School, Hannover 30625, Germany.
548. Department of Pediatric Oncology, Hematology and Clinical Immunology, Heinrich-Heine-University, Düsseldorf 40225, Germany.
549. Department of Internal Medicine/Hematology, Friedrich-Ebert-Hospital, Neumünster 24534, Germany.
550. Pediatric Hematology and Oncology, University Hospital Muenster, Muenster 24534, Germany.
551. Department of Pediatrics, University Hospital Schleswig-Holstein, Kiel 24105, Germany.
552. Department of Medicine II, University of Würzburg, Würzburg, Germany.
553. Senckenberg Institute of Pathology, University of Frankfurt Medical School, Frankfurt 60596, Germany.
554. Institute of Pathology, Charité – University Medicine Berlin, Berlin 10117, Germany.
555. Department for Internal Medicine II, University Hospital Schleswig-Holstein, Kiel 24105, Germany.
556. Institute for Medical Informatics Statistics and Epidemiology, University of Leipzig, Leipzig 04109, Germany.
557. Department of Hematology and Oncology, Georg-Augusts-University of Göttingen, Göttingen 37073, Germany.
558. Institute of Cell Biology (Cancer Research), University of Duisburg-Essen, Essen D-45147, Germany.
559. MVZ Department of Oncology, PraxisClinic am Johannisplatz, Leipzig 04109, Germany.
560. Institute of Pathology, Ulm University and University Hospital of Ulm, Ulm 89081, Germany.
561. Department of Pathology, Robert-Bosch-Hospital, Stuttgart, Germany, Stuttgart 70376, Germany.
562. University Hospital Giessen, Pediatric Hematology and Oncology, Giessen 35392, Germany.
563. Institute of Clinical Molecular Biology, Christian-Albrechts-University, Kiel 24118, Germany.
564. Institute of Pathology, University of Wuerzburg, Wuerzburg 97070, Germany.
565. Department of General Internal Medicine, University Kiel, Kiel 24118, Germany.
566. Clinic for Hematology and Oncology, St.-Antonius-Hospital, Eschweiler D-52249, Germany.
567. Department for Internal Medicine III, University of Ulm and University Hospital of Ulm, Ulm 89081, Germany.
568. Neuroblastoma Genomics, German Cancer Research Center (DKFZ), Heidelberg 69120, Germany.
569. Department of Pediatric Oncology and Hematology, University of Cologne, Cologne 50937, Germany.
570. University of Düsseldorf, Düsseldorf 40225, Germany.
571. Department of Vertebrate Genomics/Otto Warburg Laboratory Gene Regulation and Systems Biology of Cancer, Max Planck Institute for Molecular Genetics, Berlin 14195, Germany.
572. St. Jude Children's Research Hospital, Memphis, TN 38105-3678, USA.
573. Heidelberg University Hospital, Heidelberg 69120, Germany.

574. Genomics and Proteomics Core Facility High Throughput Sequencing Unit, German Cancer Research Center (DKFZ), Heidelberg 69120, Germany.
575. Epigenomics and Cancer Risk Factors, German Cancer Research Center (DKFZ), Heidelberg 69120, Germany.
576. University Medical Center Hamburg-Eppendorf, Hamburg 20251, Germany.
577. Martini-Clinic, Prostate Cancer Center, University Medical Center Hamburg-Eppendorf, Hamburg 20095, Germany.
578. Institute of Pathology, University Medical Center Hamburg-Eppendorf, Hamburg 20251, Germany.
579. Division of Cancer Genome Research, German Cancer Research Center (DKFZ), Heidelberg 69120, Germany.
580. National Institute of Biomedical Genomics, Kalyani 741235, West Bengal, India.
581. Advanced Centre for Treatment Research & Education in Cancer, Tata Memorial Centre, Navi Mumbai, Maharashtra 410210, India.
582. Department of Pathology, General Hospital of Treviso, Department of Medicine, University of Padua, Treviso 31100, Italy.
583. Department of Medicine (DIMED), Surgical Pathology Unit, University of Padua, Padua 35121, Italy.
584. Department of Hepatobiliary and Pancreatic Oncology, Hepatobiliary and Pancreatic Surgery Division, Division of Pathology and Clinical Laboratories, National Cancer Center Hospital, Chuo-ku, Tokyo, 104-0045, Japan.
585. Department of Pathology, Keio University School of Medicine, Tokyo 160-8582, Japan.
586. Department of Hepatobiliary and Pancreatic Oncology, National Cancer Center Hospital, Tokyo, 104-0045 Japan.
587. Department of Pathology, Graduate School of Medicine, The University of Tokyo, Bunkyo-ku, Tokyo 113-0033, Japan.
588. Preventive Medicine, Graduate School of Medicine, The University of Tokyo, Tokyo 113-0033, Japan.
589. Gastric Surgery Division, Division of Pathology and Clinical Laboratories, National Cancer Center Hospital, Tokyo 104-0045, Japan.
590. Department of Gastroenterology and Hepatology, Yokohama City University Graduate School of Medicine, Kanagawa 236-0004, Japan.
591. Laboratory of Molecular Medicine, Human Genome Center, The Institute of Medical Science, University of Tokyo, Tokyo 108-8639, Japan.
592. Department of Cancer Genome Informatics, Graduate School of Medicine, Osaka University, Osaka 565-0871, Japan.
593. Hiroshima University, Hiroshima 734-8553, Japan.
594. Tokyo Women's Medical University, Tokyo 162-8666, Japan.
595. Osaka International Cancer Center, Osaka 541-8567, Japan.
596. Wakayama Medical University, Wakayama 641-8509, Japan.
597. Hokkaido University, Sapporo 060-8648, Japan.
598. Division of Medical Oncology, National Cancer Centre, Singapore 169610, Singapore.
599. Cholangiocarcinoma Screening and Care Program and Liver Fluke and Cholangiocarcinoma Research Centre, Faculty of Medicine, Khon Kaen University, Khon Kaen 40002, Thailand.
600. Lymphoma Genomic Translational Research Laboratory, National Cancer Centre, Singapore 169610, Singapore.
601. Center of Digestive Diseases and Liver Transplantation, Fundeni Clinical Institute, Bucharest 022328, Romania.
602. Division of Hepatobiliary and Pancreatic Surgery, Department of Surgery, School of Medicine, Keimyung University Dongsan Medical Center, Daegu 41931, South Korea.
603. Pathology, Hospital Clinic, Institut d'Investigacions Biomèdiques August Pi i Sunyer (IDIBAPS), University of Barcelona, Barcelona 8034, Spain.
604. Hematology, Hospital Clinic, Institut d'Investigacions Biomèdiques August Pi i Sunyer (IDIBAPS), University of Barcelona, Barcelona 8034, Spain.
605. Department of Biochemistry and Molecular Biology, Faculty of Medicine, University Institute of Oncology-IUOPA, Oviedo 33006, Spain.
606. Anatomia Patològica, Hospital Clinic, Institut d'Investigacions Biomèdiques August Pi i Sunyer (IDIBAPS), University of Barcelona, Barcelona 8036, Spain.
607. Spanish Ministry of Science and Innovation, Madrid 28046, Spain.
608. Royal National Orthopaedic Hospital - Bolsover, London W1W 5AQ, UK.
609. Department of Pathology, Oslo University Hospital, The Norwegian Radium Hospital, Oslo O310, Norway.
610. Institute of Clinical Medicine and Institute of Oral Biology, University of Oslo, Oslo O310, Norway.
611. Research Department of Pathology, University College London Cancer Institute, London, WC1E 6BT, UK.
612. East Anglian Medical Genetics Service, Cambridge University Hospitals NHS Foundation Trust, Cambridge CB2 0QQ, UK.
613. Royal National Orthopaedic Hospital - Stanmore, Stanmore, Middlesex HA7 4LP, UK.
614. Division of Orthopaedic Surgery, Oslo University Hospital, Oslo 0379, Norway.
615. Department of Pathology (Research), University College London Cancer Institute, London WC1E 6BT, UK.
616. Radcliffe Department of Medicine, University of Oxford, Oxford OX3 9DU, UK.
617. University of Pavia, Pavia 27100, Italy.
618. Karolinska Institute, Stockholm SE-171 76, Sweden.
619. Wellcome Sanger Institute, Wellcome Genome Campus, Hinxton, Cambridge, CB10 1SD, UK.
620. University of Oxford, Oxford OX3 9DU, UK.
621. Salford Royal NHS Foundation Trust, Salford M6 8HD, UK.
622. Gloucester Royal Hospital, Gloucester GL1 3NL, UK.
623. Royal Stoke University Hospital, Stoke-on-Trent ST4 6QG, UK.
624. St Thomas's Hospital, London SE1 7EH, UK.

Cancer is the second most frequent cause of death worldwide, killing more than 8 million

625. Imperial College NHS Trust, Imperial College, London W2 1NY, UK.
626. Department of Histopathology, Salford Royal NHS Foundation Trust, Salford M6 8HD, UK.
627. Faculty of Biology, Medicine and Health, The University of Manchester, Manchester M13 9PL, UK.
628. Edinburgh Royal Infirmary, Edinburgh EH16 4SA, UK.
629. Barking Havering and Redbridge University Hospitals NHS Trust, Romford, RM7 0AG, UK.
630. King's College London and Guy's and St Thomas' NHS Foundation Trust, London SE1 7EH, UK.
631. Cambridge Oesophagogastric Centre, Cambridge University Hospitals NHS Foundation Trust, Cambridge, CB2 0QQ.
632. Nottingham University Hospitals NHS Trust, Nottingham NG7 2UH, UK.
633. St Luke's Cancer Centre, Royal Surrey County Hospital NHS Foundation Trust, Guildford GU2 7XX, UK.
634. University of North Carolina at Chapel Hill, Chapel Hill, NC 27599, USA.
635. Norfolk and Norwich University Hospital NHS Trust, Norwich NR4 7UY, UK.
636. University Hospitals Coventry and Warwickshire NHS Trust, Coventry CV2 2DX, UK.
637. University Hospitals Birmingham NHS Foundation Trust, Birmingham B15 2GW, UK.
638. Centre for Cancer Research and Cell Biology, Queen's University, Belfast BT9 7AB, UK.
639. School of Cancer Sciences, Faculty of Medicine, University of Southampton, Southampton SO17 1BJ, UK.
640. Wythenshawe Hospital, Manchester M23 9LT, UK.
641. Barts Cancer Institute, Barts and the London School of Medicine and Dentistry, Queen Mary University of London, London EC1M 6BQ, UK.
642. Royal Marsden NHS Foundation Trust, London and Sutton SW3 6JJ, UK.
643. University Hospital Southampton NHS Foundation Trust, Southampton SO16 6YD, UK.
644. HCA Laboratories, London W1G 8AQ, UK.
645. University of Liverpool, Liverpool L69 3BX, UK.
646. Academic Urology Group, Department of Surgery, University of Cambridge, Cambridge CB2 0QQ, UK.
647. University of Oxford, Oxford, OX3 9DU, UK.
648. Department of Urology, James Buchanan Brady Urological Institute, Johns Hopkins University School of Medicine, Baltimore, MD 21205, USA.
649. Second Military Medical University, Shanghai 200433, China.
650. Department of Surgery and Cancer, Imperial College, London W2 1NY, UK.
651. The Chinese University of Hong Kong, Shatin, NT, Hong Kong, China.
652. Nuffield Department of Surgical Sciences, John Radcliffe Hospital, University of Oxford, Headington, Oxford OX3 9DU, UK.
653. Department of Histopathology, Cambridge University Hospitals NHS Foundation Trust, Cambridge CB2 0QQ, UK.
654. Department of Bioinformatics and Computational Biology / Department of Systems Biology, The University of Texas MD Anderson Cancer Center, Houston, TX 77030, USA.
655. Laboratory of Pathology, Center for Cancer Research, National Cancer Institute, Bethesda, MD 20892, USA.
656. Canada's Michael Smith Genome Sciences Center, BC Cancer Agency, Vancouver, BC V5Z 4S6, Canada.
657. Center for Molecular Oncology, Memorial Sloan Kettering Cancer Center, New York, NY 10065, USA.
658. University Health Network, Toronto, ON M5G 2C4, Canada.
659. Department of Pathology and Laboratory Medicine, School of Medicine, University of North Carolina at Chapel Hill, Chapel Hill, NC 27599, USA.
660. Department of Population and Quantitative Health Sciences, Case Western Reserve University School of Medicine, Cleveland, OH 44016, USA.
661. Research Health Analytics and Informatics, University Hospitals Cleveland Medical Center, Cleveland, OH 44106, USA.
662. Arnie Charbonneau Cancer Institute, University of Calgary, Calgary, AB T2N 4N2, Canada.
663. Departments of Surgery and Oncology, University of Calgary, Calgary, AB T2N 4N2, Canada.
664. Buck Institute for Research on Aging, Novato, CA 94945, USA.
665. Duke University Medical Center, Durham, NC 27710, USA.
666. USC Norris Comprehensive Cancer Center, University of Southern California, Los Angeles, CA 90033, USA.
667. The Preston Robert Tisch Brain Tumor Center, Duke University Medical Center, Durham, NC 27710, USA.
668. Departments of Dermatology and Pathology, Yale University, New Haven, CT 06510, USA.
669. Fox Chase Cancer Center, Philadelphia, PA 19111, USA.
670. Department of Surgery, Division of Thoracic Surgery, The Johns Hopkins University School of Medicine, Baltimore, MD 21287, USA.
671. University of Michigan Comprehensive Cancer Center, Ann Arbor, MI 48109, USA.
672. University of Alabama at Birmingham, Birmingham, AL 35294, USA.
673. Division of Anatomic Pathology, Mayo Clinic, Rochester, MN 55905, USA.
674. Division of Experimental Pathology, Mayo Clinic, Rochester, MN 55905, USA.
675. Department of Oncology, The Johns Hopkins School of Medicine, The Sidney Kimmel Comprehensive Cancer Center at Johns Hopkins University, Baltimore, MD 21287, USA.
676. International Genomics Consortium, Phoenix, AZ 85004, USA.
677. Departments of Pediatrics and Genetics, University of North Carolina at Chapel Hill, Chapel Hill, NC 27599, USA.
678. Department of Pathology, UPMC Shadyside, Pittsburgh, PA 15232, USA.

people every year and expected to increase by >50% over the coming decades^{19,20}. ‘Cancer’

-
679. Center for Cancer Genomics, National Cancer Institute, National Institutes of Health, Bethesda, MD 20892, USA.
680. Istituto Neurologico Besta, Department of Neuro-Oncology, Milano 20133, Italy.
681. University of Queensland Thoracic Research Centre, The Prince Charles Hospital, Brisbane, QLD 4032, Australia.
682. Department of Neurosurgery, University of Florida, Gainesville, FL 32610, USA.
683. Center for Biomedical Informatics, Harvard Medical School, Boston, MA 02115, USA.
684. Department of Cancer Biology, The University of Texas MD Anderson Cancer Center, Houston, TX 77030, USA.
685. Department of Surgical Oncology, The University of Texas MD Anderson Cancer Center, Houston, TX 77030, USA.
686. Division of Gastroenterology and Hepatology, Mayo Clinic, Rochester, MN 55905, USA.
687. University of Miami, Sylvester Comprehensive Cancer Center, Miami, FL 33136, USA.
688. Department of Internal Medicine, Division of Medical Oncology, Lineberger Comprehensive Cancer Center, University of North Carolina at Chapel Hill, Chapel Hill, NC 27599, USA.
689. University of Tennessee Health Science Center for Cancer Research, Memphis, TN 38163, USA.
690. Centre for Translational and Applied Genomics, British Columbia Cancer Agency, Vancouver, BC V5Z 1L3, Canada.
691. Department of Pathology & Immunology, Baylor College of Medicine, Houston, TX 77030, USA.
692. Michael E. DeBakey Veterans Affairs Medical Center, Houston, TX 77030, USA.
693. Carolina Center for Genome Sciences, University of North Carolina at Chapel Hill, Chapel Hill, NC 27599, USA.
694. Canada's Michael Smith Genome Sciences Centre, BC Cancer Agency, Vancouver, BC V5Z 4S6, Canada.
695. Individumed GmbH, Hamburg 20251, Germany.
696. Division of Hepatobiliary and Pancreatic Surgery, Department of Surgery, School of Medicine, Keimyung University Dong-san Medical Center, Daegu 41931, South Korea.
697. Women's Cancer Program at the Samuel Oschin Comprehensive Cancer Institute, Cedars-Sinai Medical Center, Los Angeles, CA 90048, USA.
698. Department of Surgery, The George Washington University, School of Medicine and Health Science, Washington, DC 20052, USA.
699. Endocrine Oncology Branch, Center for Cancer Research, National Cancer Institute, National Institutes of Health, Bethesda, MD 20892, USA.
700. National Cancer Center, Gyeonggi 10408, South Korea.
701. ILSbio, LLC Biobank, Chestertown, MD 21620, USA.
702. Gynecologic Oncology, NYU Laura and Isaac Perlmutter Cancer Center, New York University, New York, NY 10016, USA.
703. Division of Oncology, Stem Cell Biology Section, Washington University School of Medicine, St. Louis, MO 63110, USA.
704. Urologic Oncology Branch, Center for Cancer Research, National Cancer Institute, National Institutes of Health, Bethesda, MD 20892, USA.
705. Institute for Systems Biology, Seattle, WA 98109, USA.
706. Center for Personalized Medicine, Department of Pathology and Laboratory Medicine, Children's Hospital Los Angeles, Los Angeles, CA 90027, USA.
707. Institute for Genomic Medicine, Nationwide Children's Hospital, Columbus, OH 43215, USA.
708. Department of Surgery, Duke University, Durham, NC 27710, USA.
709. Department of Obstetrics, Gynecology and Reproductive Services, University of California San Francisco, San Francisco, CA 94143, USA.
710. Departments of Neurology and Neurosurgery, Henry Ford Hospital, Detroit, MI 48202, USA.
711. Oregon Health & Science University (OHSU) Knight Cancer Institute, Portland, OR 97210, USA.
712. Department of Pathology, Roswell Park Cancer Institute, Buffalo, NY 14263, USA.
713. Department of Obstetrics and Gynecology, Division of Gynecologic Oncology, Washington University School of Medicine, St. Louis, MO 63110, USA.
714. Department of Palliative, Rehabilitation and Integrative Medicine, The University of Texas MD Anderson Cancer Center, Houston, TX 77030, USA.
715. Penrose St. Francis Health Services, Colorado Springs, CO 80907, USA.
716. The University of Chicago, Chicago, IL 60637, USA.
717. Department of Neurology, Mayo Clinic, Rochester, MN 55905, USA.
718. Center for Liver Cancer, Research Institute and Hospital, National Cancer Center, Gyeonggi 410-769, South Korea.
719. Department of Genetics and Lineberger Comprehensive Cancer Center, University of North Carolina at Chapel Hill, Chapel Hill, NC 27599, USA.
720. NYU Langone Medical Center, New York, NY 10016, USA.
721. Department of Hematology and Medical Oncology, Cleveland Clinic, Cleveland, OH 44195, USA.
722. Department of Genetics, Department of Pathology and Laboratory Medicine, School of Medicine, University of North Carolina at Chapel Hill, Chapel Hill, NC 27599, USA.
723. Helen F. Graham Cancer Center at Christiana Care Health Systems, Newark, DE 19713, USA.
724. Cureline, Inc, South San Francisco, CA 94080, USA.
725. Department of Obstetrics and Gynecology, Medical College of Wisconsin, Milwaukee, WI 53226, USA.
726. Hematology and Medical Oncology, Winship Cancer Institute of Emory University, Atlanta, GA 30322, USA.
727. Vanderbilt Ingram Cancer Center, Vanderbilt University, Nashville, TN 37232, USA.

is a catch-all term used to denote a set of diseases characterised by autonomous expansion

728. Ohio State University College of Medicine and Arthur G. James Comprehensive Cancer Center, Columbus, OH 43210, USA.
 729. Research Computing Center, University of North Carolina at Chapel Hill, Chapel Hill, NC 27599, USA.
 730. Analytical Biological Services, Inc, Wilmington, DE 19801, USA.
 731. Department of Dermatology, University Hospital Essen, Westdeutsches Tumorzentrum & German Cancer Consortium, Essen 45122, Germany.
 732. University of Pittsburgh, Pittsburgh, PA 15213, USA.
 733. Murtha Cancer Center, Walter Reed National Military Medical Center, Bethesda, MD 20889, USA.
 734. Brigham and Women's Hospital, Harvard Medical School, Boston, MA 02115, USA.
 735. Department of Surgery, Memorial Sloan Kettering Cancer Center, New York, NY 10065, USA.
 736. Department of Gynecologic Oncology and Reproductive Medicine, and Center for RNA Interference and Non-Coding RNA, The University of Texas MD Anderson Cancer Center, Houston, TX 77030, USA.
 737. Department of Urology, Mayo Clinic, Rochester, MN 55905, USA.
 738. Department of Surgery, Johns Hopkins University School of Medicine, Baltimore, MD 21205, USA.
 739. Departments of Neurosurgery and Hematology and Medical Oncology, Winship Cancer Institute and School of Medicine, Emory University, Atlanta, GA 30322, USA.
 740. Georgia Regents University Cancer Center, Augusta, GA 30912, USA.
 741. Thoracic Oncology Laboratory, Mayo Clinic, Rochester, MN 55905, USA.
 742. Institute for Genomic Medicine, Nationwide Children's Hospital, Columbus, OH 43205, USA.
 743. Department of Obstetrics & Gynecology, Division of Gynecologic Oncology, Mayo Clinic, Rochester, MN 55905, USA.
 744. International Institute for Molecular Oncology, Poznań 60-203, Poland.
 745. Poznań University of Medical Sciences, Poznań 61-701, Poland.
 746. Edison Family Center for Genome Sciences and Systems Biology, Washington University, St. Louis, MO 63110, USA.

Competing interests

The following authors declare that they have competing interests: **Hikmat Al-Ahmadie** (H. A. is consultant to AstraZeneca and Bristol-Myers-Squibb); **Samuel Aparicio** (Founder and shareholder of Contextual Genomics Inc.); **Pratiti Bandopadhyay** (P.B. receives grant funding from Novartis from an unrelated project.); **Rameen Beroukhi** (R.B. owns equity in Ampressa Therapeutics); **Andrew Biankin** (Grant funding from Celgene, AstraZeneca; Consultancies/Advisory boards: AstraZeneca, Celgene, Elstar Therapeutics, Clovis Oncology, Roche.); **E Birney** (Consultant to Oxford Nanopore, Dovetail and GSK); **Marcus Bosenberg** (Eli Lilly and Company); **Atul Butte** (A.B. is a co-founder and consultant to Personalis, NuMedii; consultant to Samsung, Geisinger Health, Mango Tree Corporation, Regenstrief Institute, and in the recent past 10x Genomics and Helix; shareholder in Personalis; minor shareholder in Apple, Twitter, Facebook, Google, Microsoft, Sarepta, 10x Genomics, Amazon, Biogen, CVS, Illumina, Snap, and Sutro; and has received honoraria and travel reimbursement for invited talks from Genentech, Roche, Pfizer, Optum, AbbVie, and many academic institutions and health systems.); **C Caldas** (C.C. has served on the Scientific Advisory Board of Illumina.); **Lorraine Chantrill** (L.C. acted on an advisory board for AMGEN Australia in the last 2 years.); **Andrew D Cherniack** (A.D.C. receives research funding from Bayer AG.); **Helen Davies** (Helen Davies is an inventor on a number of patent filings encompassing the use of mutational signatures); **Francisco De La Vega** (Employment at Annai Systems Inc. during part of the project.); **Ronny Drapkin** (R.D. serves on the SAB of Repare Therapeutics and Siamab Therapeutics.); **Rosalind Eeles** (GU-ASCO meeting in San Francisco – Jan 2016 – Honorarium as speaker \$500. 2. RMH FR meeting – Nov 2017 – support from Janssen, honorarium as speaker £1100 (Title: Genetics and Prostate Cancer). 3. University of Chicago invited talk May 2018 – Honorarium as speaker \$1000. 4. EUR 200 educational honorarium paid by Bayer & Ipsen to attend GU Connect “Treatment sequencing for mCRPC patients within the changing landscape of mHSPC” at a venue at ESMO, Barcelona, 28 September 2019.); **Paul Flicek** (Member of the Scientific Advisory Boards of Fabric Genomics, Inc., and Eagle Genomics, Ltd.); **Gad Getz** (G.G. receives research funds from IBM and Pharmacyclics and is an inventor on patent applications related to MuTect, ABSOLUTE, MutSig, MSMuTect, MSMutSig and POLYSOLVER); **Ronald Ghossein** (veracyte, inc); **D Glodzik** (D.G. is an inventor on a number of patent filings encompassing the use of mutational signatures.); **Eoghan Harrington** (Eoghan Harrington is a full-time employee of Oxford Nanopore Technologies Inc. and is a stock option holder); **Yann Joly** (Responsible for the Data Access Compliance Office (DACO) of ICGC 2009-2018.); **Sissel Juul** (SJ is a full-time employee of Oxford Nanopore Technologies Inc. and is a stock option holder); **Vincent Khoo** (VK has received personal fees and non-financial support from Accuray, Astellas, Bayer, Boston Scientific, and Janssen.); **Stian Knappskog** (co-PI on clinical trial receiving research funding from AstraZeneca and Pfizer); **Ignaty Leshchiner** (Consulting-PACT Pharma); **Yong-Jie Lu** (CA16672 and R50CA221675); **Carlos López-Otín** (CLO has ownership interest (including stock, patents, etc.) from DREAMgenics); **Matthew Meyerson** (Scientific advisory board chair of, and consultant for, OrigamiMed. Research funding from Bayer and Ono Pharma. Patent royalties from LabCorp.); **Serena Nik-Zainal** (S. N.-Z. is an inventor on a number of patent filings encompassing the use of mutational signatures.); **Nathan Pennell** (N.P. has done consulting work with Merck, Astrazeneca, Eli Lilly, and BMS.); **Xose Puente** (XSP has ownership interest (including stock, patents, etc.) from DREAMgenics); **Benjamin Raphael** (BJR is a consultant at and has ownership interest (including stock, patents, etc.) in Medley Genomics.); **Jorge Reis-Filho** (Consultant of Goldman Sachs and REPARE Therapeutics; member of the scientific advisory board of Volition RX and Paige.AI; ad hoc member of the scientific advisory board of Ventana Medical Systems, Roche Tissue Diagnostics, InVivo, Roche, Genentech and Novartis); **Lewis Roberts** (LRR has received grant support from ARIAD Pharmaceuticals, Bayer, BTG International, Exact Sciences, Gilead Sciences, Glycotest, Inc., RedHill Biopharma, Inc., Target PharmaSolutions, and Wako Diagnostics; he has provided advisory services to Bayer, Exact Sciences, Gilead Sciences, GRAIL, Inc., QED Therapeutics and TAVEC Pharmaceuticals Inc.); **Richard Scolyer** (Richard A. Scolyer reports receiving fees for professional services from Merck Sharp & Dohme, GlaxoSmithKline Australia, Bristol-Myers

and spread of a somatic clone. To achieve this behaviour, the cancer clone must co-opt multiple cellular pathways that enable it to disregard the normal constraints on cell growth, to modify the local microenvironment favouring its own proliferation, to invade through tissue barriers, to spread to other organs, and to evade immune surveillance²¹. No single cellular programme directs these behaviours. Rather, there is a large pool of potential pathogenic abnormalities from which individual cancers draw their own combinations: the commonalities of macroscopic features across tumours belie a vastly heterogeneous landscape of cellular abnormalities.

This heterogeneity arises from the stochastic nature of Darwinian evolution. The preconditions for Darwinian evolution are three: characteristics must vary within a population; this variation must be heritable from parent to offspring; and there must be competition for survival within the population. In the context of somatic cells, heritable variation arises from mutations acquired stochastically throughout life, notwithstanding additional contributions from germline and epigenetic variation. A subset of these mutations alter cellular phenotype, and a small subset of those variants confer an advantage on clones in their competition to escape the tight physiological controls wired into somatic cells. Mutations providing selective advantage to the clone are termed 'driver' mutations, as opposed to selectively neutral 'passenger' mutations.

Initial studies using massively parallel sequencing demonstrated the feasibility of identifying every somatic point mutation, copy number change, and structural variant in a given cancer¹⁻³. In 2008, recognising the opportunity this advance in technology provided, the global cancer genomics community established the International Cancer Genome Consortium (ICGC) with the goal of systematically documenting the somatic mutations driving common tumour types²².

Pan-Cancer Analysis of Whole Genomes

The maturing of whole genome sequencing studies from individual ICGC and TCGA working groups presented the opportunity to undertake a meta-analysis of genomic features across tumour types. To achieve this, the Pan-Cancer Analysis of Whole Genomes (PCAWG) consortium was established. A Technical Working Group implemented informatics analyses, aggregating the raw sequencing data from working groups studying individual tumour types, aligning to the human genome, and delivering a set of high-quality somatic mutation calls for downstream analysis (Extended Figure 1). Given the recent meta-

Squibb, Dermepedia, Novartis Pharmaceuticals Australia Pty Ltd, Myriad, NeraCare GmbH and Amgen); **Tal Shmaya** (Employment at Annai Systems, Inc.); **Reiner Siebert** (Speakers Honorary Roche, AstraZeneca); **Sabina Signoretti** (Consulting: Bristol-Myers Squibb, AstraZeneca, Merck, AACR, NCI. Funding: Bristol-Myers Squibb, AstraZeneca, Exelixis. Royalties: Biogenex.); **Jared Simpson** (Research funding and travel support from Oxford Nanopore Technologies); **Anil K Sood** (Consulting – Merck, Kiyatec); Research funding (M-Trap); Shareholder (BioPath)); **Simon Tavaré** (I am on the SAB of Ipsen, and a consultant for Kallyope Inc.); **John Thompson** (J.F.T. has received honoraria and travel support for attending advisory board meetings of GlaxoSmithKline and Provectus Inc. He has received honoraria for participation in advisory boards for MSD Australia and BMS Australia.); **Daniel Turner** (DT is a full-time employee of Oxford Nanopore Technologies Ltd. and is a stock option holder); **Naveen Vasudev** (Speaker honoraria and/or consultancy fees from Bristol Myers Squibb, Pfizer, EUSA pharma, MSD, Novartis); **Jeremiah Wala** (J.A.W. is a consultant for Nference Inc.); **Daniel Weisenberger** (D.J.W. is a consultant for Zymo Research Corporation.); **Dai-Ying Wu** (Employment at Annai Systems, Inc.); **Cheng-Zhong Zhang** (C.-Z.Z. is a co-founder and equity holder of Pillar Biosciences, a for-profit company specializing in the development of targeted sequencing assays.)

analysis of exome data from the TCGA Pan-Cancer Atlas^{23–25}, scientific working groups concentrated their efforts on analyses best informed by whole genome sequencing data.

We collected genome data from 2,834 donors (Extended Table 1), of which 176 were excluded after quality assurance. A further 75 had minor issues that could impact some analyses (grey-listed donors), and 2,583 had data of optimal quality (white-listed donors; Supplementary Table 1). Across the 2,658 white- and grey-listed donors, whole genome sequencing data were available from 2,605 primary tumours and 173 metastases or local recurrences. Mean read coverage was 39x for normal samples, while tumours had a bimodal coverage distribution with modes at 38x and 60x (Supplementary Figure 1). RNA-sequencing data was available for 1,222 donors. The final cohort comprised 1,469 males (55%) and 1,189 females (45%), with a mean age of 56 years (range, 1-90 years) across 38 tumour types (Extended Table 1; Supplementary Table 1).

In order to identify somatic mutations, we analysed all 6,835 samples using a uniform set of algorithms for alignment, variant calling and quality control (Extended Figure 1; Supplementary Figure 2; Supplementary Methods S2). We deployed three established pipelines to call somatic single nucleotide variations (SNVs), small insertions and deletions (indels), copy number alterations (CNAs), and structural variants (SVs). Somatic retrotransposition events, mitochondrial DNA mutations and telomere lengths were also called by bespoke algorithms. RNA-Sequencing data were uniformly processed to call transcriptomic alterations. Germline variants identified via three separate pipelines included single nucleotide polymorphisms (SNPs), indels, structural variants and mobile element insertions (Supplementary Table 2).

The requirement to uniformly realign and call variants on ~5,800 whole genomes presented significant computational challenges, and raised ethical issues due to the use of data from different jurisdictions (Box 1). We used cloud computing^{26,27} to distribute alignment and variant calling across 13 data centres in three continents (Supplementary Table 3). Core pipelines were packaged into Docker containers²⁸ as reproducible, stand-alone packages, which we have made available for download. Data repositories for raw and derived datasets, together with portals for data visualisation and exploration have also been created (Box 1; Supplementary Table 4).

Benchmarking of genetic variant calls

To benchmark mutation calling, we ran the three core pipelines, together with 10 additional pipelines, on 63 representative tumour/normal genome pairs (Supplementary Note 1). For 50 of these cases, we performed validation by hybridisation of tumour and matched normal DNA to a custom bait-set with deep sequencing²⁹. The three core somatic variant-calling pipelines had individual estimates of sensitivity of 80-90% to detect a true somatic SNV called by any of the 13 pipelines; with >95% of SNV calls made by each of the core pipelines being genuine somatic variants (Figure 1A). For indels, a more challenging class of variants to identify with short-read sequencing, the three core algorithms had individual sensitivity estimates in the range 40-50%, with precision 70-95% (Figure 1B). For individual

SV callers, we estimated precision to be in the range 80-95% for samples in the pilot-63 dataset.

Next, we defined a strategy to merge results from the three pipelines into one final call-set to be used for downstream scientific analyses (Methods, Supplementary Note 2). Sensitivity and precision of consensus somatic variant calls were 95% ($CI_{90\%}=88-98\%$) and 95% ($CI_{90\%}=71-99\%$) respectively for SNVs (Extended Figure 2). For somatic indels, sensitivity and precision were 60% (34-72%) and 91% (73-96%) respectively (Extended Figure 2). Regarding somatic SVs, we estimate the sensitivity of merged calls to be 90% for true calls generated by any one caller; precision was estimated as 97.5%. The improvement in calling accuracy from combining different callers was most noticeable in variants having low variant allele fractions, which likely originate in tumour subclones (Figure 1C-D). Germline variant calls, phased using a haplotype-reference panel, displayed a precision >99% and sensitivity of 92%-98% (Supplementary Note 2).

Analysis of PCAWG data

The uniformly generated, high quality set of variant calls across >2,500 donors provided the springboard for a series of scientific working groups to explore the biology of cancer. A comprehensive suite of companion papers detailing the analyses and discoveries across these thematic areas is co-published with this paper (Extended Table 3).

Pan-cancer burden of somatic mutations

Across the 2,583 white-listed PCAWG donors, we called 43,778,859 somatic SNVs; 410,123 somatic multi-nucleotide variants; 2,418,247 somatic indels; 288,416 somatic structural variants; 19,166 somatic retrotransposition events; and 8,185 *de novo* mitochondrial DNA mutations (Supplementary Table 1). There was considerable heterogeneity in the burden of somatic mutations across patients and tumour types, with a broad correlation in mutation burden among different classes of somatic variation (Extended Figure 3). Analysed at a per-patient level, this correlation held, even when considering tumours with similar purity and ploidy (Supplementary Figure 3). Why such correlation should apply on a pan-cancer basis is unclear. It is likely that age plays some role, as we observe a correlation of most classes of somatic mutation with age at diagnosis (~190 SNVs/year, $p=0.02$; ~22 indels/year, $p=5\times 10^{-5}$; 1.5 SVs/year, $p<2\times 10^{-16}$; linear regression with likelihood ratio tests; Supplementary Figure 4). Other factors are also likely to contribute to the correlations among classes of somatic mutation, since there is evidence that some DNA repair defects can cause multiple types of somatic mutation³⁰, and a single carcinogen can cause a range of DNA lesions³¹.

Panorama of driver mutations in cancer

We extracted the subset of somatic mutations in PCAWG tumours that have high confidence to be driver events, based on current knowledge. One challenge to pinpointing the specific driver mutations in an individual tumour is that not all point mutations in recurrently mutated cancer genes are drivers³². For genomic elements significantly mutated in the

PCAWG, we developed a ‘*rank-and-cut*’ approach to identify the likely drivers (Supplementary Methods 8.1). This works by *ranking* the observed mutations in a given genomic element based on recurrence, estimated functional consequence, and expected pattern of drivers in that element. We then estimate the excess burden of somatic mutations in that genomic element above that expected for the background mutation rate, and *cut* the ranked mutations at this level. Mutations in that element with the highest driver ranking will then be assigned as likely drivers; those below the threshold will probably have arisen through chance, and be assigned as likely passengers. Improvements to features employed to rank the mutations and the methods used to measure them will contribute to further maturation of the rank-and-cut approach.

We also needed to account for the fact that some *bona fide* cancer genomic elements were not rediscovered in PCAWG data because of low statistical power. We therefore added previously known cancer genes to the discovery set, creating a ‘Compendium of Mutational Driver Elements’ (Supplementary Methods 8.2). Then, using stringent rules to nominate driver point mutations affecting these genomic elements on the basis of prior knowledge³³, we separated likely driver from passenger point mutations. To cover all classes of variant, we also created a compendium of known driver SVs, using analogous rules to identify which somatic CNAs and SVs most likely act as drivers in each tumour. For likely pathogenic germline variants, we identified all truncating germline point mutations and SVs affecting high-penetrance germline cancer genes.

This analysis defined a set of mutations that we could confidently assert, based on current knowledge, drove tumorigenesis in the >2,500 tumours of PCAWG. We found that 91% of tumours had at least one identified driver mutation, with an average of 4.6 drivers per tumour identified, showing extensive variation across cancer types (Figure 2A). For coding point mutations, the average was 2.6 drivers per tumour, similar to numbers estimated in known cancer genes in TCGA tumours using similar approaches³².

To address the frequency of non-coding driver point mutations, we combined promoters and enhancers that are known targets of non-coding drivers^{34–37} with those newly discovered on PCAWG data, reported in a companion paper⁴. Using this approach, only 13% (785/5913) of driver point mutations were non-coding in PCAWG. Nonetheless, 25% of PCAWG tumours bear at least one putative non-coding driver point mutation, with one third (237/785) affecting the *TERT* promoter (9% of PCAWG tumours). Overall, then, non-coding driver point mutations are less frequent than coding drivers. With the exception of the *TERT* promoter, individual enhancers and promoters are only infrequent targets of driver mutations⁴.

Across tumour types, SVs and point mutations make different relative contribution to tumorigenesis. Driver SVs are more prevalent in breast adenocarcinomas (6.4±3.7 SVs vs. 2.2±1.3 point mutations on average±SD; $p < 10^{-16}$, Mann-Whitney U test) and ovary adenocarcinomas (5.8±2.6 SVs vs. 1.9±1.0 point mutations; $p < 10^{-16}$), while driver point mutations make a larger contribution in colorectal adenocarcinomas (2.4±1.4 SVs vs. 7.4±7.0 point mutations; $p = 4 \times 10^{-10}$) and mature B-cell lymphomas (2.2±1.3 SVs vs. 6±3.8

point mutations; $p < 10^{-16}$), as shown previously³⁸. Across tumour types, there are differences in which classes of mutation affect a given genomic element (Figure 2B).

We confirmed that many driver mutations affecting tumour suppressor genes are two-hit inactivation events (Figure 2C). For example, of the 954 tumours in the cohort with driver mutations in *TP53*, 736 (77%) had both alleles mutated, 96% of which (707/736) combined a somatic point mutation affecting one allele with somatic deletion of the other allele. Overall, 17% of patients harboured rare germline protein-truncating variants (PTVs) in cancer predisposition genes³⁹, DNA damage response genes⁴⁰ and somatic driver genes. Biallelic inactivation due to somatic alteration on top of a germline PTV was observed in 4.5% of patients overall, with 81% of these affecting known cancer predisposition genes (such as *BRCA1*, *BRCA2* and *ATM*).

PCAWG tumours with no apparent drivers

Although >90% PCAWG cases had identified drivers, we found none in 181 tumours (Extended Figure 4A). Reasons for missing drivers have not yet been systematically evaluated in a pan-cancer cohort, and could arise from either technical or biological causes.

Technical explanations could include poor quality samples; inadequate sequencing; or failures in the bioinformatic algorithms deployed. Assessing the quality of samples, four of the 181 ‘missed-driver’ cases had >5% tumour DNA contamination in their matched normal (Figure 3A). Using an algorithm designed to correct for this contamination⁴¹, we identified previously missed mutations in genes relevant to the respective cancer types. Similarly, if the fraction of tumour cells in the cancer sample is low through stromal contamination, detection of driver mutations can be impaired. Most missed-driver tumours had an average power to detect mutations close to 100%, but a few had power in the 70-90% range (Figure 3B; Extended Figure 4B). Even in adequately sequenced genomes, lack of read depth at specific driver loci can impair mutation detection. For example, only ~50% of PCAWG tumours had sufficient coverage to call a mutation (90% power) at the two *TERT* promoter hotspots, likely because of the region’s high GC-content causing biased coverage (Figure 3C). In fact, six Liver-HCC and two Biliary-AdenoCa tumours among the 181 missed-driver cases actually did carry *TERT* mutations upon deep targeted sequencing⁴².

Finally, technical reasons for missing driver mutations include failures in the bioinformatic algorithms. This affected 35 myeloproliferative neoplasms in PCAWG, where the *JAK2*^{V617F} driver mutation should have been called. Our somatic variant-calling algorithms rely on ‘panels of normals’, typically from blood samples, to remove recurrent sequencing artefacts. Since 2-5% healthy individuals carry occult haematopoietic clones⁴³, recurrent driver mutations in these clones can enter panels of normals.

Turning to biological causes, tumours may be driven by mutations in cancer genes not yet discovered in that tumour type. Using driver discovery algorithms on missed-driver tumours, no individual genes reached significance for point mutations. However, we identified a recurrent CNA spanning *SETD2* in medulloblastomas lacking known drivers (Figure 3D), indicating that restricting hypothesis-testing to missed-driver cases can improve power if

undiscovered genes are enriched in such tumours. Inactivation of *SETD2* in medulloblastoma significantly decreased gene expression ($p=0.002$; Extended Figure 4C). Interestingly, *SETD2* mutations occurred exclusively in medulloblastoma group 4 tumours ($p<1\times 10^{-4}$). Group 4 medulloblastomas are known for frequent mutations in other chromatin-modifying genes⁴⁴, and our results suggest that *SETD2* loss-of-function is an additional driver affecting chromatin regulators in this subgroup.

Two tumour types had a surprisingly high fraction of patients without identified driver mutations: chromophobe renal cell carcinoma (44%; 19/43) and pancreatic neuroendocrine cancers (22%; 18/81) (Extended Data Figure 4A). A striking feature of the missed-driver cases in both tumour types was a remarkably consistent profile of chromosomal aneuploidy, patterns that have been reported previously^{45,46} (Figure 3E). The absence of other identified driver mutations in these patients raises the intriguing hypothesis that certain combinations of whole chromosome gains and losses may be sufficient to initiate a cancer in the absence of more targeted driver events such as point mutations, fusion genes or focal CNAs.

Even after accounting for technical issues and novel drivers, 5.3% of PCAWG tumours still had no identifiable driver events. In a research setting, where we are interested in drawing conclusions about populations of patients, the consequences of technical issues affecting occasional samples will be mitigated by sample size. In a clinical setting, where we are interested in the driver mutations in a specific patient, these issues become substantially more important. Careful and critical appraisal of the whole pipeline, including sample acquisition, genome sequencing, mapping, variant calling, and driver annotation, as done here, should be required for laboratories offering clinical sequencing of cancer genomes.

Patterns of clustered mutations and SVs

Some mutational processes generate multiple mutations in a single catastrophic event, typically clustered in genomic space, leading to substantial reconfiguration of the genome. Three such processes have been described: (i) chromoplexy, in which repair of co-occurring dsDNA breaks, typically on different chromosomes, results in shuffled chains of rearrangements^{47,48} (example in Extended Figure 5A); (ii) kataegis, a focal hypermutation process leading to locally clustered nucleotide substitutions, biased towards a single DNA strand^{49–51} (Extended Figure 5B); and (iii) chromothripsis, in which tens to hundreds of DNA breakages occur simultaneously, clustered on one or a few chromosomes, with near-random stitching together of the resulting fragments^{52–55} (Extended Figure 5C). We characterised the PCAWG genomes for these three processes (Figure 4).

Chromoplexy events and reciprocal translocations were identified in 467 (17.8%) samples (Figure 4A,C). Chromoplexy was prominent in prostate adenocarcinoma and lymphoid malignancies, as described previously^{47,48}, and, unexpectedly, thyroid adenocarcinoma. Different genomic loci were recurrently rearranged by chromoplexy across the three tumour types, mediated by positive selection for particular fusion genes or enhancer-hijacking events. Of 13 fusion genes or enhancer hijacking events in 48 thyroid adenocarcinomas, at least 4 (31%) were caused by chromoplexy, with a further 4 (31%) part of complexes containing chromoplexy footprints (Extended Figure 5A). These generated fusion genes

involving *RET* (2 cases) and *NTRK3* (1 case)⁵⁶, and juxtaposition of the oncogene *IGF2BP3* with regulatory elements from highly expressed genes (5 cases).

Kataegis events were seen in 60.5% of all cancers, with particularly high abundance in lung squamous cell carcinoma, bladder cancer, acral melanoma and sarcomas (Figure 4A,B). Typically, kataegis comprises C>N mutations in TpC context, likely due to APOBEC activity^{49–51}, although a T>N at TpT or CpT process attributed to error-prone polymerases has recently been described⁵⁷. The APOBEC signature accounted for 81.7% of kataegis events and correlated positively with *APOBEC3B* expression levels, somatic SV burden and age at diagnosis (Supplementary Figure 5). 5.7% of kataegis events involved the T>N error-prone polymerase signature and 2.3% of events, most notably in sarcomas, showed cytidine deamination in an alternative GpC or CpC context.

Kataegis events were frequently associated with somatic SV breakpoints (Figure 4A, Supplementary Figure 6A), as previously described^{50,51}. Deletions and complex rearrangements were most strongly associated with kataegis, while tandem duplications and other simple SV classes were only infrequently associated (Supplementary Figure 6B). The C[T>N]T-type kataegis was enriched near deletions, specifically those in the 10-25kbp range (Supplementary Figure 6C).

Samples with extreme kataegis burden (>30 foci) comprise four types of focal hypermutation (Extended Figure 6): (i) off-target somatic hypermutation and C[T>N]T foci in B-cell non-Hodgkin lymphoma and oesophageal adenocarcinomas, respectively; (ii) APOBEC kataegis associated with complex rearrangements, notably in sarcoma and melanoma; (iii) rearrangement-independent APOBEC kataegis on the lagging strand and in early-replicating regions, mainly in bladder and head and neck cancer; (iv) a mix of the previous two types. Kataegis only occasionally led to driver mutations (Supplementary Table 5).

We identified *chromothripsis* in 587 samples (22.3%), most frequently amongst sarcoma, glioblastoma, lung squamous cell carcinoma, melanoma, and breast adenocarcinoma⁵⁸. Chromothripsis increased with whole genome duplications in most cancer types (Extended Figure 7A), as previously shown in medulloblastoma⁵⁹. The most recurrently associated driver was *TP53*⁵² (pan-cancer odds ratio=3.22; pan-cancer p=8.3x10⁻³⁵; q<0.05 in breast lobular (OR=13), colorectal (OR=25), prostate (OR=2.6) and hepatocellular cancers (OR=3.9); Fisher-Boschloo tests). In two cancer types (osteosarcoma and B-cell lymphoma), females showed higher incidence of chromothripsis than males (Extended Figure 7B). In prostate cancer, we observed a higher incidence of chromothripsis in patients with late-onset than early-onset disease⁶⁰ (Extended Figure 7C).

Chromothripsis regions coincided with 3.6% of all identified drivers in PCAWG and ~7% of copy number drivers (Figure 4D). These proportions are considerably enriched compared to expectation if selection were not acting on these events (Extended Figure 7D). The majority of coinciding driver events were amplifications (58%), followed by homozygous deletions (34%), and SVs within genes or promoter regions (8%). We frequently observed 2-fold increased or decreased expression of amplified or deleted drivers, respectively, when these

loci were part of a chromothripsis event, compared to samples without chromothripsis (Extended Figure 7E).

Chromothripsis manifested in diverse patterns and frequencies across tumour types, which we categorised based on five characteristics (Figure 4A). In liposarcoma for example, chromothripsis events often involved multiple chromosomes, with universal *MDM2* amplification⁶¹ and co-amplification of *TERT* in 4 of 19 cases (Figure 4D). In contrast, in glioblastoma, the events tended to affect a smaller region on a single chromosome, distant from the telomere, resulting in focal *EGFR* and *MDM2* amplification, and *CDKN2A* loss. Acral melanomas frequently exhibited *CCND1* amplification, and lung squamous cell carcinomas *SOX2* amplifications. In both cases, these drivers were more frequently altered by chromothripsis compared to other drivers in the same cancer type, and to other cancer types for the same driver (Figure 4D, Extended Figure 7F). Finally, in chromophobe renal cell carcinoma, chromothripsis nearly always affected chromosome 5 (Supplementary Figure 7): these samples had breakpoints immediately adjacent to *TERT*, increasing *TERT* expression 80-fold on average over samples without rearrangements ($p=0.0004$; Mann-Whitney U test).

Timing clustered mutations in evolution

An unanswered question for clustered mutational processes is whether they occur early or late in cancer evolution. To address this, we used molecular clocks to define broad epochs in each tumour's life history^{49,62}. One transition point is between clonal and subclonal mutations: clonal mutations occurred before, and subclonal mutations after, emergence of the most recent common ancestor. In regions with copy number gains, molecular time can be further divided according to whether mutations preceded the copy number gain (and were themselves duplicated) or occurred after the gain (and therefore present on only one chromosomal copy)⁶³.

Chromothripsis tended to have greater relative odds of being clonal than subclonal, suggesting it occurs early in cancer evolution, especially in liposarcomas, prostate adenocarcinoma and squamous cell lung cancer, among others (Figure 5A). As previously reported, chromothripsis was especially common in melanomas⁶⁴. We identified 89 separate chromothripsis events affecting 66 melanomas (61%), with 47/89 events affecting genes known to be recurrently altered in melanoma⁶⁵ (Supplementary Table 6). Involvement of a region on chromosome 11 that includes the cell-cycle regulator *CCND1* occurred in 21 cases (10/86 cutaneous, 11/21 acral or mucosal melanomas), typically combining chromothripsis with amplification (19/21 cases; Extended Figure 8). Co-involvement of other cancer genes in the same chromothripsis event was also frequent, including *TERT* (5 cases), *CDKN2A* (3 cases), *TP53* (2 cases) and *MYC* (2 cases) (Figure 5B). In these co-amplifications, a chromothripsis event involving multiple chromosomes initiated the process, creating a derivative chromosome in which hundreds of fragments were stitched together in near-random order (Figure 5B). This derivative then rearranged further, leading to massive co-amplification of the multiple target oncogenes together with regions located nearby on the derivative chromosome.

In these cases of amplified chromothripsis, we can use the inferred number of copies bearing each SNV to time the amplification process. SNVs present on the chromosome before amplification will themselves be amplified, and therefore reported in a high fraction of sequence reads (Figure 5B; Extended Figure 8). In contrast, late SNVs that occur after the amplification has concluded, will be present on only one chromosome copy out of many, and thus have low variant allele fraction. Regions of *CCND1* amplification had few, sometimes zero, mutations at high variant allele fraction in acral melanomas, contrasting with later *CCND1* amplifications in cutaneous melanomas (Figure 5B; Extended Figure 9A,B). Thus, both chromothripsis and the subsequent amplification generally occurred very early during the evolution of acral melanoma. By comparison, in lung squamous cell carcinomas, similar patterns of chromothripsis followed by *SOX2* amplification are characterised by many amplified SNVs, suggesting a later event in the evolution of these cancers (Extended Figure 9C).

Interestingly, in cancer types where mutational load was sufficiently high, we could detect a larger than expected number of SNVs on an intermediate number of DNA copies, suggesting that they appeared during the amplification process (Supplementary Figure 8).

Germline effects on somatic mutations

We integrated the set of 88 million germline genetic variant calls with somatic mutations in PCAWG, to study germline determinants of somatic mutation rates and patterns. First, we performed a genome-wide association study (GWAS) of somatic mutational processes with common germline variants (minor allele frequency (MAF) >5%) in individuals with inferred European ancestry. An independent GWAS was performed in East Asian individuals from Asian cancer genome projects. We focused on two prevalent endogenous mutational processes: spontaneous deamination of 5methyl-C at CpG dinucleotides⁶⁶ (signature 1) and activity of the APOBEC3 family of cytidine deaminases⁶⁷ (signatures 2 and 13). No locus reached genome-wide significance ($p < 5 \times 10^{-8}$) for signature 1 (Extended Figure 10A,B). However, a locus at 22q13.1 predicted APOBEC3B-like mutagenesis at the pan-cancer level⁶⁸ (Figure 6A). The strongest signal at 22q13.1 was driven by rs12628403, and the minor (non-reference) allele was protective against APOBEC3B-like mutagenesis ($\beta = -0.43$, $p = 5.6 \times 10^{-9}$, MAF=8.2%, $n = 1,201$ donors; Extended Figure 10C). This variant tags a common ~30kb germline SV that deletes the *APOBEC3B* coding sequence and fuses the *APOBEC3B* 3'-UTR with the coding sequence of *APOBEC3A*. The deletion is known to increase breast cancer risk and APOBEC mutagenesis in breast cancer genomes^{69,70}. Here, we found that rs12628403 reduces APOBEC3B-like mutagenesis specifically in cancer types with low levels of APOBEC mutagenesis ($\beta_{\text{low}} = -0.50$, $p_{\text{low}} = 1 \times 10^{-8}$; $\beta_{\text{high}} = +0.17$, $p_{\text{high}} = 0.2$), and increases APOBEC3A-like mutagenesis in cancer types with high levels of APOBEC mutagenesis ($\beta_{\text{high}} = +0.44$, $p_{\text{high}} = 8 \times 10^{-4}$; $\beta_{\text{low}} = -0.21$, $p_{\text{low}} = 0.02$). Moreover, we identified a second, novel locus at 22q13.1 that associated with APOBEC3B-like mutagenesis across cancer types (rs2142833, $\beta = +0.23$, $p = 1.3 \times 10^{-8}$). We independently validated the association between both loci and APOBEC3B-like mutagenesis using East Asian individuals from Asian cancer genome projects ($\beta_{\text{rs12628403}} = +0.57$, $p_{\text{rs12628403}} = 4.2 \times 10^{-12}$; $\beta_{\text{rs2142833}} = +0.58$, $p_{\text{rs2142833}} = 8 \times 10^{-15}$; Extended Figure 10D). Of note, in a conditional analysis that accounted for rs12628403, rs2142833 and rs12628403

are inherited independently in Europeans ($r^2 < 0.1$), while rs2142833 remained significantly associated with APOBEC3B-like mutagenesis in Europeans ($\beta_{\text{EUR}} = +0.17$, $p_{\text{EUR}} = 3 \times 10^{-5}$) and East Asians ($\beta_{\text{ASN}} = +0.25$, $p_{\text{ASN}} = 2 \times 10^{-3}$) (Extended Figure 10E,F). Analysis of donor-matched expression data further suggests that rs2142833 is a *cis*-eQTL for *APOBEC3B* at the pan-cancer level ($\beta = +0.19$, $p = 2 \times 10^{-6}$; Extended Figure 10G-H), consistent with *cis*-eQTL studies in normal cells^{71,72}.

Second, we performed a rare variant association study (RVAS) (MAF < 0.5%) to investigate the relationship between germline protein-truncating variants (PTVs) and somatic DNA rearrangements in individuals with European ancestry (Extended Figure 11A-C). Germline *BRCA2* and *BRCA1* PTVs associated with an increased burden of small (<10kb) somatic SV deletions ($p = 1 \times 10^{-8}$) and tandem duplications ($p = 6 \times 10^{-13}$), respectively, corroborating recent studies in breast and ovarian cancer^{30,73}. In PCAWG data, this pattern extends to other tumour types as well, including adenocarcinomas of the prostate and pancreas⁶, typically in the setting of biallelic inactivation. In addition, tumours with high levels of small SV tandem duplications frequently exhibited a novel and distinct class of SVs termed ‘cycles of templated insertions’⁶. These complex SV events consist of DNA templates that are copied from across the genome, joined into one contiguous sequence, and inserted into a single derivative chromosome. We found a significant association between germline *BRCA1* PTVs and templated insertions at the pan-cancer level ($p = 4 \times 10^{-15}$; Extended Figure 11D,E). Whole genome long-read sequencing data generated for a *BRCA1*-deficient PCAWG prostate tumour verified the small tandem duplication and templated insertion SV phenotypes (Figure 6B). Virtually all (20/21) of *BRCA1*-associated tumours with a templated insertion SV phenotype displayed combined germline and somatic hits in the gene. Together, these data suggest that biallelic inactivation of *BRCA1* is a driver of the templated insertion SV phenotype.

Third, rare variant association analysis revealed that patients with germline *MBD4* PTVs exhibited increased rates of somatic C>T mutation rates at CpG dinucleotides ($P < 2.5 \times 10^{-6}$; Figure 6C; Extended Figure 11F,G). Analysis of previously published TCGA WES samples ($n = 8,134$) replicated the association between germline *MBD4* PTVs and increased somatic CpG mutagenesis at the pan-cancer level ($P = 7.1 \times 10^{-4}$; Extended Figure 11H). Moreover, gene expression profiling revealed a significant but modest correlation between *MBD4* expression and somatic CpG mutation rates between and within PCAWG tumour types (Extended Figure 11I-K). *MBD4* encodes a DNA repair gene that removes thymidines from T:G mismatches within methylated CpG sites⁷⁴, a suggestive functionality for CpG mutational signatures in cancer.

Fourth, we assessed LINE-1 (L1) elements that mediate somatic retrotransposition events⁷⁵⁻⁷⁷. We identified 114 germline source L1 elements capable of active somatic retrotransposition, including 70 that represent insertions with respect to the human reference genome (Figure 6D, Supplementary Table 7), and 53 that were tagged by SNPs in strong linkage disequilibrium (Supplementary Table 7). Only 16 germline L1 elements accounted for 67% (2,440/3,669) of all L1-mediated transductions¹⁰ detected in the PCAWG dataset (Extended Figure 12A). These 16 hot-L1 elements followed two broad patterns of somatic activity (8 of each), which we term Strombolian and Plinian in analogy to patterns of

volcanic activity. Strombolian L1s are frequently active in cancer, but mediate only small to modest eruptions of somatic L1 activity in cancer samples (Extended Figure 12B). In contrast, Plinian L1s are more rarely seen, but display aggressive somatic activity. Whereas Strombolian elements are typically relatively common (MAF>2%) and sometimes even fixed in the human population, all Plinian elements were infrequent (MAF < 2%) in PCAWG donors (Extended Figure 12C; $p=0.001$; Mann-Whitney U test). This dichotomous pattern of activity and allele frequency may reflect differences in age and selective pressures, with Plinian elements potentially inserted into the human germline more recently. PCAWG donors bear on average between 50-60 L1 source elements and 5-7 elements with hot activity (Extended Figure 12D), but only 38% (1075/2814) of PCAWG donors carry 1 Plinian element. Some L1 germline source loci caused somatic loss of tumour suppressor genes (Extended Figure 12E). Many are restricted to individual continental population ancestries (Extended Figure 12F-J).

Replicative immortality

One of the hallmarks of cancer is its ability to evade cellular senescence²¹. Normal somatic cells typically have finite cell division potential, with telomere attrition one mechanism to limit numbers of mitoses⁷⁸. Cancers enlist multiple strategies to achieve replicative immortality. Over-expression of the telomerase gene, *TERT*, which maintains telomere lengths, is especially prevalent. This can be achieved via point mutations in the promoter that lead to *de novo* transcription factor binding^{34,37}; hitching *TERT* to highly active regulatory elements elsewhere in the genome^{46,79}; insertions of viral enhancers upstream of the gene^{80,81}; and increased dosage through chromosomal amplification, as we have seen in melanoma (Figure 5B). In addition, there is an ‘alternative lengthening of telomeres’ (ALT) pathway, in which telomeres are lengthened through homologous recombination, mediated by loss-of-function mutations in the *ATRX* and *DAXX* genes⁸².

As reported in a companion paper, 16% of tumours in the PCAWG dataset exhibited somatic mutations in at least one of *ATRX*, *DAXX* and *TERT*⁸³. *TERT* alterations were detected in 270 samples, whereas 128 tumours had alterations in *ATRX* or *DAXX*, of which 71 were protein-truncating. In the companion paper, which focused on describing patterns of ALT and *TERT*-mediated telomere maintenance⁸³, twelve features of telomeric sequence were measured on the PCAWG cohort. These included counts of nine variants of the core hexameric sequence, the number of ectopic telomere-like insertions within the genome, the number of genomic breakpoints, and telomere length as a ratio between tumour and normal. Here we used the twelve features to overview telomere integrity across all tumours in the PCAWG dataset.

Based on these twelve features, tumour samples formed four distinct sub-clusters (Figure 7A, Extended Figure 13A), suggesting that telomere maintenance mechanisms are more diverse than the well-established *TERT*/ALT dichotomy. Clusters C1 (47 tumours) and C2 (42 tumours) were enriched for traits of the ALT pathway, having longer telomeres, more genomic breakpoints, more ectopic telomere insertions, and variant telomere sequence motifs (Supplementary Figure 9). C1 and C2 were distinguished from one another by the latter having striking elevation in the number of TTCGGG and TGAGGG variant motifs

among the telomeric hexamers. Thyroid adenocarcinomas were strikingly enriched among C3 samples (26/33 C3 samples; $p < 10^{-16}$); the C1 cluster (ALT subtype 1) was common among sarcomas; and both pancreatic endocrine neoplasms and low-grade gliomas had a high proportion of samples in the C2 cluster (ALT subtype 2) (Figure 7B). Interestingly, some of the thyroid adenocarcinomas and pancreatic neuroendocrine tumours that cluster together (Cluster C3) had matched normals that also cluster together (Normal cluster N3, Extended Figure 13A), and which share common properties. For example, the GTAGGG repeat was overrepresented among samples in this group (Supplementary Figure 10).

Somatic driver mutations were also unevenly distributed across the four clusters (Figure 7C). C1 tumours were enriched for *RB1* mutations or structural variants ($p = 3 \times 10^{-5}$), as well as frequent structural variants affecting *ATRX* ($p = 6 \times 10^{-14}$), but not *DAXX*. *RB1* and *ATRX* mutations were largely mutually exclusive (Extended Figure 13B). In contrast, C2 tumours were enriched for somatic point mutations in *ATRX* and *DAXX* ($p = 6 \times 10^{-5}$), but not *RB1*. The enrichment of *RB1* mutations in C1 remained significant when only leiomyosarcomas and osteosarcomas were considered, confirming that this enrichment is not merely a consequence of the different distribution of tumour types across clusters. C3 samples had frequent *TERT* promoter mutations (30%; $p = 2 \times 10^{-6}$).

The predominance of *RB1* mutations in C1 was striking. Nearly a third of the samples in C1 contained an *RB1* alteration, evenly distributed across truncating SNVs, SVs and shallow deletions (Extended Figure 13C). Previous work has shown that *RB1* mutations are associated with long telomeres in the absence of *TERT* mutations and *ATRX* inactivation⁸⁴, and mouse models have revealed that knock-out of Rb-family proteins causes elongated telomeres⁸⁵. The association with the C1 cluster here suggests that *RB1* mutations can represent another route to activating the ALT pathway, with subtly different properties of telomeric sequence compared to inactivating *DAXX*, which fall almost exclusively in cluster C2.

Tumour types with the highest rates of abnormal telomere maintenance mechanisms often originate in tissues that have low endogenous replicative activity (Figure 7D). In support of this, we found an inverse correlation between previously estimated rates of stem cell division across tissues⁸⁶ and the frequency of telomere maintenance abnormalities ($p = 0.01$, Poisson regression; Extended Figure 13D). This suggests that restriction of telomere maintenance is a critical tumour suppression mechanism, particularly in tissues with low steady-state cellular proliferation, in which a clone must overcome this constraint to achieve replicative immortality.

Conclusions and future perspectives

The resource reported in this paper and its companion papers has yielded insights into the nature and timing of the many mutational processes that shape large and small-scale somatic variation in the cancer genome; the patterns of selection acting on these variations; the widespread impact of somatic variants on transcription; the complementary roles of coding and non-coding genome, for both germline and somatic mutations; the ubiquity of intratumoral heterogeneity; and the distinctive evolutionary trajectory of each cancer type.

Many of these insights can only be obtained from an integrated analysis of all classes of somatic mutation on a whole genome scale, and would not be accessible with, for example, targeted exome sequencing.

The promise of precision medicine is to match patients to targeted therapies using genomics. A major barrier to its evidence-based implementation is the daunting heterogeneity of cancer chronicled in these pages, from tumour type to tumour type, from patient to patient, from clone to clone and from cell to cell. Building meaningful clinical predictors from genomic data can be achieved, but will require knowledge banks comprising tens of thousands of patients with comprehensive clinical characterisation⁸⁷. Since these sample sizes will be too large for any single funding agency, pharmaceutical company or health system, international collaboration and data sharing will be required. The next phase of ICGC, ICGC-ARGO (<https://icgc-argo.org/>), will bring the cancer genomics community together with healthcare providers, pharma, data science and clinical trials groups to build comprehensive knowledge banks of clinical outcome and treatment data from patients with a wide variety of cancers, matched with detailed molecular profiling.

Extending the story begun by TCGA, ICGC and other cancer genomics projects, PCAWG has brought us closer to a comprehensive narrative of the causal biological changes that drive cancer phenotypes. We must now translate this knowledge into sustainable, meaningful clinical impacts.

Methods

Samples

We compiled an inventory of matched tumour/normal whole cancer genomes in the ICGC Data Coordinating Centre. Most samples came from treatment-naïve, primary cancers, but there were a small number of donors with multiple samples of primary, metastatic and/or recurrent tumours. Our inclusion criteria were: (i) matched tumour and normal specimen pair; (ii) a minimal set of clinical fields; and (iii) characterisation of tumour and normal whole genomes using Illumina HiSeq paired-end sequencing reads.

We collected genome data from 2,834 donors, representing all ICGC and TCGA donors that met these criteria at the time of the final data freeze in autumn 2014 (Extended Table 1). After quality assurance (Supplementary Methods S2.5), data from 176 donors were excluded as unusable, 75 had minor issues that could impact some analyses (grey-listed donors), and 2,583 had data of optimal quality (white-listed donors; Supplementary Table 1). Across the 2,658 white- and grey-listed donors, there were whole genome sequences from 2,605 primary tumours and 173 metastases or local recurrences. Matching normal samples were obtained from blood (2,064 donors), tissue adjacent to the primary (87 donors), or distant sites (507 donors). Whole genome sequencing data were available on tumour and normal DNA for the entire cohort. The mean read coverage was 39x for normal samples, while tumours had a bimodal coverage distribution with modes at 38x and 60x (Supplementary Figure 1). The majority of specimens (65.3%) were sequenced using 101 bp paired-end reads. An additional 28% were sequenced with 100 bp paired-end reads. Of the remaining specimens, 4.7% were sequenced with read lengths longer than 101 bp, and 1.9% with read

lengths shorter than 100 bp. The distribution of read lengths by tumour cohort is shown in Supplementary Figure 11. Median read length for WGS paired end reads was 101 bp (mean=106.2, SD=16.7; min-max=50-151). RNA-sequencing data was collected and re-analysed centrally for 1,222 donors, including 1,178 primary tumours, 67 metastases or local recurrences, and 153 matched normal tissue samples adjacent to the primary tumour.

Demographically, the cohort included 1,469 males (55%) and 1,189 females (45%), with a mean age of 56 years (range, 1-90 years) (Supplementary Table 1). Using population ancestry-differentiated single nucleotide polymorphisms (SNPs), the ancestry distribution was heavily weighted towards donors of European descent (77% of total) followed by East Asians (16%), as expected for large contributions from European, North American and Australian projects (Supplementary Table 1).

We consolidated histopathology descriptions of the tumour samples, using the ICD-0-3 tumour site controlled vocabulary⁹³. Overall, the PCAWG data set comprises 38 distinct tumour types (Extended Table 1; Supplementary Table 1). While the most common tumour types are included in the dataset, their distribution does not match the relative population incidences, largely due to differences among contributing ICGC/TCGA groups in numbers sequenced.

Uniform processing and somatic variant calling

In order to generate a consistent set of somatic mutation calls that could be used for cross-tumour analyses, we analysed all 6,835 samples using a uniform set of algorithms for alignment, variant calling, and quality control (Extended Figure 1; Supplementary Figure 2; Supplementary Table 3; Supplementary Methods S2). We used the BWA-MEM algorithm⁹⁴ to align each tumour and normal sample to human reference build hs37d5 (as used in the 1000 Genomes Project⁹⁵). Somatic mutations were identified in the aligned data using three established pipelines, run independently on each tumour/normal pair. Each of the three pipelines, labelled “Sanger”^{96–99}, “EMBL/DKFZ”^{100,101} and “Broad”^{102–105} after the computational biology groups that created or assembled them, consisted of multiple software packages for calling somatic single nucleotide variations (SNVs), small insertions and deletions (indels), copy number alterations (CNAs), and somatic structural variants (SVs; with intrachromosomal SVs defined as those >100bp). Two additional variant callers^{106,107} were included to further improve accuracy across a broad range of clonal and subclonal mutations. We tested different merging strategies using validation data, choosing the optimal method for each variant type to generate a final consensus set of mutation calls (Supplementary Methods S2.4).

Somatic retrotransposition events, including *Alu* and LINE/L1 insertions⁷⁵, L1-mediated transductions⁷⁶ and pseudogene formation¹⁰⁸, were called using a dedicated pipeline⁷⁶. We removed these retrotransposition events from the somatic SV call-set. Mitochondrial DNA mutations were called using a published algorithm¹⁰⁹. RNA-Sequencing data were uniformly processed to quantify normalised gene-level expression, splicing variation and allele-specific expression, and to identify fusion transcripts, alternative promoter usage and sites of RNA editing¹¹⁰.

Integration, phasing, and validation of germline variant call-sets

Calls of common (≥ 1% frequency in PCAWG) and rare (<1%) germline variants including single nucleotide polymorphisms (SNPs), indels, structural variants and mobile element insertions were generated using a population-scale genetic polymorphism detection approach^{95,111}. The uniform germline data processing workflow comprised variant identification using six different variant callers^{100,112,113}, and orchestrated via the Butler workflow system¹¹⁴.

We performed call-set benchmarking, merging, variant genotyping and statistical haplotype-block phasing⁹⁵ (Supplementary Methods S3.4). Using this strategy, we identified 80.1 million germline SNPs, 5.9 million germline indels, 1.8 million multi-allelic short (<50bp-sized) germline variants, as well as germline SVs ≥ 50bp in size including 29,492 biallelic deletions and 27,254 mobile element insertions (MEIs) (Supplementary Table 2). We statistically phased this germline variant set utilising 1000 Genomes Project⁹⁵ haplotypes as a reference panel, yielding an N50 phased block length of 265 kb based on haploid chromosomes from donor-matched tumour genomes. Precision estimates for germline SNVs and indels were >99% for the phased merged call-set, and sensitivity estimates ranged from 92% to 98%.

Core alignment and variant calling by cloud computing

The requirement to uniformly realign and call variants on nearly 5,800 whole genomes (tumour plus normal) presented significant computational challenges, and raised ethical issues due to the use of data from different jurisdictions (Box 1). To process the data, we adopted a cloud-computing architecture²⁶ in which the alignment and variant calling was spread across 13 data centres in three continents, representing a mixture of commercial, infrastructure-as-a-service, academic cloud compute, and traditional academic high-performance computer clusters (Supplementary Table 3). Altogether, the effort used 10 million CPU core-hours.

To generate reproducible variant-calling across the 13 data centres, we built the core pipelines into Docker containers²⁸, in which the workflow description, required code and all associated dependencies were packaged together in stand-alone packages. These heavily tested, extensively validated workflows are available for download (Box 1).

Validation, benchmarking and merging of somatic variant calls

In order to evaluate the performance of each of the mutation-calling pipelines and determine an integration strategy, we performed a large-scale deep sequencing validation experiment (Supplementary Notes 1). We selected a pilot set of 63 representative tumour/normal pairs, on which we ran the three core pipelines, together with a set of 10 additional somatic variant-calling pipelines contributed by members of the SNV Calling Working Group. Sufficient DNA remained for 50 of the 63 cases for validation, which was performed by hybridisation of tumour and matched normal DNA to a custom RNA bait-set, followed by deep sequencing, as described previously²⁹. Although performed using the same sequencing chemistry as the original whole genome sequencing, the considerably greater depth achieved in the validation experiment enabled accurate assessment of sensitivity and precision of

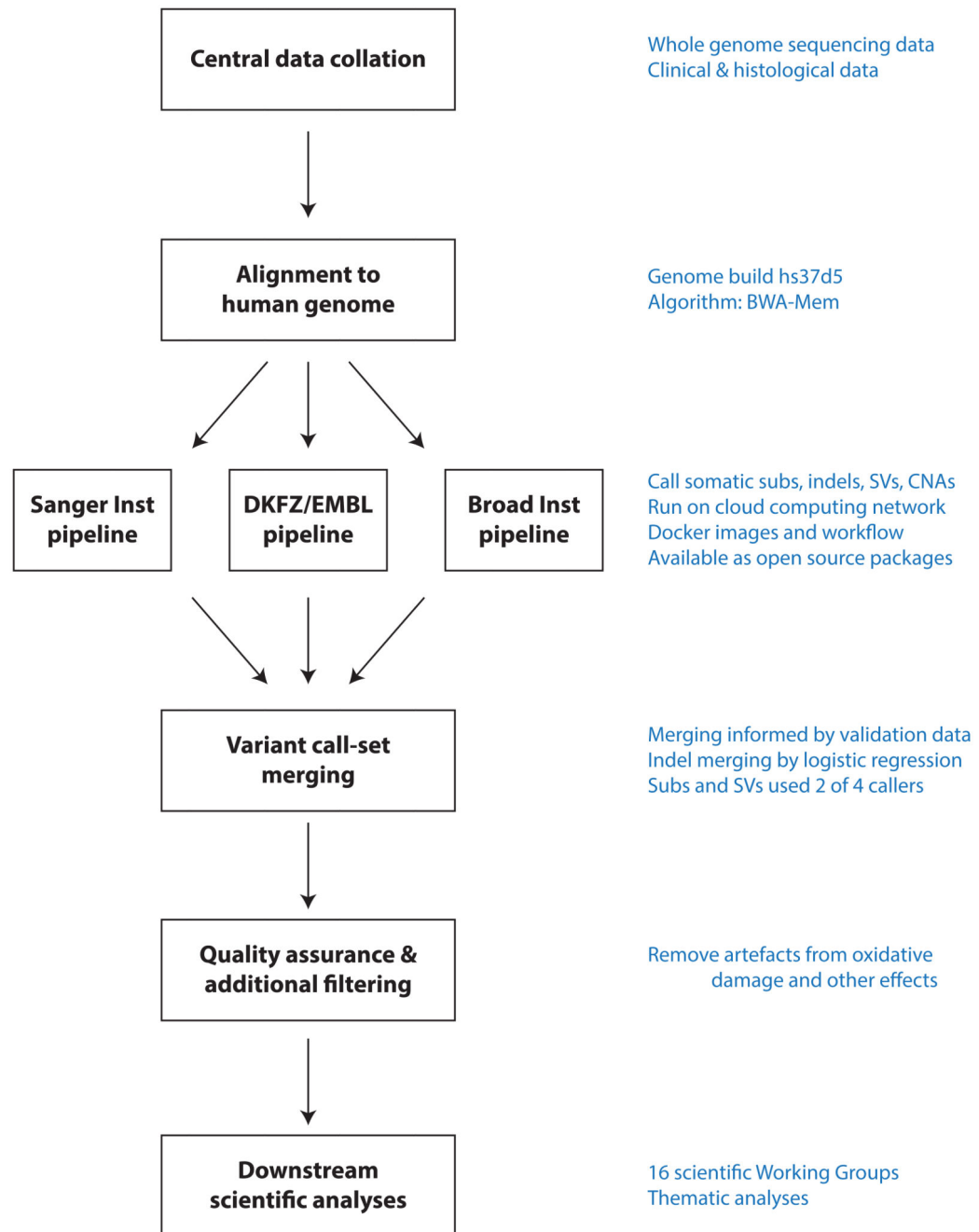
variant calls. Variant calls in repeat-masked regions were not tested due to the challenge of designing reliable validation probes in these areas.

The three core pipelines had individual estimates of sensitivity of 80-90% to detect a true somatic SNV called by any of the 13 pipelines; with >95% of SNV calls made by each of the core pipelines being genuine somatic variants (Figure 1A). For indels, a more challenging class of variants to identify in short read sequencing data, the three core algorithms had individual sensitivity estimates in the range 40-50%, with precision 70-95% (Figure 1B). Validation of SV calls is inherently more difficult because methods based on PCR or hybridisation to RNA baits often fails to isolate DNA spanning the breakpoint. To assess accuracy of SV calls, we therefore used the property that an SV must either generate a copy number change or be balanced, whereas artefactual calls will not respect this property. For individual SV callers, we estimated precision to be in the range 80-95% for samples in the pilot-63 dataset.

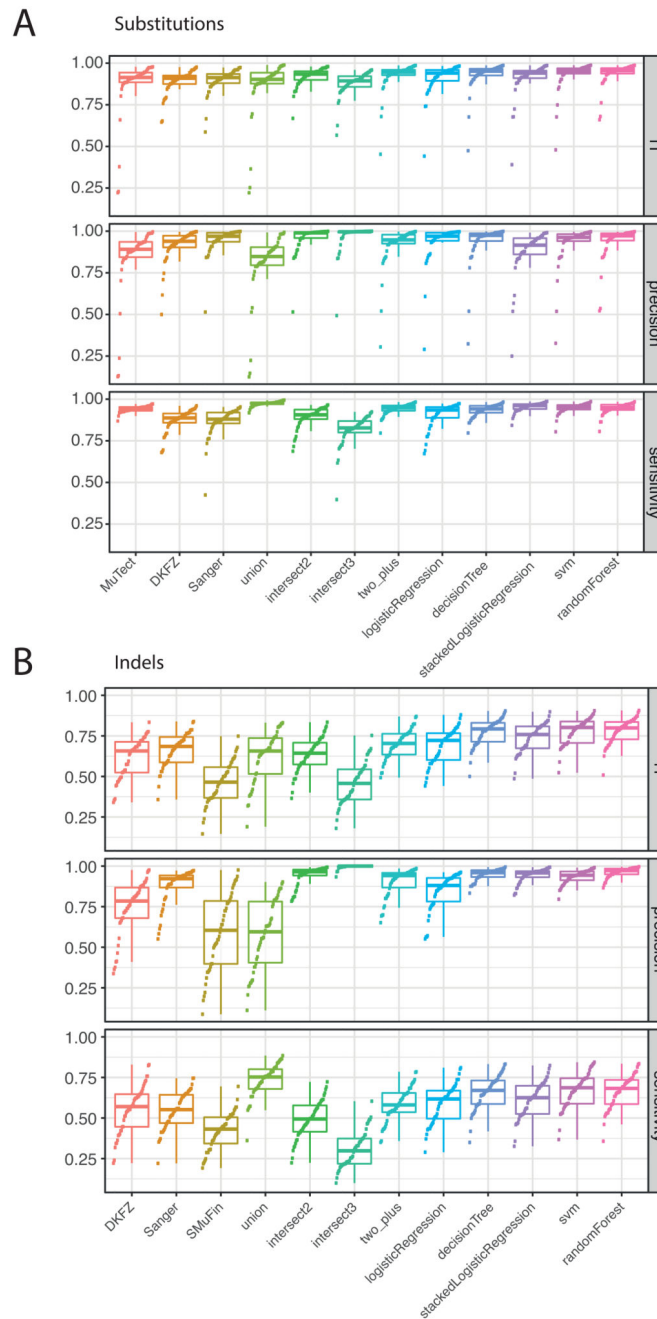
Next, we examined multiple methods for merging calls made by several algorithms into a single definitive call-set to be used for downstream analysis. The final consensus calls for SNVs were based on a simple approach that required two or more methods to agree on a call. For indels, because methods were less concordant, we used stacked logistic regression^{115,116} to integrate the calls. The merged SV set includes all calls made by two or more of the four primary SV callers^{100,104,117,118}. Consensus CNA calls were obtained by joining the outputs of six individual CNA callers with SV consensus breakpoints to obtain base-pair resolution CNAs (Supplementary Methods 2.4.3). Consensus purity and ploidy were derived, and a multi-tier system was developed for consensus copy number calls (Supplementary Methods 2.4.3, and described in detail elsewhere⁶³).

Overall, the sensitivity and precision of the consensus somatic variant calls were 95% (CI_{90%}: 88-98%) and 95% (CI_{90%}: 71-99%) respectively for SNVs (Extended Figure 2). For somatic indels, sensitivity and precision were 60% (34-72%) and 91% (73-96%) respectively. Regarding SVs, we estimate the sensitivity of the merging algorithm to be 90% for true calls generated by any one caller; precision was estimated as 97.5%. That is, 97.5% of SVs in the merged SV call-set have an associated copy number change or balanced partner rearrangement. The improvement in calling accuracy from combining different callers was most noticeable in variants having low variant allele fractions, which are likely to originate in subclonal populations of the tumour (Figure 1C-D). There remains much work to be done in improving indel callers; we still lack sensitivity for calling even fully clonal complex indels from short-read sequencing data.

Extended Data



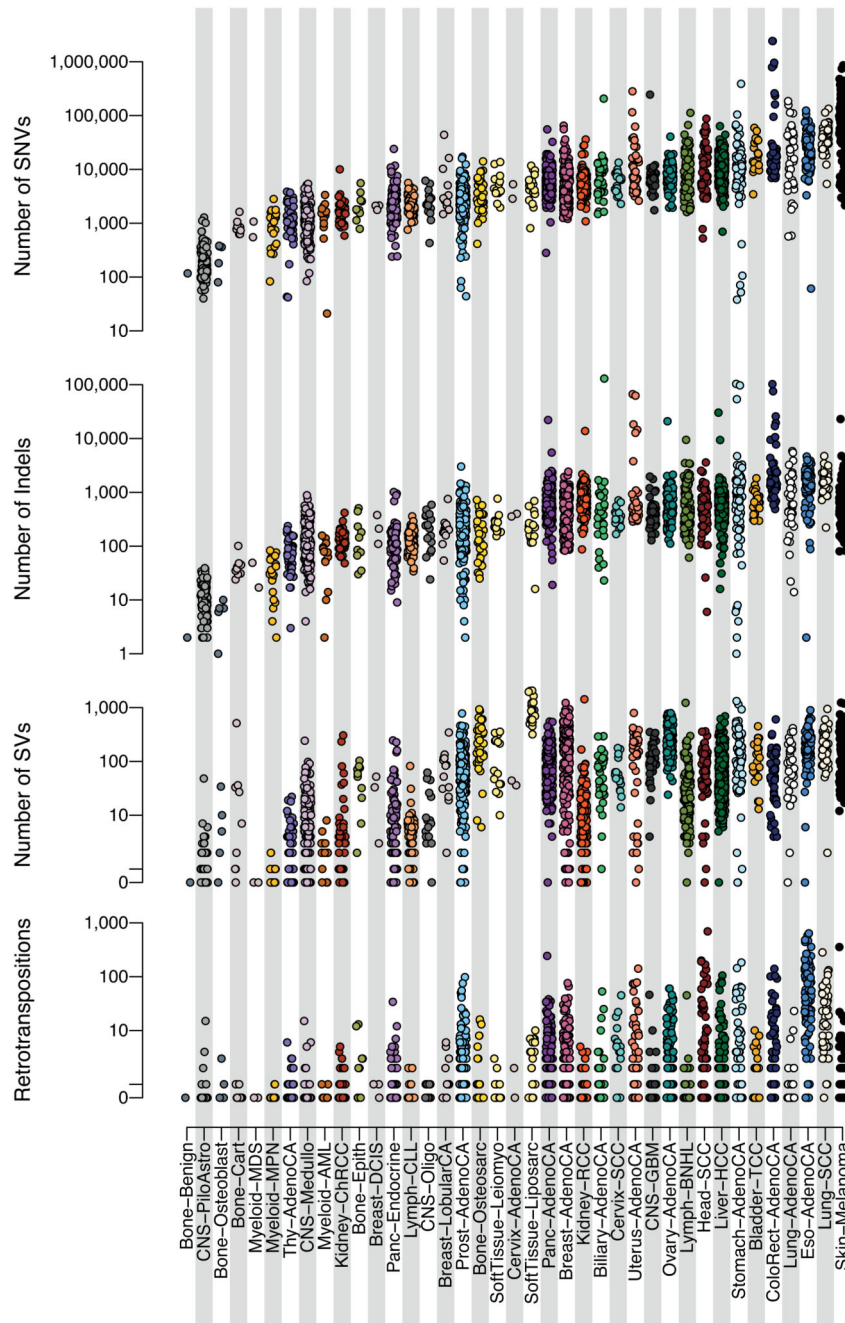
Extended Figure 1. Flow-chart showing key steps in the analysis of PCAWG genomes.



Extended Figure 2. Distribution of accuracy estimates across algorithms and samples from validation data.

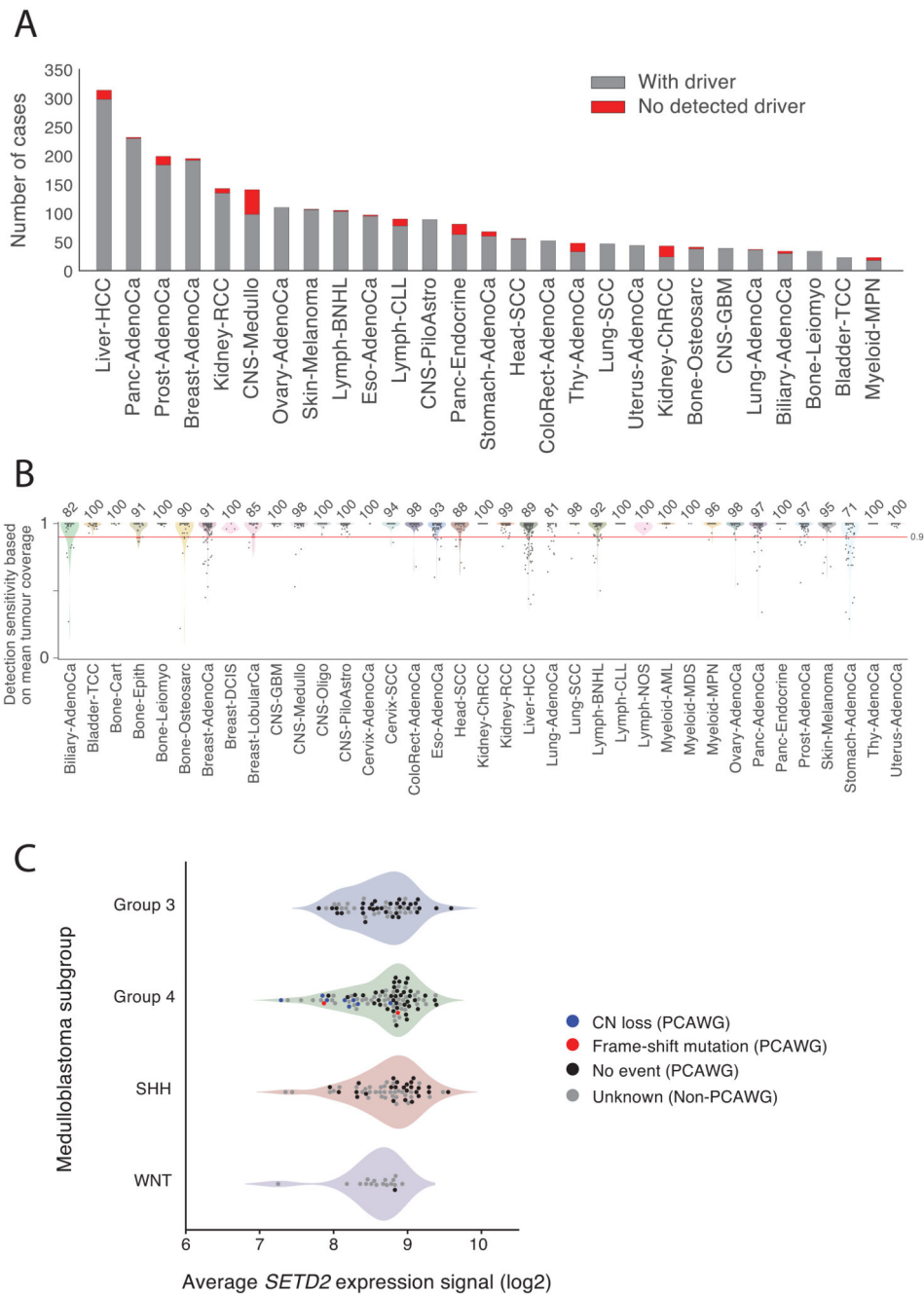
(A) F_1 accuracy, precision and sensitivity estimates for somatic SNVs across the core algorithms and different approaches to merging the call sets. The box plots demarcate the interquartile range and median of estimates across the $n=50$ samples in the validation dataset. (B) F_1 accuracy, precision and sensitivity estimates for somatic indels ($n=50$ samples). SVM, support vector machine; union, calls made by all variant callers; intersect2,

calls made by any combination of two variant callers; intersect3, calls made by any three variant callers.



Extended Figure 3. Distribution of numbers of somatic mutations of different classes across tumour types.

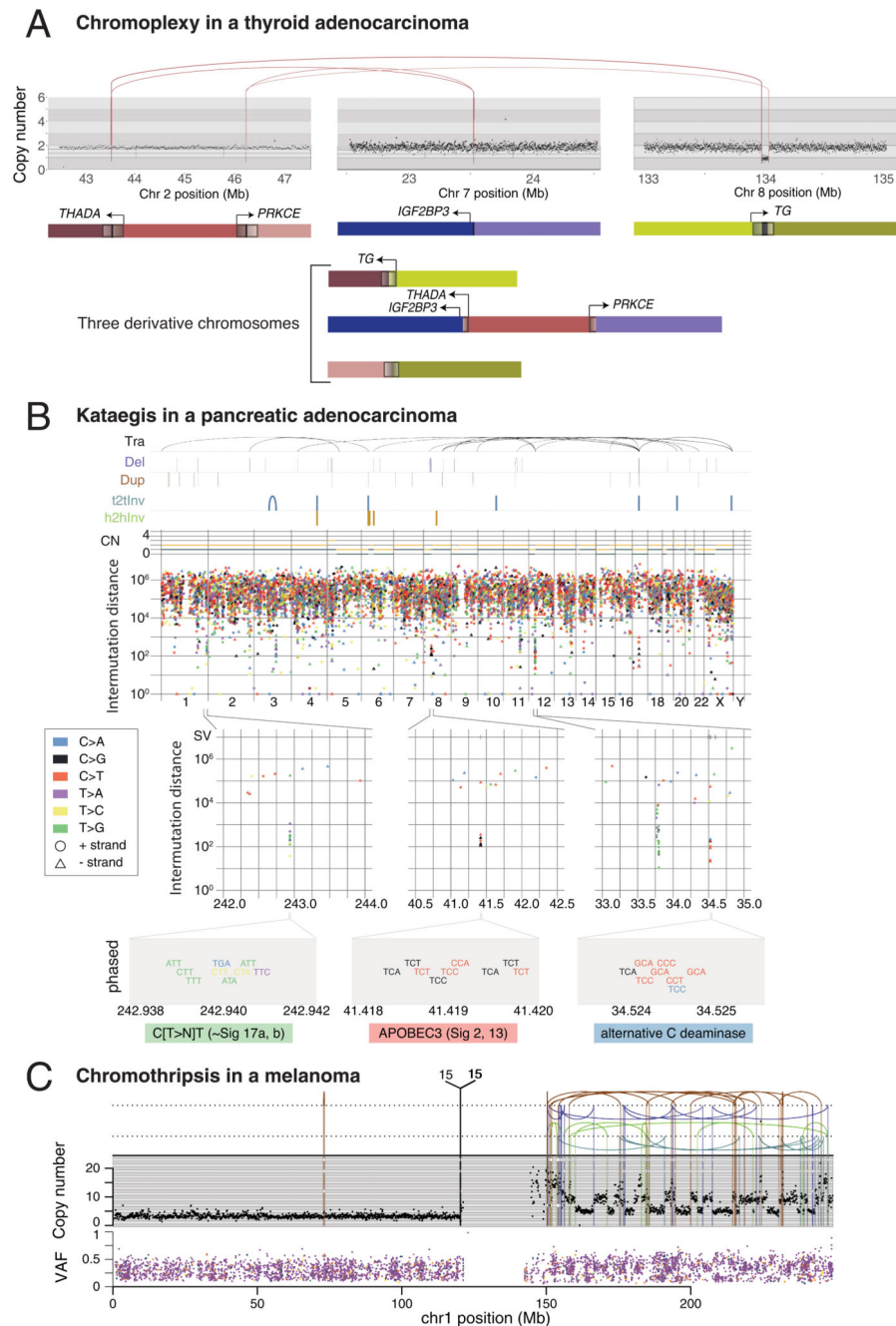
The y axis is on a log scale. Plotted are the 2,583 donors with the highest quality metrics (white-listed donors). SNVs, single nucleotide variants (substitutions); Indels, insertions or deletions <100 base pairs in size; SVs, structural variants; Retrotranspositions, counts of somatic retrotransposon insertions, transductions and somatic pseudogene insertions combined.



Extended Figure 4. Patients with no detected driver mutations in PCAWG.

(A) Number (red) of patients without detected driver mutations distributed across the different tumour types studied. (B) Estimated sensitivity for detecting somatic point mutations genome-wide across tumour types (total sample size: $n=2,583$ patients). Each point represents the estimate for a single patient, layered on violin plots representing the estimated density distribution of sensitivity values for that tumour type (width proportional to density). (C) *SETD2* expression levels across different medulloblastoma subtypes. Points represent individual patients, coloured by whether the gene exhibited focal copy number

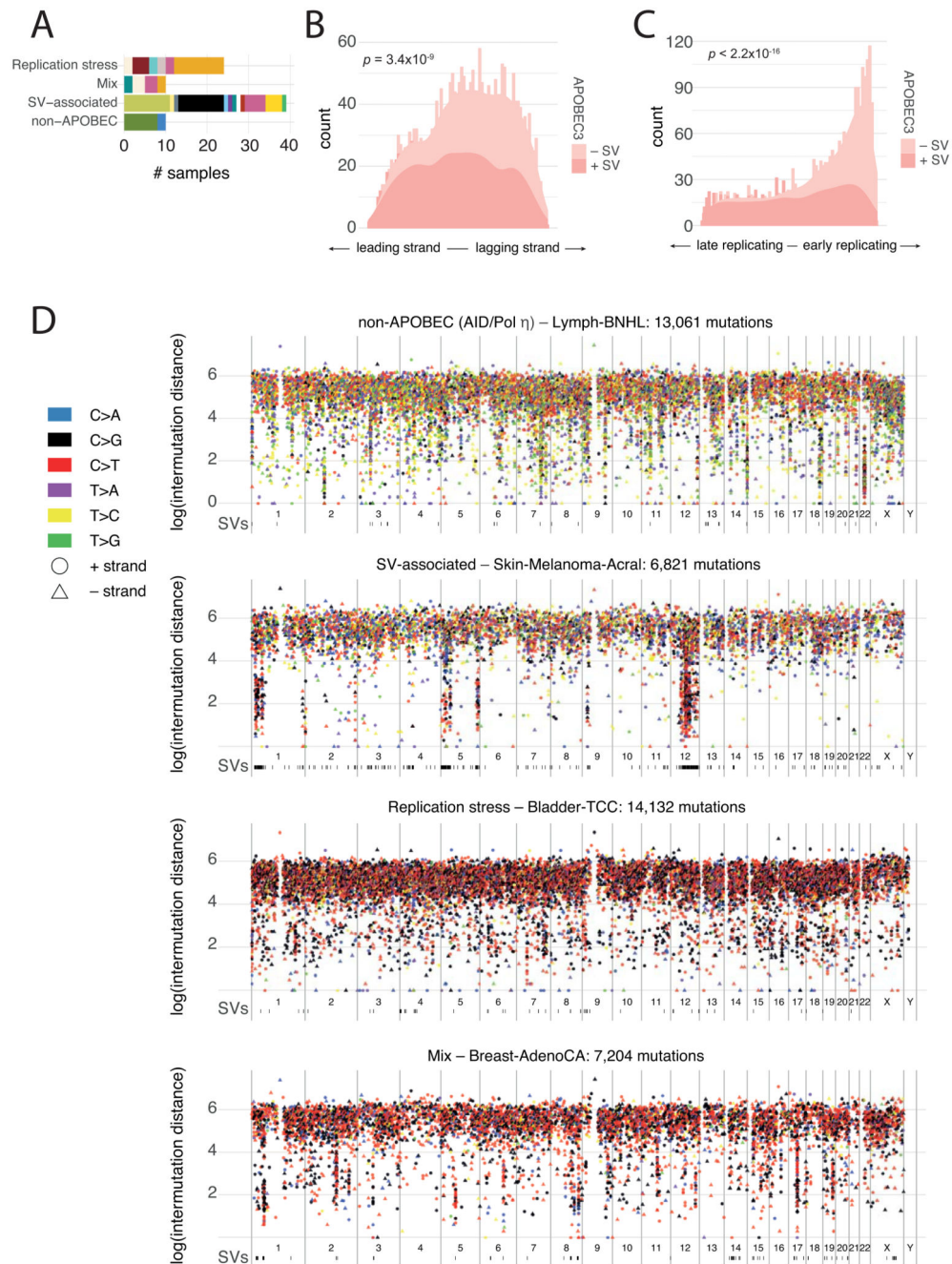
loss, truncating point mutation, or was wild-type. The coloured areas are violin plots representing the estimated density distribution of expression values for that medulloblastoma subtype (width proportional to density).



Extended Figure 5. Examples of clustered mutational processes.

(A) Chromoplexy example in a thyroid adenocarcinoma. Genes at the breakpoints are schematically depicted in their normal genomic context and again in the reconstructed derivative chromosomes below. (B) Distinct kataegis signatures in the genome of a pancreatic adenocarcinoma sample. SVs and their classification are shown above the main rainfall plot (Tra, translocation; Del, deletion; Dup, duplication; t2tInv, tail-to-tail inversion; h2hInv, head-to-head inversion), as well as the total and minor allele copy number. Zooming into three foci on chr1, chr8 and chr12, respectively, exemplifies distinct manifestations of

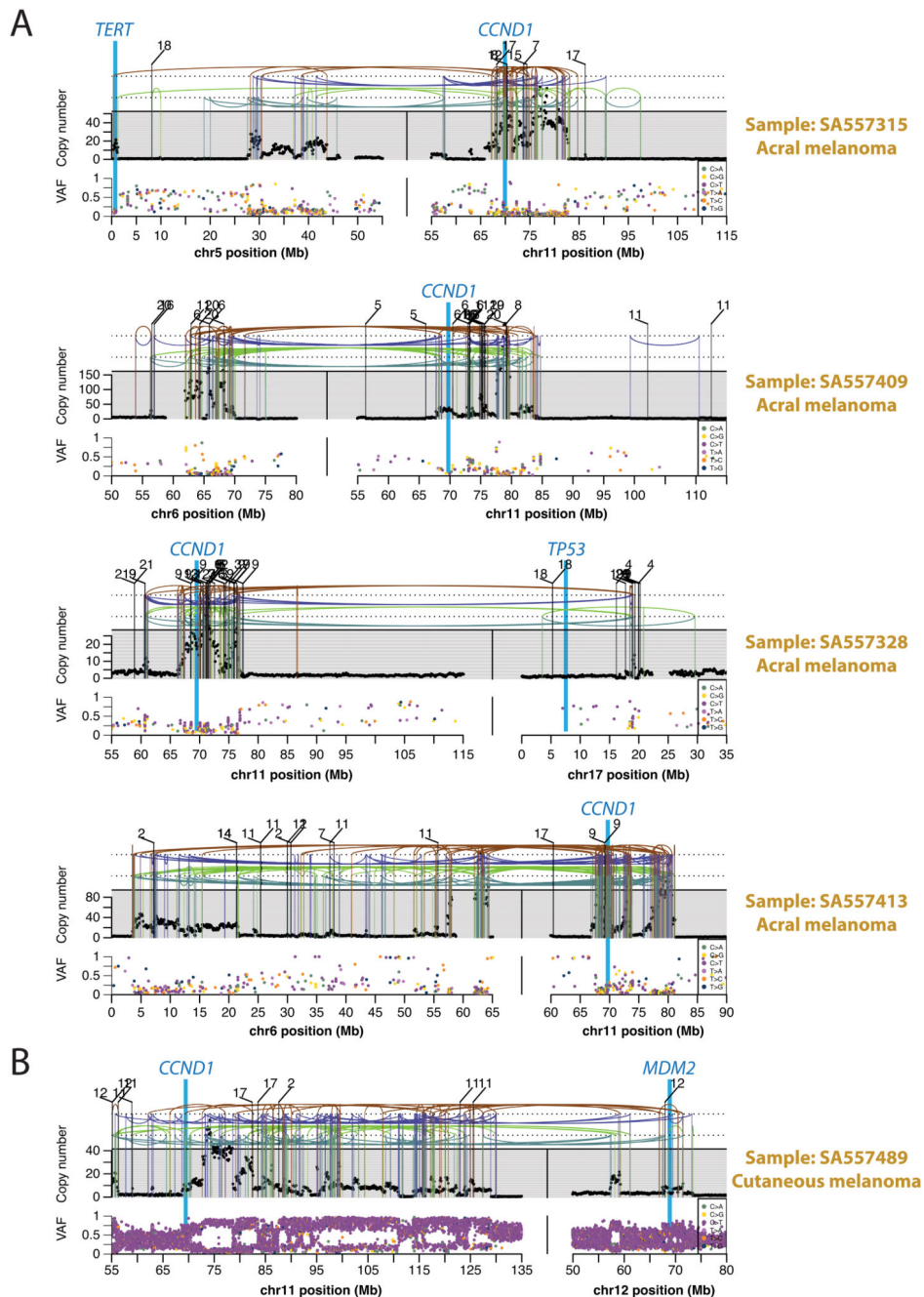
kataegis: (left) a novel process similar to Signature 17 with T>N mutations at CT or TT dinucleotides; (middle) the prototypical APOBEC3A/B type with C>T (Signature 2) and/or C>G/A (Signature 13) substitutions at TpC; (right) an alternative cytidine deaminase(s) with a preference for substitutions at C/GpC. Most of the SNVs in each of these foci can be phased to the same allele and no evidence of anti-phasing is observed. (C) Example of a chromothripsis event in a melanoma. The black points in the upper panel represent copy number estimates from individual genomic bins, with structural variants shown as coloured arcs (translocation in black, deletion in purple, duplication in brown, tail-to-tail inversion in cyan, head-to-head inversion in green), mostly demarcating copy number changes. The mate chromosomes are displayed above translocations. The lower panel shows the variant allele fraction (VAF) of somatic mutations distributed along the relevant chromosomal region.



Extended Figure 6. Patterns of intense kataegis.

(A) Bar plot showing the tumour type distribution (colour-coded as in Extended Figure 3) of samples in the top 5% of kataegis intensity in each of the four genome-wide patterns identified: non-APOBEC, replication stress, rearrangement-associated and combination of the latter two. (B,C) Distribution of leading/lagging strand (B) and replication timing bias (C) for rearrangement-(in)dependent APOBEC kataegis, based on $n=2,583$ tumours. P-values were derived using a two-sided Mann-Whitney U test. (D) Example rainfall plots for each of the four kataegis patterns identified.

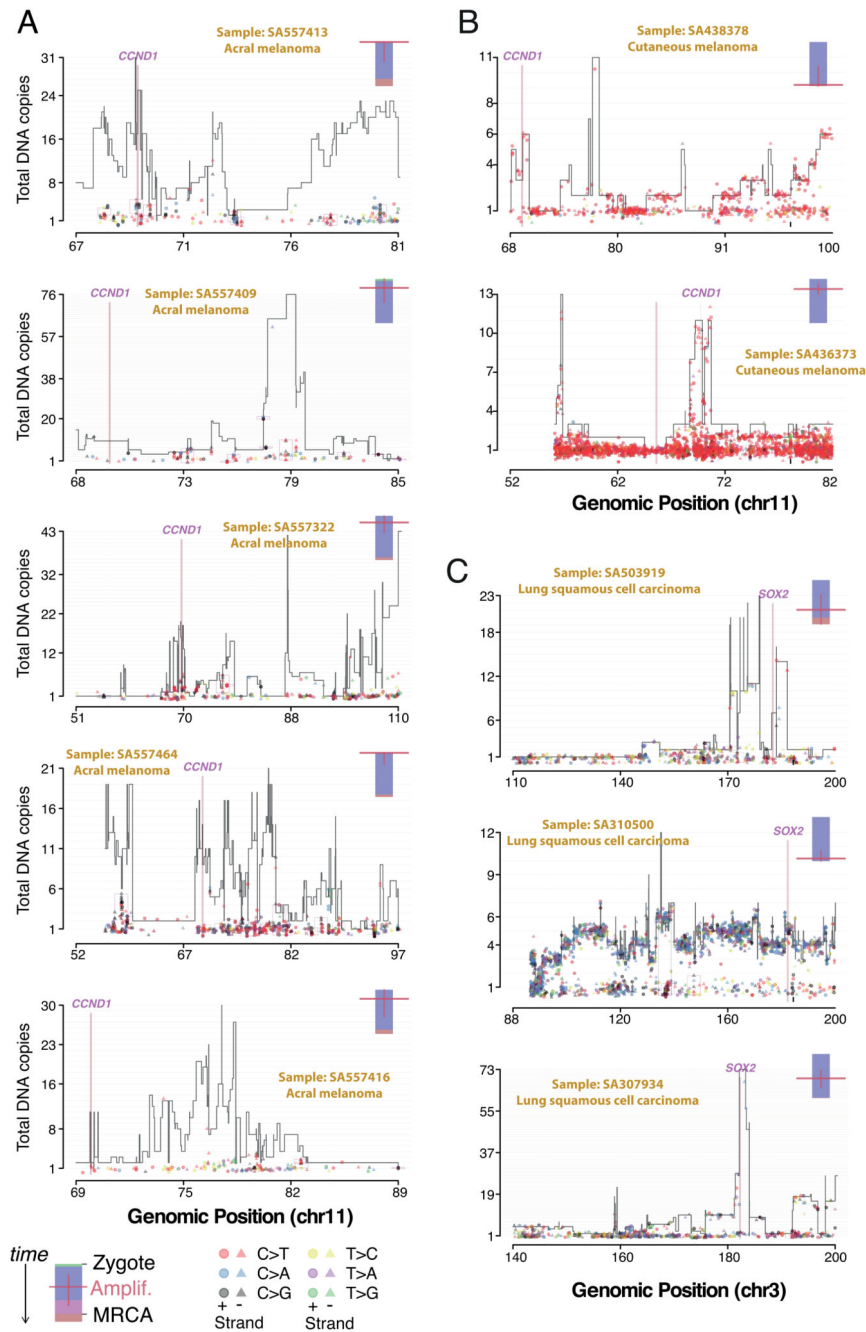
lower depth. For the box-and-whisker plots, the box denotes the interquartile range, with the median marked as a horizontal line. The whiskers extend as far as the range or 1.5x the interquartile range, whichever is less. Two-sided hypothesis testing was performed using Mann-Whitney U tests. **(D)** Counts of co-occurrence of chromothripsis with amplification (blue) and homozygous deletions (red) in driver regions: observed (thick line) vs. randomised (shaded area and thin line). The cumulative number of drivers hit is plotted as a function of the number of times those drivers are hit. **(E)** For each sample where chromothripsis coincided with a driver event in those genes, we show the gene expression fold change compared to the median expression of the gene in non-chromothripsis samples of the same cancer type, coloured by cancer type and shaped by the type of driver event. We show with added transparency the fold changes calculated the same way for samples with driver mutations hitting the same driver genes but no evidence for chromothripsis. Analysis is based on n=1,222 patients with RNA-sequencing data. **(F)** Enrichment of co-occurrence of chromothripsis with driver events. The x-axis indicates the association of chromothripsis with a driver in a given cancer type compared to its rate of association with that driver in all other cancer types. The y-axis show the association of chromothripsis with a driver in a given cancer type compared to its rate of association with all other drivers in that type. Exact binomial tests are used and p-values are corrected for multiple testing according to Benjamini and Hochberg.



Extended Figure 8. Further examples of chromothripsis-induced amplification targeting multiple cancer genes simultaneously in melanoma.

(A) Examples of amplifications that occurred early in melanoma development. The black points in the upper panel represent copy number estimates from individual genomic bins, with structural variants shown as coloured arcs (translocation in black, deletion in purple, duplication in brown, tail-to-tail inversion in cyan, head-to-head inversion in green), mostly demarcating copy number changes. The mate chromosomes are displayed above translocations. The lower panel shows the variant allele fraction (VAF) of SNVs distributed

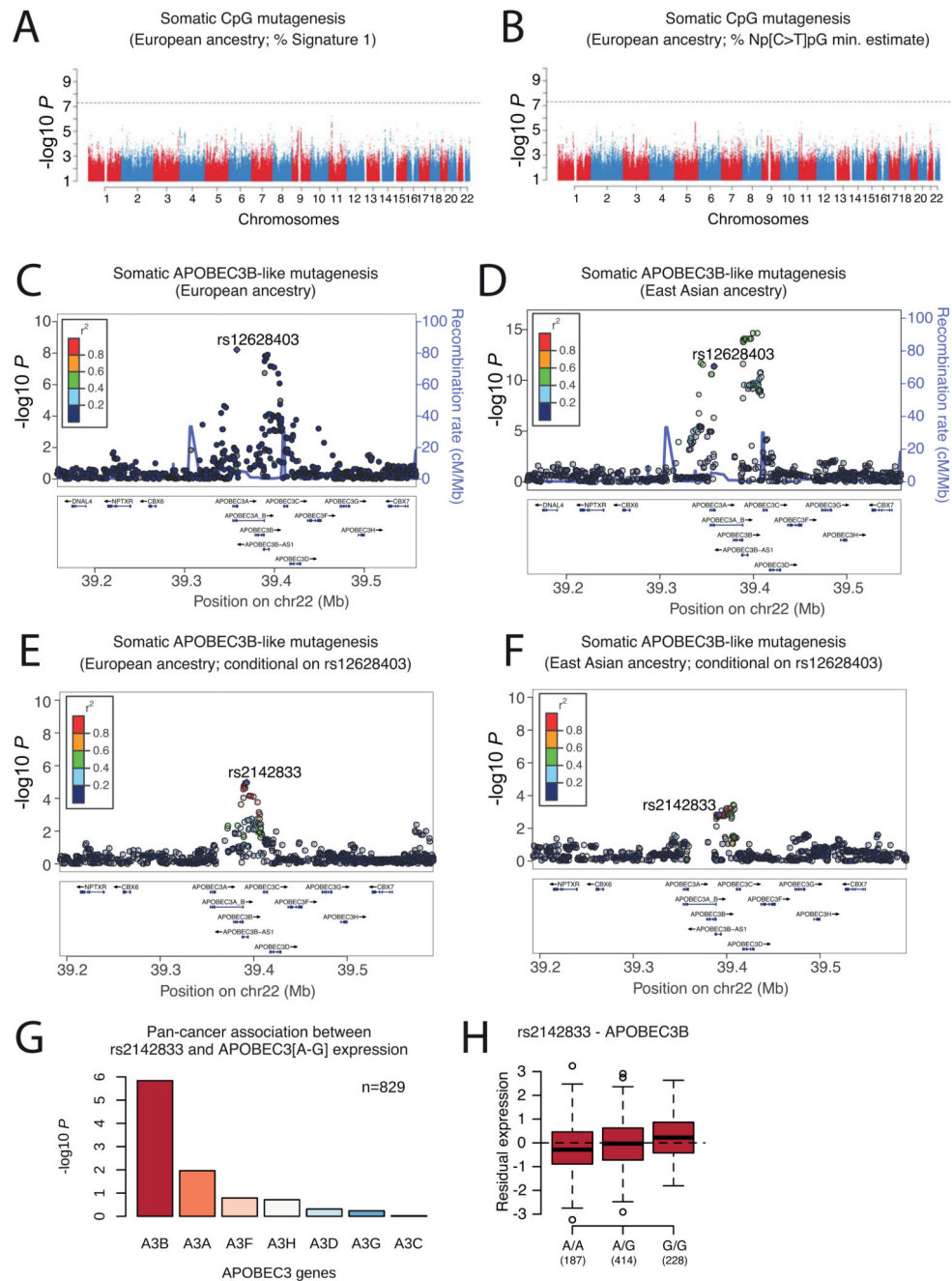
along the relevant chromosomal region. The paucity of somatic mutations at high variant allele fraction in the most heavily amplified regions indicates that these amplifications began very early in tumour evolution, before the lineage had had opportunity to acquire many SNVs. **(B)** Example of an amplification that occurred late in melanoma development. The large numbers of somatic mutations at high variant allele fraction in the most heavily amplified regions indicates that these amplifications began late in tumour evolution, after the lineage had already acquired many SNVs.



Extended Figure 9. Timing the amplifications following chromothripsis in molecular time – 10 selected cases.

(A) Copy number plot of chromothriptic regions categorised as “liposarc-like” in 5 acral melanomas showing *CCND1* amplification. Segments indicate the copy number of the major allele. Points represent SNV multiplicities, i.e. the estimated number of copies carrying them, coloured by base change and shaped by strand. Small vertical arrows link SNVs to their corresponding copy number segment. Kataegis foci are shown within black boxes, and show typical strand-specificity (all triangles or all circles), similar multiplicities and base

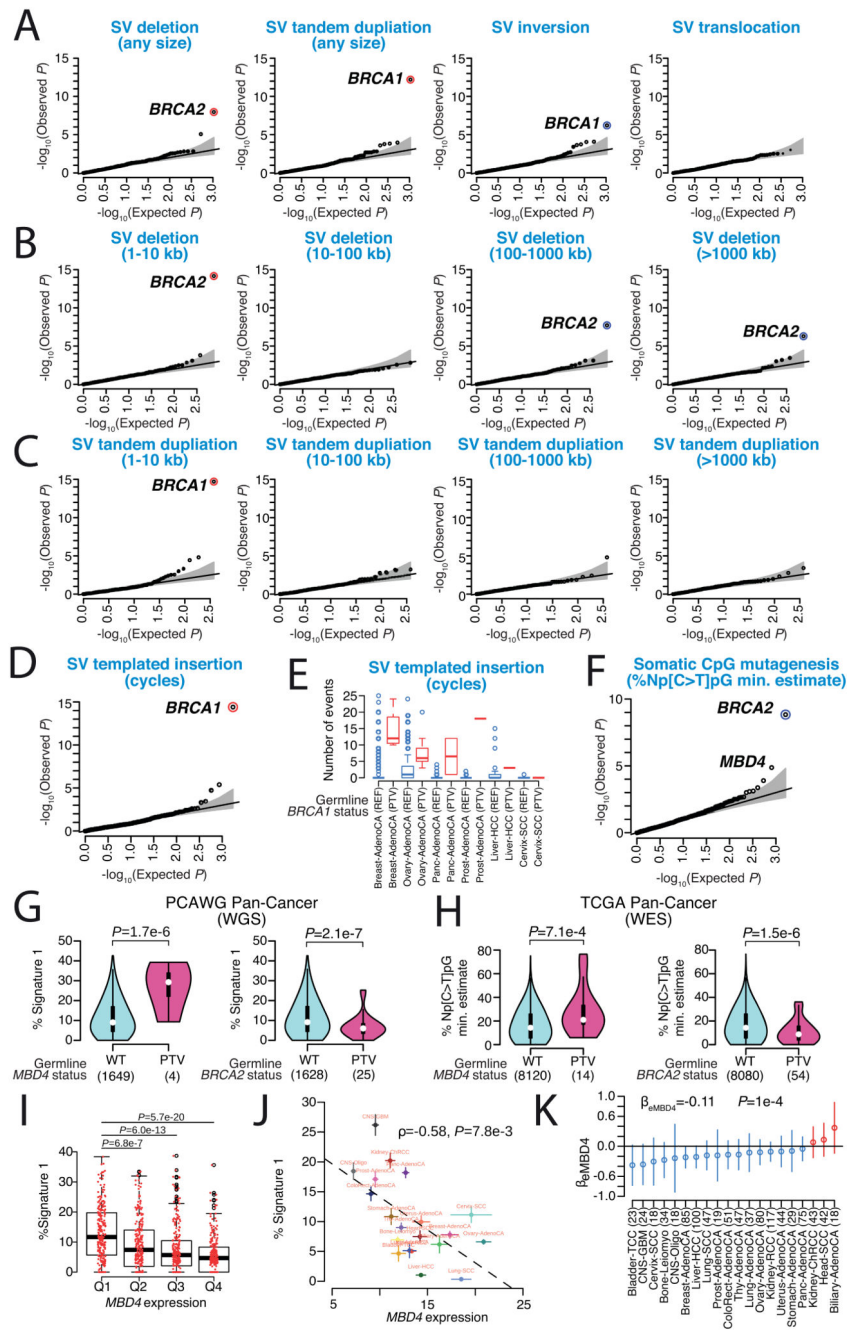
changes of signatures 2 and 13 (red and black). A coloured bar on the top right represents the molecular timing of the amplification (red bar; high is early, low is late) and is coloured by the fraction of total SNVs assigned to timing categories clonal[early], clonal[NA], clonal[late] and subclonal. **(B)** Same as A in 2 cutaneous melanomas, one shows an early amplification, the other a late one. **(C)** Same as A-B for 3 lung squamous cell carcinomas and late amplification of *SOX2*.



Extended Figure 10. Association between common germline variants and endogenous mutational processes.

Genome-wide association of somatic CpG mutagenesis in individuals of European ancestry (n=1,201 patients) based on mutational signature analysis (A) and NpCpG motif analysis (B). Two-sided hypothesis-testing was performed using PLINK v1.9. To mitigate multiple hypothesis-testing, the significance threshold was set at genome-wide significance ($p < 5 \times 10^{-8}$). (C,D) Locuszoom plot for somatic APOBEC3B-like mutagenesis association results, LD, and recombination rates around the genome-wide significant 22q13.1 locus in

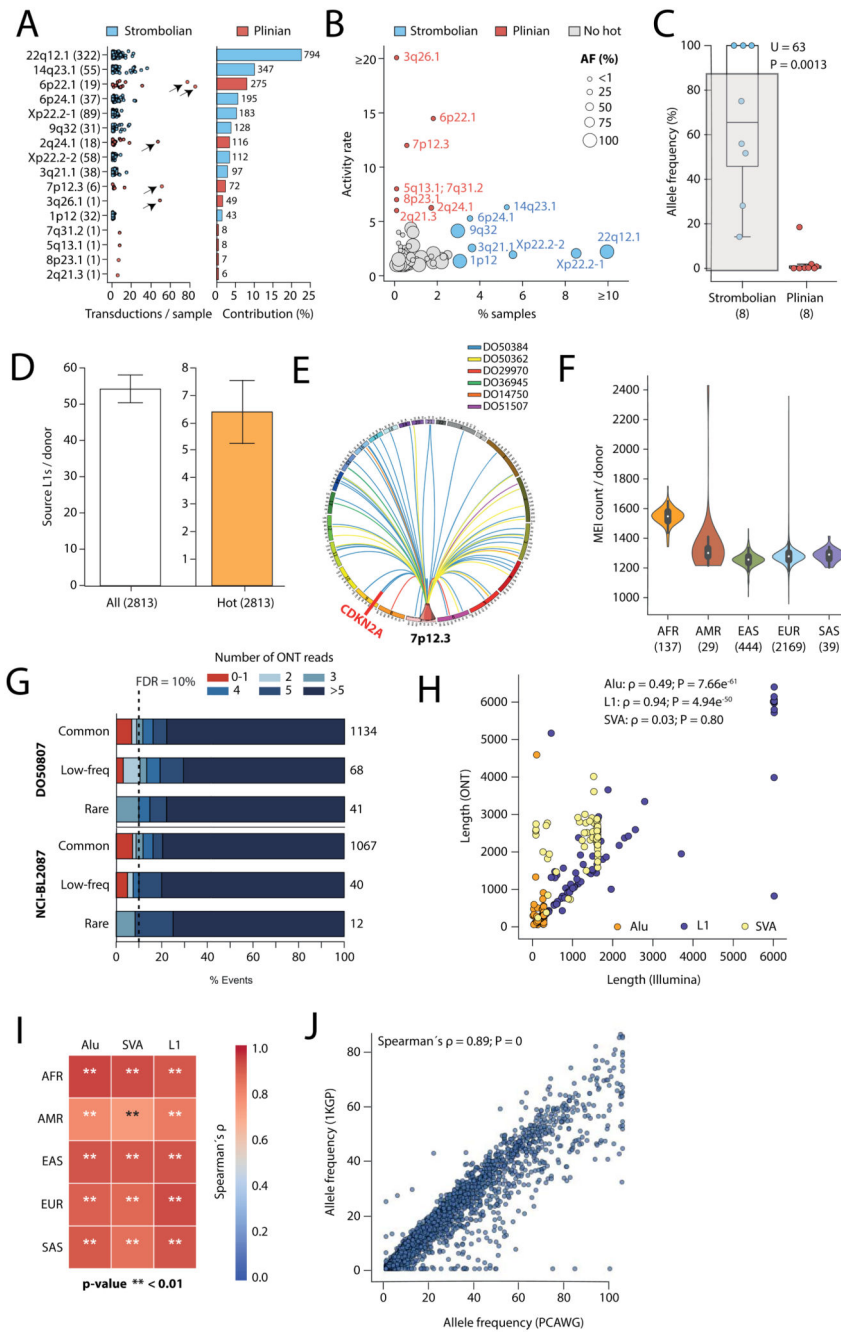
individuals with European (**C**) and East Asian (**D**) ancestry (n=1,201 and 318 patients respectively). Locuszoom plot for somatic APOBEC3B-like mutagenesis association results around the 22q13.1 locus in individuals of European (**E**) and East Asian (**F**) ancestry after conditioning on rs12628403. (**G,H**) Association between rs2142833 and expression of *APOBEC3* genes in PCAWG tumour samples (adjusted for sex, age at diagnosis, histology, and population structure in linear regression models with two-sided hypothesis testing not corrected for multiple tests). For the box-and-whisker plot, the box denotes the interquartile range, with the median marked as a horizontal line. The whiskers extend as far as the range or 1.5x the interquartile range, whichever is less. Outlier patients are shown as points.



Extended Figure 11. Association between rare germline PTVs in protein-coding genes and somatic mutational phenotypes.

For panels A-D and F, the data are based on two-sided rare-variant association testing across $n=2,583$ patients, with a stringent p-value threshold of $P < 2.5 \times 10^{-6}$ used to mitigate multiple hypothesis testing (significant genes marked with coloured circles). Blue/red circles mark genes that decrease/increase somatic mutation rates. The black line represents the identity line which would be followed if the observed p values followed the null expectation, with the shaded area showing 95% confidence intervals. (A) QQ plots for proportion of somatic

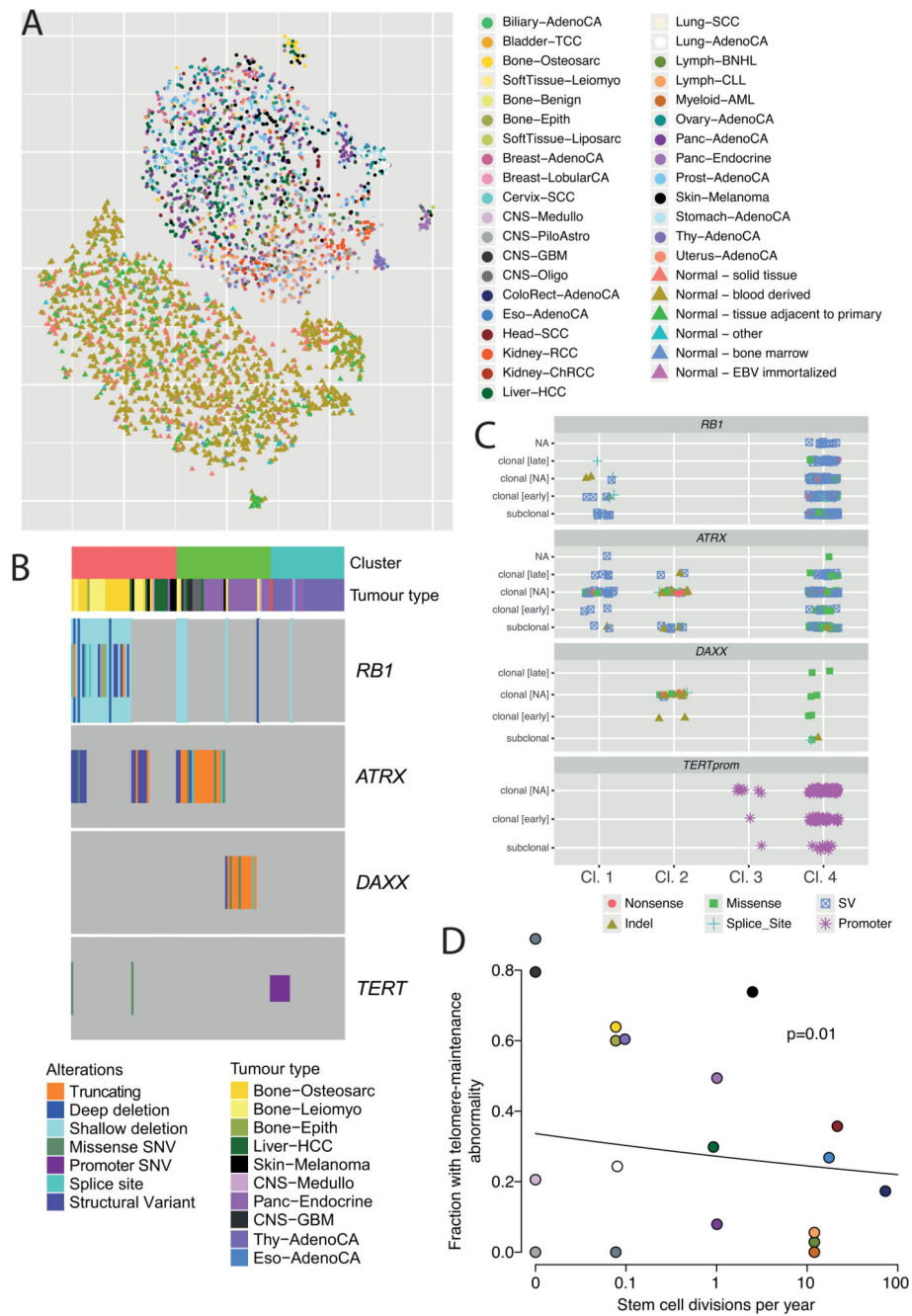
SV deletions, tandem duplications, inversions, and translocation in cancer genomes. **(B)** QQ plots for proportion of somatic SV deletions in cancer genomes stratified by four size groups (1-10 kb; 10-100 kb; 100-1000 kb; >1000 kb). **(C)** QQ plots for proportion of somatic SV tandem duplications in cancer genomes stratified by four size groups (1-10 kb; 10-100 kb; 100-1000 kb; >1000 kb). **(D)** QQ plot for presence/absence of somatic SV templated insertion (cycles) in cancer genomes. **(E)** Number of SV templated insertion cycles in PCAWG tumours with germline *BRCA1* PTVs. Only histologies with at least one germline *BRCA1* PTV carrier are shown (n=1,095 patients combined). The box denotes the interquartile range, with the median marked as a horizontal line. The whiskers extend as far as the range or 1.5x the interquartile range, whichever is less. Outlier patients are shown as points. **(F)** QQ plot for somatic CpG mutagenesis in cancer genomes based on NpCpG motif analysis. **(G)** Violin plots show estimated density of the proportion of somatic CpG mutations in PCAWG donors with germline *MBD4* and *BRCA2* PTVs. The box denotes the interquartile range, with the median marked as a white point. The whiskers extend as far as the range or 1.5x the interquartile range, whichever is less. Two-sided hypothesis testing, not corrected for multiple testing, was performed using linear regression models. **(H)** Replication of germline *MBD4* and *BRCA2* PTV associations with somatic CpG mutagenesis in TCGA WES donors. Violin plots show estimated density of the proportion of somatic CpG mutations in TCGA exomes with germline *MBD4* and *BRCA2* PTVs. The box denotes the interquartile range, with the median marked as a white point. The whiskers extend as far as the range or 1.5x the interquartile range, whichever is less. Two-sided hypothesis testing, not corrected for multiple testing, was performed using linear regression models. **(I)** Correlation between *MBD4* expression and somatic CpG mutagenesis in primary solid PCAWG tumours. Hypothesis testing was two-sided and not corrected for multiple testing, using linear regression models. The box denotes the interquartile range, with the median marked as a horizontal line. The whiskers extend as far as the range or 1.5x the interquartile range, whichever is less. **(J)** Points represent means across n=20 tumour types and error bars represent standard error of the mean. The dashed black line shows the fitted line to the data, estimated with linear regression models. Hypothesis testing was two-sided and not corrected for multiple testing, performed with Spearman's rank correlation method. **(K)** *MBD4* effect sizes (open circles) with 95% confidence intervals (error bars) for individual cancer types were estimated with linear regression analysis after (if available) accounting for sex, age at diagnosis (low/high), and ICGC project. Hypothesis testing was two-sided and not corrected for multiple testing.



Extended Figure 12. Germline mobile element insertion (MEI) callset.

(A) On the left, dots show the number of transductions promoted by each hot element in individual samples. Arrows highlight retrotransposition burst. On the right, the contribution of each hot locus is represented. The total number of transductions mediated by each source element is shown on the right side. (B) Source L1 activity rate (*i.e.*, measured as the average number of transductions mediated by an element) versus the percentage of samples with retrotransposition activity in which the germline element is active. For visualization purposes, extreme points observed for a source L1 with an activity rate of 49 and for a L1

active in 31% of the samples are shown at “ 20” and “ 10”, respectively. **(C)** Contrasting allele frequencies for Strombolian and Plinian source loci (sample sizes shown under each axis label). The box denotes the interquartile range, with the median marked as a white point. The whiskers extend as far as the range or 1.5x the interquartile range, whichever is less. Hypothesis-testing was performed using two-sided Mann-Whitney tests without correction for multiple tests. **(D)** Number of active and hot source L1 elements per donor. The bar height represents the mean number of elements per donor and error bars the standard deviation. **(E)** Novel Plinian source element on 7p12.3 mediates 72 transductions amongst only six cancer samples. This includes a transduction that induces the deletion of the tumour suppressor gene *CDKN2A*. **(F)** Violin plots show estimated number of distinct germline MEI alleles per PCAWG donor. The box denotes the interquartile range, with the median marked as a white point. The whiskers extend as far as the range or 1.5x the interquartile range, whichever is less. Donors are grouped according to their genetic ancestry: AFR, African; AMR, Ad Mixed American; EAS, East Asian; EUR, European; SAS, South Asian. Sample sizes are shown under each axis label. **(G)** For each type of MEI (L1, Alu and SVA) identified both in PCAWG and in the 1000 Genomes Project (1KGP), the correlations between allele frequency estimates per ancestry derived from both projects are displayed in a blue (0) to a red (1) coloured gradient. Sample size was n=2,583 PCAWG patients. Two-sided hypothesis-testing was performed using Spearman’s rank correlation without correction for multiple tests. **(H)** Example displaying the correlation between PCAWG and 1KGP derived MEI allele frequencies in individuals with European ancestry (n=1201 patients in PCAWG). Two-sided hypothesis-testing was performed using Spearman’s rank correlation without correction for multiple tests. **(I)** Evaluation of TraFiC-mem false discovery rate on a liver hepatocellular carcinoma donor (DO50807) and a cell-line (NCI-BL2087) sequenced through single-molecule sequencing with MinION (Oxford Nanopore). For each allele frequency bin (common, >5%; low-freq, 1-5%; rare, <1%), the percentage of events supported by N long-reads is represented (N from 0-1 to more than 5). MEIs supported by at least two Nanopore reads were considered true positives (blue palette) and false positives (red), otherwise. The total number of germline MEIs per allele frequency bin is shown on the right side of the panels. **(J)** Correlation between predicted MEI lengths from Illumina and Nanopore data. Two-sided hypothesis testing was performed using Spearman’s rank correlation without correction for multiple testing.



Extended Figure 13. Different mechanisms of telomere lengthening in cancer.

(A) Scatter plot showing the four clusters of tumour-specific telomere patterns identified across PCAWG samples, together with the clusters of matched normal samples, generated by t-Distributed Stochastic Neighbour Embedding. Circles represent tumour samples and triangles represent matched normal samples. Points are coloured by tissue of origin. Data are based on $n=2,518$ tumour samples and their matched normal samples. (B) Patterns of co-mutation of the relevant driver mutations across individual patients. Columns in plot represent individual patients, coloured by type of abnormality observed. (C) Clonal [early]

denotes clonal mutations occurring before duplications involving the relevant chromosome (including whole genome duplications); clonal [late] to clonal mutations occurring after such duplications; and clonal [NA] to mutations occurring when no duplication was observed. **(D)** Relationship between estimated number of stem cell divisions per year and rate of telomere maintenance abnormalities across tumour types. The analysis uses data on estimated rates of stem cell division per year across n=19 tissue types previously collated from the literature⁸⁶. Tumour types are coloured according to the scheme shown in Extended Figure 3. Two-sided hypothesis testing was performed using likelihood ratio tests on Poisson regression models with no correction for multiple tests.

Extended Table 1
Overview of tumour types included in PCAWG project.

Med, Median; F, Female; M, Male; 10-90th, 10-90th centile; Adeno., Adenocarcinoma; Comb., Combined; SCC, squamous cell carcinoma; HCC, hepatocellular carcinoma; Ca. Carcinoma.

Organ	Abbreviation	Included subtypes	Cases	Sex		Age	
				F	M	Med.	10 th -90 th
Neural Crest			Num.	F	M	Med.	10th-90th
CNS	CNS-GBM	Glioblastoma	41	13	28	60	43-72
CNS	CNS-Medullo	Medulloblastoma and variants	146	67	79	9	3-28
CNS	CNS-Oligo	Oligodendroglioma	18	9	9	41	21-62
CNS	CNS-PiloAstro	Pilocytic astrocytoma	89	47	42	8	2-17
Skin	Skin-Melanoma	Malignant melanoma	107	38	69	57	37-78
Endoderm							
Biliary	Biliary-AdenoCA	Papillary cholangiocarcinoma	34	15	19	64	53-76
Bladder	Bladder-TCC	Transitional cell carcinoma	23	8	15	65	52-80
Colon/Rectum	ColoRect-AdenoCA	Adenocarcinoma; Mucinous adeno.	60	30	30	67	46-81
Oesophagus	Eso-AdenoCA	Adenocarcinoma	98	14	84	70	56-79
Liver	Liver-HCC	Hepatocellular carcinoma; Comb. HCC/cholangio	317	89	228	67	50-78
Lung	Lung-AdenoCA	Adenocarcinoma; Adenocarcinoma <i>in situ</i>	38	20	18	66	47-77
Lung	Lung-SCC	Squamous cell carcinoma; Basaloid SCC	48	10	38	68	54-77
Pancreas	Panc-AdenoCA	Adeno.; Acinar cell Ca.; Mucinous adeno.	239	119	120	67	50-79
Pancreas	Panc-Endocrine	Neuroendocrine carcinoma	85	30	55	59	38-75
Prostate	Prost-AdenoCA	Adenocarcinoma	210	0	210	59	47-71
Stomach	Stomach-AdenoCA	Adenocarcinoma; Mucinous; Papillary; Tubular	75	18	57	65	47-79
Thyroid	Thy-AdenoCA	Adenocarcinoma; Columnar cell; Follicular type	48	37	11	51	26-75
Mesoderm							

Organ	Abbreviation	Included subtypes	Cases	Sex	Age		
Bone/Soft Tissue	Bone-Benign	Osteoblastoma; Osteofibrous dysplasia	7	4	3	18	12-30
Bone/Soft Tissue	Bone-Benign	Chondroblastoma; Chondromyxoid fibroma	9	2	7	16	14-38
Bone/Soft Tissue	Bone-Epith	Adamantinoma; Chordoma	10	4	6	60	37-67
Bone/Soft Tissue	Bone-Osteosarc	Osteosarcoma	38	20	18	20	9-58
Bone/Soft Tissue	SoftTissue-Leiomyo	Leiomyosarcoma	15	10	5	61	51-78
Bone/Soft Tissue	SoftTissue-Liposarc	Liposarcoma	19	5	14	n/a	n/a
Cervix	Cervix-AdenoCA	Adenocarcinoma	2	2	0	39	33-46
Cervix	Cervix-SCC	Squamous cell carcinoma	18	18	0	39	25-58
Head/Neck	Head-SCC	Squamous cell carcinoma	57	10	47	53	34-71
Kidney	Kidney-ChRCC	Adenocarcinoma, chromophobe type	45	19	26	47	34-69
Kidney	Kidney-RCC	Clear cell adenocarcinoma; papillary type	144	54	90	60	48-75
Lymphoid	Lymph-BNHL	Burkitt; Diffuse large B-cell; Follicular; Marginal	107	51	56	57	10-74
Lymphoid	Lymph-CLL	Chronic lymphocytic leukaemia	95	31	64	62	46-78
Myeloid	Myeloid-AML	Acute myeloid leukaemia	10	3	7	50	35-56
Myeloid	Myeloid-MDS	Myelodysplastic syndrome	2	1	1	76	74-77
Myeloid	Myeloid-MPN	Myeloproliferative neoplasm	26	14	12	56	38-75
Ovary	Ovary-AdenoCA	Adenocarcinoma; Serous cystadenocarcinoma	113	113	0	60	48-74
Uterus	Uterus-AdenoCA	Adeno., endometrioid; Serous cystadeno.	51	51	0	69	57-81
Ectoderm							
Breast	Breast-AdenoCA	Infiltrating duct carcinoma; Medullary; Mucinous	198	197	1	56	39-76
Breast	Breast-DCIS	Duct micropapillary carcinoma	3	3	0	55	43-60
Breast	Breast-LobularCA	Lobular carcinoma	13	13	0	53	42-69
Total			2658	1189	1469	59	21-76

Extended Table 2
Ethical considerations of genomic cloud computing.

Ethical Considerations of Genomic Cloud Computing

The PCAWG project represents the first large-scale use of distributed cloud computing in genomics. The project involved the movement of large quantities of personal health information across multiple legal jurisdictions and responsible use of this data by several hundred international researchers. Donor consents were written to explicitly allow for broad research use of the data and for international data sharing. PCAWG was granted permission by the leads of each of the tumour data providers to store, analyse and distribute the data on academic and/or commercial compute clouds.

To ensure that the PCAWG personal data were handled in a manner consistent with the donor consents, authorised representatives of each of the academic clouds and high-performance computing facilities signed a commitment not to access controlled tier data beyond the minimum needed to administer it. We negotiated similar contractual terms with commercial cloud partners. Prior to accessing the data, each PCAWG researcher was required to obtain local Institutional Review Board approval for their proposed analytic projects, and obtained controlled tier authorisation from dbGaP (National Center for Biotechnology Information) and the ICGC DACO (Centre of Genomics and Policy at McGill University). To handle the data securely, we encrypted it while in motion and at rest. We used a central authentication and digital token generating system to enforce a strong data access protocol that required researchers to provide their TCGA and/or ICGC credentials prior to accessing controlled tier data. No data breach or other compromise of donor confidentiality is known to have occurred over the course of the PCAWG project, despite its extensive use of cloud computing.

Extended Table 3
Scientific output using PCAWG data, in bite-size chunks.

Scientific	Key findings	Citation
Driver mutations		
Discovery of non-coding drivers	<ul style="list-style-type: none"> Estimated ~10-fold more coding than non-coding driver point mutations. Variation in point mutation density in non-coding regions influenced more by mutational processes than selection. 	4
Drivers by pathways and networks	<ul style="list-style-type: none"> Both coding and non-coding alterations contribute to cancer pathways. Some pathways, such as RNA splicing, are primarily driven by non-coding mutations. 	16
Evolution and heterogeneity		
Timing of cancer evolution	<ul style="list-style-type: none"> Each tumour type has a distinct pattern of early and late-occurring driver events. Earliest somatic mutations may occur decades prior to diagnosis, providing opportunities for early diagnosis. Intra-tumour heterogeneity is widespread and tumour subclones contain drivers that are under positive selection. 	7
Structural variants		
Patterns of structural variation	<ul style="list-style-type: none"> Replication-based mechanisms of genome rearrangement frequent in many cancers, often causing driver structural variants. 16 signatures of SV, including break-and-ligate patterns and copy-and-insert patterns, varying by size range, replication timing, tumour type and patient. 	6
Functional consequence of structural variation	<ul style="list-style-type: none"> 52 regions with recurrent structural breakpoints and 90 recurrently fused pairs of loci show evidence of positive selection. Oncogenic fusions are shaped by juxtaposition of proto-oncogenes with tissue-specific regulatory elements. 	4
Patterns of retrotransposition	<ul style="list-style-type: none"> Many flavours of somatic retrotransposition in many cancers: LINE element mobilisation; transductions, pseudogenes, Alu elements. 	10

Scientific	Key findings	Citation
	<ul style="list-style-type: none"> Retrotranspositions can induce genomic instability, including large deletions and breakage-fusion-bridge cycles amplifying cancer genes. 	
Chromothripsis	<ul style="list-style-type: none"> Chromothripsis pervasive across cancers, with frequency > 50% in several tumour types. Replicative processes and templated insertions contribute to rearrangement. 	18
Mutational signatures		
Signatures of point mutations	<ul style="list-style-type: none"> >70 distinct mutational signatures, encompassing SNVs, doublet subs and indels. Multiple signatures from unknown processes of DNA damage, repair and replication. 	5
Mutation distribution across genome	<ul style="list-style-type: none"> Uneven distribution of somatic mutations and structural variants across the genome explained by epigenetic state of tissue, cell of origin and topological associated domains. Can be used to identify a tumour's type and presumed tissue/cell of origin. 	11,12,15
Transcriptional consequences of somatic mutation		
RNA effects of somatic mutation	<ul style="list-style-type: none"> Genomic basis for RNA alterations across ~1200 tumours, including quantitative trait loci, allele specific expression and alternative splicing. Link between mutational signatures and expression; classification of gene fusions; identification of genes recurrently altered at RNA level. 	8,9
Others		
Tumour subtypes from genome sequencing	<ul style="list-style-type: none"> Genomic distribution of somatic mutations, mutational signatures and driver mutations accurately distinguish major tumour types of primaries and metastases. 	12
Mitochondrial DNA mutations	<ul style="list-style-type: none"> Somatic mitochondrial truncating mutations frequent in certain cancer types, associated with activation of critical signaling pathways. 	14
Telomere biology and sequences	<ul style="list-style-type: none"> Activating <i>TERT</i> promoter mutations are the single most frequent non-coding driver. In <i>ATRX/DAXX</i>-mutant tumours, aberrant telomere variant repeat distribution is common. 	4,13

Supplementary Material

Refer to Web version on PubMed Central for supplementary material.

Acknowledgements

We thank research participants who generously donated samples and data, the physicians and clinical staff who contributed to sample annotation and collection, and the numerous funding agencies that contributed to the collection and analysis of this data set.

References

1. Pleasance ED, et al. A comprehensive catalogue of somatic mutations from a human cancer genome. *Nature*. 2010; 463:191–196. [PubMed: 20016485]
2. Pleasance ED, et al. A small-cell lung cancer genome with complex signatures of tobacco exposure. *Nature*. 2010; 463:184–190. [PubMed: 20016488]
3. Ley TJ, Mardis ER, Ding L, Fulton B, McLellan MD. DNA sequencing of a cytogenetically normal acute myeloid leukaemia genome. *Nature*. 2008
4. Rheinbay E, et al. Analyses of non-coding somatic drivers in 2,693 cancer whole genomes. *Nature*. 2019
5. Alexandrov LB, et al. The Repertoire of Mutational Signatures in Human Cancer. *Nature*. 2019
6. Li Y, et al. Patterns of somatic structural variation in human cancer genomes. *Nature*. 2019
7. Gerstung M, et al. The evolutionary history of 2,658 cancers. *Nature*. 2019
8. PCAWG Transcriptome Core Group *et al.* Genomic basis of RNA alterations in cancer. *Nature*. 2019
9. Zhang Y, et al. High-coverage whole-genome analysis of 1220 cancers reveals hundreds of genes deregulated by rearrangement-mediated cis-regulatory alterations. *Nat Commun*. 2019
10. Rodriguez-Martin B, et al. Pan-cancer analysis of whole genomes identifies driver rearrangements promoted by LINE-1 retrotransposition. *Nat Genet*. 2019
11. Kübler K, et al. Tumor mutational landscape is a record of the pre-malignant state. *Nature*. 2019; doi: 10.1101/517565
12. Jiao W, et al. A deep learning system can accurately classify primary and metastatic cancers based on patterns of passenger mutations. *Nat Commun*. 2019
13. Sieverling L, et al. Genomic footprints of activated telomere maintenance mechanisms in cancer. *Nat Commun*. 2019
14. Yuan Y, et al. Comprehensive Molecular Characterization of Mitochondrial Genomes in Human Cancers. *Nat Genet*. 2019
15. Akdemir KC, et al. Chromatin Folding Domains Disruptions by Somatic Genomic Rearrangements in Human Cancers. *Nat Genet*. 2019
16. Reyna MA, et al. Pathway and network analysis of more than 2,500 whole cancer genomes. *Nat Commun*. 2019
17. Bailey MH, et al. Retrospective evaluation of whole exome and genome mutation calls in 746 cancer samples. *Nat Commun*. 2019
18. Cortes-Ciriano I, et al. Comprehensive analysis of chromothripsis in 2,658 human cancers using whole-genome sequencing. *Nature Genetics*. 2019
19. Bray F, Ren J-S, Masuyer E, Ferlay J. Global estimates of cancer prevalence for 27 sites in the adult population in 2008. *Int J Cancer*. 2013; 132:1133–1145. [PubMed: 22752881]
20. Tarver T. Cancer Facts & Figures 2012. American Cancer Society (ACS). *Journal of Consumer Health On the Internet*. 2012; 16:366–367.
21. Hanahan D, Weinberg RA. Hallmarks of Cancer: The Next Generation. *Cell*. 2011; 144:646–674. [PubMed: 21376230]
22. International Cancer Genome Consortium. et al. International network of cancer genome projects. *Nature*. 2010; 464:993–998. [PubMed: 20393554]
23. Bailey MH, et al. Comprehensive Characterization of Cancer Driver Genes and Mutations. *Cell*. 2018; 173:371–385.e18. [PubMed: 29625053]
24. Sanchez-Vega F, et al. Oncogenic Signaling Pathways in The Cancer Genome Atlas. *Cell*. 2018; 173:321–337.e10. [PubMed: 29625050]
25. Hoadley KA, et al. Cell-of-Origin Patterns Dominate the Molecular Classification of 10,000 Tumors from 33 Types of Cancer. *Cell*. 2018; 173:291–304.e6. [PubMed: 29625048]
26. Stein LD, Knoppers BM, Campbell P, Getz G, Korbel JO. Data analysis: Create a cloud commons. *Nature*. 2015; 523:149–151. [PubMed: 26156357]
27. Phillips M, et al. Of Clouds and Genomic Data Protection. *Nature*. 2019
28. Krochmalski, J. *Developing with Docker*. Packt Publishing Ltd; 2016.

29. Welch JS, et al. The origin and evolution of mutations in acute myeloid leukemia. *Cell*. 2012; 150:264–278. [PubMed: 22817890]
30. Nik-Zainal S, et al. Landscape of somatic mutations in 560 breast cancer whole-genome sequences. *Nature*. 2016; 534:47–54. [PubMed: 27135926]
31. Meier B, et al. *C. elegans* whole-genome sequencing reveals mutational signatures related to carcinogens and DNA repair deficiency. *Genome Research*. 2014; 24:1624–1636. [PubMed: 25030888]
32. Martincorena I, et al. Universal Patterns of Selection in Cancer and Somatic Tissues. *Cell*. 2018; 173:1823.
33. Tamborero D, et al. Cancer Genome Interpreter annotates the biological and clinical relevance of tumor alterations. *Genome Med*. 2018; 10:25. [PubMed: 29592813]
34. Huang FW, et al. Highly recurrent TERT promoter mutations in human melanoma. *Science*. 2013; 339:957–959. [PubMed: 23348506]
35. Rheinbay E, et al. Recurrent and functional regulatory mutations in breast cancer. *Nature*. 2017; 547:55–60. [PubMed: 28658208]
36. Fredriksson NJ, Ny L, Nilsson JA, Larsson E. Systematic analysis of noncoding somatic mutations and gene expression alterations across 14 tumor types. *Nat Genet*. 2014; 46:1258–1263. [PubMed: 25383969]
37. Horn S, et al. TERT promoter mutations in familial and sporadic melanoma. *Science*. 2013; 339:959–961. [PubMed: 23348503]
38. Ciriello G, et al. Emerging landscape of oncogenic signatures across human cancers. *Nat Genet*. 2013; 45:1127–1133. [PubMed: 24071851]
39. Rahman N. Realizing the promise of cancer predisposition genes. *Nature*. 2014; 505:302–308. [PubMed: 24429628]
40. Pearl LH, Schierz AC, Ward SE, Al-Lazikani B, Pearl FMG. Therapeutic opportunities within the DNA damage response. *Nat Rev Cancer*. 2015; 15:166–180. [PubMed: 25709118]
41. Taylor-Weiner A, et al. DeTiN: overcoming tumor-in-normal contamination. *Nat Methods*. 2018; 15:531–534. [PubMed: 29941871]
42. Fujimoto A, et al. Whole-genome mutational landscape and characterization of noncoding and structural mutations in liver cancer. *Nature Genetics*. 2016; 48:500–509. [PubMed: 27064257]
43. Shlush LI. Age-related clonal hematopoiesis. *Blood*. 2018; 131:496–504. [PubMed: 29141946]
44. Northcott PA, et al. The whole-genome landscape of medulloblastoma subtypes. *Nature*. 2017; 547:311–317. [PubMed: 28726821]
45. Scarpa A, et al. Whole-genome landscape of pancreatic neuroendocrine tumours. *Nature*. 2017; 543:65–71. [PubMed: 28199314]
46. Davis CF, et al. The somatic genomic landscape of chromophobe renal cell carcinoma. *Cancer Cell*. 2014; 26:319–330. [PubMed: 25155756]
47. Berger MF, et al. The genomic complexity of primary human prostate cancer. *Nature*. 2011; 470:214–220. [PubMed: 21307934]
48. Baca SC, et al. Punctuated evolution of prostate cancer genomes. *Cell*. 2013; 153:666–677. [PubMed: 23622249]
49. Nik-Zainal S, et al. The Life History of 21 Breast Cancers. *Cell*. 2012; 149:994–1007. [PubMed: 22608083]
50. Nik-Zainal S, et al. Mutational processes molding the genomes of 21 breast cancers. *Cell*. 2012; 149:979–993. [PubMed: 22608084]
51. Roberts SA, et al. Clustered mutations in yeast and in human cancers can arise from damaged long single-strand DNA regions. *Mol Cell*. 2012; 46:424–435. [PubMed: 22607975]
52. Rausch T, et al. Genome sequencing of pediatric medulloblastoma links catastrophic DNA rearrangements with TP53 mutations. *Cell*. 2012; 148:59–71. [PubMed: 22265402]
53. Stephens PJ, et al. Massive Genomic Rearrangement Acquired in a Single Catastrophic Event during Cancer Development. *Cell*. 2011; 144:27–40. [PubMed: 21215367]
54. Korbel JO, Campbell PJ. Criteria for inference of chromothripsis in cancer genomes. *Cell*. 2013; 152:1226–1236. [PubMed: 23498933]

55. Zhang C-Z, et al. Chromothripsis from DNA damage in micronuclei. *Nature*. 2015; 522:179–184. [PubMed: 26017310]
56. Cancer Genome Atlas Research Network. Integrated genomic characterization of papillary thyroid carcinoma. *Cell*. 2014; 159:676–690. [PubMed: 25417114]
57. Supek F, Lehner B. Clustered Mutation Signatures Reveal that Error-Prone DNA Repair Targets Mutations to Active Genes. *Cell*. 2017; 170:534–547.e23. [PubMed: 28753428]
58. Cortes-Ciriano I, et al. Comprehensive analysis of chromothripsis in 2,658 human cancers using whole-genome sequencing. *Genomics*. 2018
59. Mardin BR, et al. A cell-based model system links chromothripsis with hyperploidy. *Mol Syst Biol*. 2015; 11:828. [PubMed: 26415501]
60. Weischenfeldt J, et al. Integrative genomic analyses reveal an androgen-driven somatic alteration landscape in early-onset prostate cancer. *Cancer Cell*. 2013; 23:159–170. [PubMed: 23410972]
61. Garsed DW, et al. The architecture and evolution of cancer neochromosomes. *Cancer Cell*. 2014; 26:653–667. [PubMed: 25517748]
62. Durinck S, et al. Temporal dissection of tumorigenesis in primary cancers. *Cancer Discov*. 2011; 1:137–143. [PubMed: 21984974]
63. Dentre SC, et al. Portraits of genetic intra-tumour heterogeneity and subclonal selection across cancer types.
64. Hayward NK, et al. Whole-genome landscapes of major melanoma subtypes. *Nature*. 2017; 545:175–180. [PubMed: 28467829]
65. Cancer Genome Atlas Network. Genomic Classification of Cutaneous Melanoma. *Cell*. 2015; 161:1681–1696. [PubMed: 26091043]
66. Alexandrov LB, et al. The Repertoire of Mutational Signatures in Human Cancer. *Nature*. 2019
67. Alexandrov LB, et al. Signatures of mutational processes in human cancer. *Nature*. 2013; 500:415–421. [PubMed: 23945592]
68. Chan K, et al. An APOBEC3A hypermutation signature is distinguishable from the signature of background mutagenesis by APOBEC3B in human cancers. *Nat Genet*. 2015; 47:1067–1072. [PubMed: 26258849]
69. Nik-Zainal S, et al. Association of a germline copy number polymorphism of APOBEC3A and APOBEC3B with burden of putative APOBEC-dependent mutations in breast cancer. *Nat Genet*. 2014; 46:487–491. [PubMed: 24728294]
70. Middlebrooks CD, et al. Association of germline variants in the APOBEC3 region with cancer risk and enrichment with APOBEC-signature mutations in tumors. *Nat Genet*. 2016; 48:1330–1338. [PubMed: 27643540]
71. Westra H-J, et al. Systematic identification of trans eQTLs as putative drivers of known disease associations. *Nat Genet*. 2013; 45:1238–1243. [PubMed: 24013639]
72. Stranger BE, et al. Population genomics of human gene expression. *Nat Genet*. 2007; 39:1217–1224. [PubMed: 17873874]
73. Menghi F, et al. The tandem duplicator phenotype as a distinct genomic configuration in cancer. *Proc Natl Acad Sci U S A*. 2016; 113:E2373–82. [PubMed: 27071093]
74. Hendrich B, Hardeland U, Ng HH, Jiricny J, Bird A. The thymine glycosylase MBD4 can bind to the product of deamination at methylated CpG sites. *Nature*. 1999; 401:301–304. [PubMed: 10499592]
75. Lee E, et al. Landscape of Somatic Retrotransposition in Human Cancers. *Science*. 2012; 337:967–971. [PubMed: 22745252]
76. Tubio JMC, et al. Extensive transduction of nonrepetitive DNA mediated by L1 retrotransposition in cancer genomes. *Science*. 2014; 345
77. Helman E, et al. Somatic retrotransposition in human cancer revealed by whole-genome and exome sequencing. *Genome Res*. 2014; 24:1053–1063. [PubMed: 24823667]
78. Shay JW, Wright WE. Hayflick, his limit, and cellular ageing. *Nat Rev Mol Cell Biol*. 2000; 1:72–76. [PubMed: 11413492]
79. Peifer M, et al. Telomerase activation by genomic rearrangements in high-risk neuroblastoma. *Nature*. 2015; 526:700–704. [PubMed: 26466568]

80. Totoki Y, et al. Trans-ancestry mutational landscape of hepatocellular carcinoma genomes. *Nat Genet.* 2014; 46:1267–1273. [PubMed: 25362482]
81. Paterlini-Bréchet P, et al. Hepatitis B virus-related insertional mutagenesis occurs frequently in human liver cancers and recurrently targets human telomerase gene. *Oncogene.* 2003; 22:3911–3916. [PubMed: 12813464]
82. Heaphy CM, et al. Prevalence of the alternative lengthening of telomeres telomere maintenance mechanism in human cancer subtypes. *Am J Pathol.* 2011; 179:1608–1615. [PubMed: 21888887]
83. Sieverling L, et al. Genomic footprints of activated telomere maintenance mechanisms in cancer. *Genomics.* 2017
84. Barthel FP, et al. Systematic analysis of telomere length and somatic alterations in 31 cancer types. *Nat Genet.* 2017; 49:349–357. [PubMed: 28135248]
85. García-Cao M, Gonzalo S, Dean D, Blasco MA. A role for the Rb family of proteins in controlling telomere length. *Nat Genet.* 2002; 32:415–419. [PubMed: 12379853]
86. Tomasetti C, Vogelstein B. Cancer etiology. Variation in cancer risk among tissues can be explained by the number of stem cell divisions. *Science.* 2015; 347:78–81. [PubMed: 25554788]
87. Gerstung M, et al. Precision oncology for acute myeloid leukemia using a knowledge bank approach. *Nat Genet.* 2017; 49:332–340. [PubMed: 28092685]
88. O'Connor BD, et al. The Dockstore: enabling modular, community-focused sharing of Docker-based genomics tools and workflows. *F1000Research.* 2017; 6:52. [PubMed: 28344774]
89. Zhang J, et al. The International Cancer Genome Consortium Data Portal. *Nat Biotechnol.* 2019; 37:367–369. [PubMed: 30877282]
90. Miller CA, Qiao Y, DiSera T, D'Astous B, Marth GT. bam.iobio: a web-based, real-time, sequence alignment file inspector. *Nature Methods.* 2014; 11:1189–1189. [PubMed: 25423016]
91. Goldman M, et al. The UCSC Xena platform for public and private cancer genomics data visualization and interpretation.
92. Papatheodorou I, et al. Expression Atlas: gene and protein expression across multiple studies and organisms. *Nucleic Acids Research.* 2018; 46:D246–D251. [PubMed: 29165655]
93. SEER ICD-O-3 Coding Materials. Available at: <https://seer.cancer.gov/icd-o-3/>
94. Li H, Durbin R. Fast and accurate long-read alignment with Burrows–Wheeler transform. *Bioinformatics.* 2010; 26:589–595. [PubMed: 20080505]
95. 1000 Genomes Project Consortium *et al.* A global reference for human genetic variation. *Nature.* 2015; 526:68–74. [PubMed: 26432245]
96. Raine KM, et al. ascatNgs: Identifying Somatic Copy-Number Alterations from Whole-Genome Sequencing Data. *Curr Protoc Bioinformatics.* 2016; 56:15.9.1–15.9.17.
97. Jones D, et al. cgpCaVEManWrapper: Simple Execution of CaVEMan in Order to Detect Somatic Single Nucleotide Variants in NGS Data. *Curr Protoc Bioinformatics.* 2016; 56:15.10.1–15.10.18.
98. Raine KM, et al. cgpPindel: Identifying Somatic Acquired Insertion and Deletion Events from Paired End Sequencing. *Curr Protoc Bioinformatics.* 2015; 52:15.7.1–12.
99. Ye K, Schulz MH, Long Q, Apweiler R, Ning Z. Pindel: a pattern growth approach to detect break points of large deletions and medium sized insertions from paired-end short reads. *Bioinformatics.* 2009; 25:2865–2871. [PubMed: 19561018]
100. Rausch T, et al. DELLY: structural variant discovery by integrated paired-end and split-read analysis. *Bioinformatics.* 2012; 28:i333–i339. [PubMed: 22962449]
101. Rimmer A, et al. Integrating mapping-, assembly- and haplotype-based approaches for calling variants in clinical sequencing applications. *Nature Genetics.* 2014; 46:912–918. [PubMed: 25017105]
102. Cibulskis K, et al. Sensitive detection of somatic point mutations in impure and heterogeneous cancer samples. *Nat Biotechnol.* 2013; 31:213–219. [PubMed: 23396013]
103. Carter SL, et al. Absolute quantification of somatic DNA alterations in human cancer. *Nat Biotechnol.* 2012; 30:413–421. [PubMed: 22544022]
104. Drier Y, et al. Somatic rearrangements across cancer reveal classes of samples with distinct patterns of DNA breakage and rearrangement-induced hypermutability. *Genome Research.* 2013; 23:228–235. [PubMed: 23124520]

105. Ramos AH, et al. Oncotator: Cancer Variant Annotation Tool. *Human Mutation*. 2015; 36:E2423–E2429. [PubMed: 25703262]
106. Moncunill V, et al. Comprehensive characterization of complex structural variations in cancer by directly comparing genome sequence reads. *Nat Biotechnol*. 2014; 32:1106–1112. [PubMed: 25344728]
107. Fan Y, et al. MuSE: accounting for tumor heterogeneity using a sample-specific error model improves sensitivity and specificity in mutation calling from sequencing data. *Genome Biol*. 2016; 17:178. [PubMed: 27557938]
108. Cooke SL, et al. Processed pseudogenes acquired somatically during cancer development. *Nature Communications*. 2014; 5
109. Ju YS, et al. Origins and functional consequences of somatic mitochondrial DNA mutations in human cancer. *eLife*. 2014; 3
110. Group PTC, et al. Genomic basis for RNA alterations revealed by whole-genome analyses of 27 cancer types.
111. Sudmant PH, et al. An integrated map of structural variation in 2,504 human genomes. *Nature*. 2015; 526:75–81. [PubMed: 26432246]
112. Garrison E, Marth G. Haplotype-based variant detection from short-read sequencing. *arXiv [q-bio.GN]*. 2012
113. DePristo MA, et al. A framework for variation discovery and genotyping using next-generation DNA sequencing data. *Nature Genetics*. 2011; 43:491–498. [PubMed: 21478889]
114. Yakneen S, Waszak SM, Gertz M, Korbel JO, PCAWG Consortium. Enabling rapid cloud-based analysis of thousands of human genomes via Butler. *Nat Biotechnol*. 2019
115. Kim SY, Jacob L, Speed TP. Combining calls from multiple somatic mutation-callers. *BMC Bioinformatics*. 2014; 15:154. [PubMed: 24885750]
116. Breiman L. Stacked regressions. *Mach Learn*. 1996; 24:49–64.
117. Campbell PJ, et al. Identification of somatically acquired rearrangements in cancer using genome-wide massively parallel paired-end sequencing. *Nat Genet*. 2008; 40:722–729. [PubMed: 18438408]
118. Wala JA, et al. SvABA: genome-wide detection of structural variants and indels by local assembly. *Genome Research*. 2018; 28:581–591. [PubMed: 29535149]

BOX 1**Online resources for data access, visualisation and analysis**

The PCAWG Landing Page at <http://docs.icgc.org/pcawg> provides links to several data resources for interactive online browsing, analysis and download of PCAWG data and results (Supplementary Table 4).

Direct download of PCAWG data

Aligned PCAWG read data in BAM format are also available at the European Genome Phenome Archive (EGA; <https://www.ebi.ac.uk/ega/search/site/pcawg> under accession EGAS00001001692). In addition, all open tier PCAWG genomics data, as well as reference data sets used for analysis, can be downloaded from the ICGC Data Portal at <http://docs.icgc.org/pcawg/data/>. Controlled tier genomic data, including SNVs and indels that originated from TCGA projects (in VCF format), and aligned reads (in BAM format) can be downloaded using the Score (<https://www.overture.bio/>) software package, which implements accelerated and secure file transfer, as well as BAM slicing facilities to selectively download defined regions of genomic alignments.

PCAWG computational pipelines

The core alignment, somatic variant-calling, quality control and variant consensus generation pipelines used by PCAWG have each been packaged into portable cross-platform images using the Dockstore system⁸⁸ and released under an Open Source license that allows for unrestricted usage and redistribution. All PCAWG Dockstore images are available to the public at <https://dockstore.org>.

ICGC Data Portal (<https://dcc.icgc.org>).

The ICGC Data Portal⁸⁹ serves as the main entry point for accessing PCAWG datasets with a single uniform web interface and a high-performance data download client. This uniform interface gives users easy access to the myriad of PCAWG sequencing data and variant calls that reside in many repositories and compute clouds worldwide. Streaming technology⁹⁰ gives users high-level visualisations in real time of BAM and VCF files stored remotely on the Cancer Genome Collaboratory.

UCSC Xena (<https://pcawg.xenahubs.net>)

UCSC Xena⁹¹ visualises all PCAWG primary results, including copy number, gene expression, gene fusion, promoter usage, simple somatic mutations, large somatic structural variation, mutational signatures and phenotypic data. These open-access data are available through a public Xena hub, while consensus simple somatic mutations can be loaded into a user's local computer private Xena hub. Kaplan-Meier plots, histograms, boxplots, scatterplots and transcript-specific views offer additional visualisation options and statistical analyses.

Expression Atlas (<https://www.ebi.ac.uk/gxa/home>)

The Expression Atlas contains RNAseq and expression microarray data for querying gene expression across tissues, cell types, developmental stages and/or experimental

conditions⁹². Two different views of the data are provided: summarised expression levels for each tumour type and gene expression at the level of individual samples, including reference gene expression datasets for matching normal tissues.

PCAWG-Scout (<http://pcawgscout.bsc.es/>)

PCAWG-Scout provides a framework for 'omics workflow and website templating to make on-demand, in-depth analyses over the PCAWG data openly available to the whole research community. Views of protected data are available that still safeguard sensitive data. Through the PCAWG-Scout web interface, users can access an array of reports and visualisations that leverage on-demand bioinformatic computing infrastructure to produce results in real-time, allowing users to discover trends as well as form and test hypotheses.

Chromothripsis Explorer (<http://compbio.med.harvard.edu/chromothripsis/>)

Chromothripsis Explorer is a portal that allows structural variation in the PCAWG dataset to be explored on an individual patient basis through the use of circos plots. Patterns of chromothripsis can also be explored in aggregated formats.

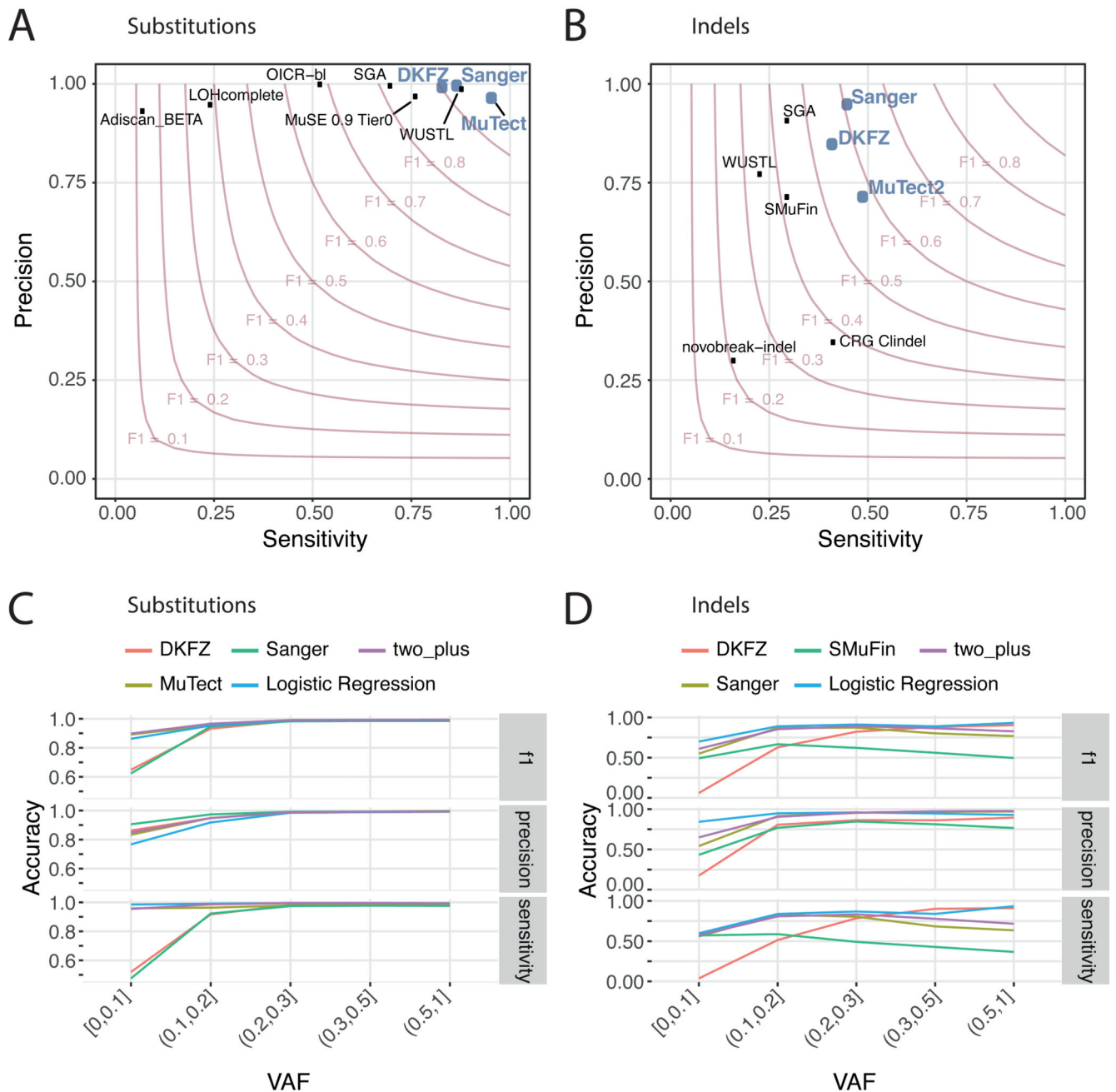


Figure 1. Validation of variant-calling pipelines in PCAWG.

(A) Scatter plot of estimated sensitivity and precision for somatic SNVs across individual algorithms assessed in the validation exercise across $n=63$ PCAWG samples. Core algorithms included in the final PCAWG call-set are shown in blue. (B) Sensitivity and precision estimates across individual algorithms for somatic indels. (C) Accuracy (F_1 score, precision and sensitivity) of somatic SNV calls across variant allele fractions (VAF) for the core algorithms. Also shown is the accuracy for two methods of combining variant calls

(two-plus, which was used in the final data-set, and logistic regression). **(D)** Accuracy of indel calls across VAFs.

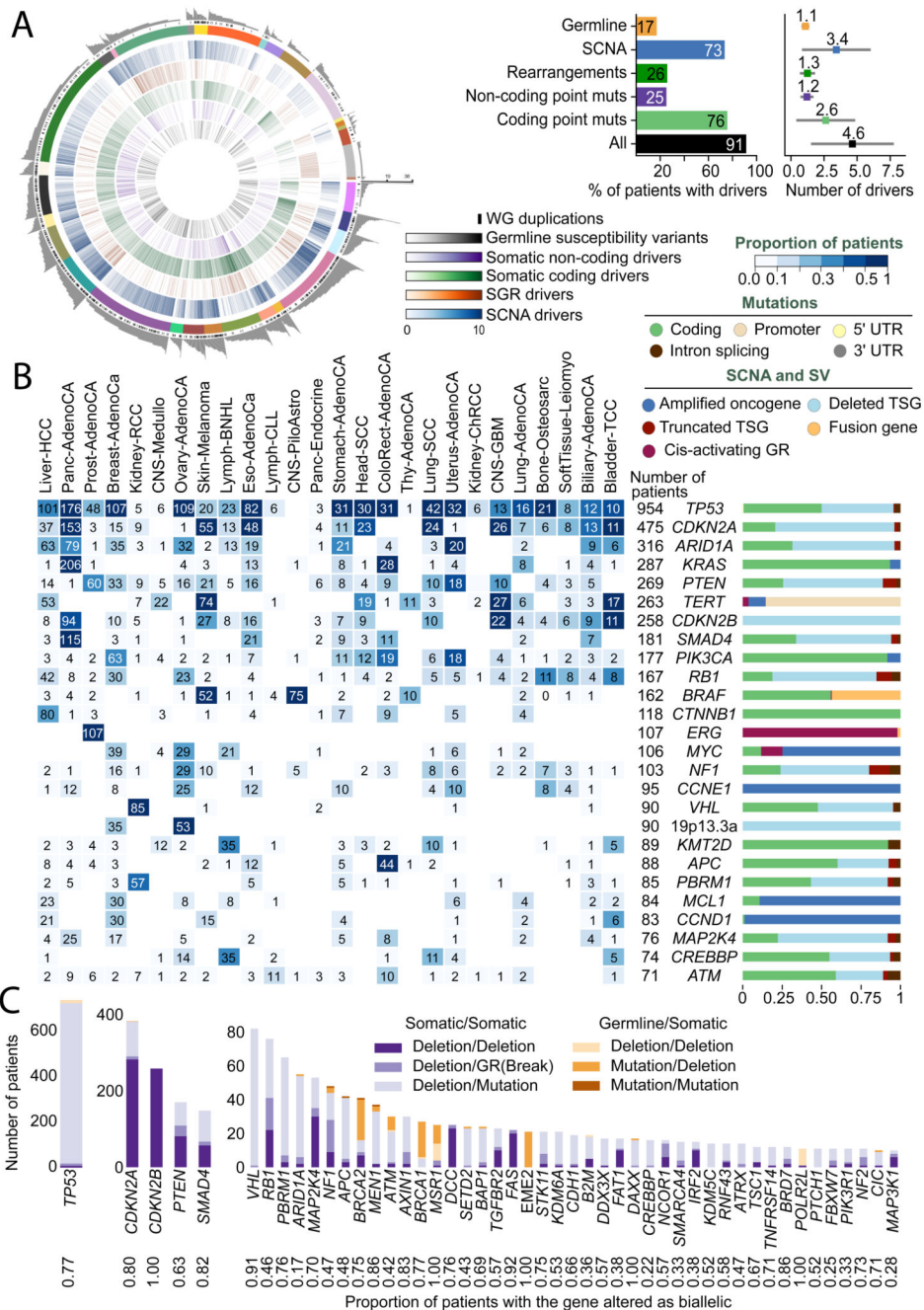


Figure 2. Panorama of driver mutations in PCAWG.

(A) **Left panel:** putative driver mutations in PCAWG, represented as a circos plot. Each sector represents a tumour in the cohort. From the periphery to the centre of the plot the concentric rings represent: i) the total number of driver alterations; ii) presence of whole genome duplication; iii) the tumour type; iv) the number of driver copy number alterations; v) the number of driver genomic rearrangements; vi) driver coding point mutations; vii) driver non-coding point mutations; and viii) pathogenic germline variants. **Right panel:** Snapshots of the panorama of driver mutations. The horizontal bar plot at the left represents

the proportion of patients with different types of drivers. The dot plot at the right represents the mean number of each type of driver mutation across tumours with at least one event (the square dot), and its standard deviation (gray whiskers), based on $n=2,583$ patients. **(B)** Genomic elements targeted by different types of mutations in the cohort in more than 65 tumours. Both germline and somatic variants are included. The heatmap shows the recurrence of alterations experienced across cancer types (with the colour indicating the proportion, and the number indicating the absolute count of mutated tumours); the barplot at the right reflects the proportion of each type of alteration affecting each genomic element. **(C)** Tumour suppressor genes with biallelic inactivation in 10 or more patients. The values quoted under the gene labels represent the proportions of patients who have biallelic mutations of the gene out of all patients with a somatic mutation in that gene.

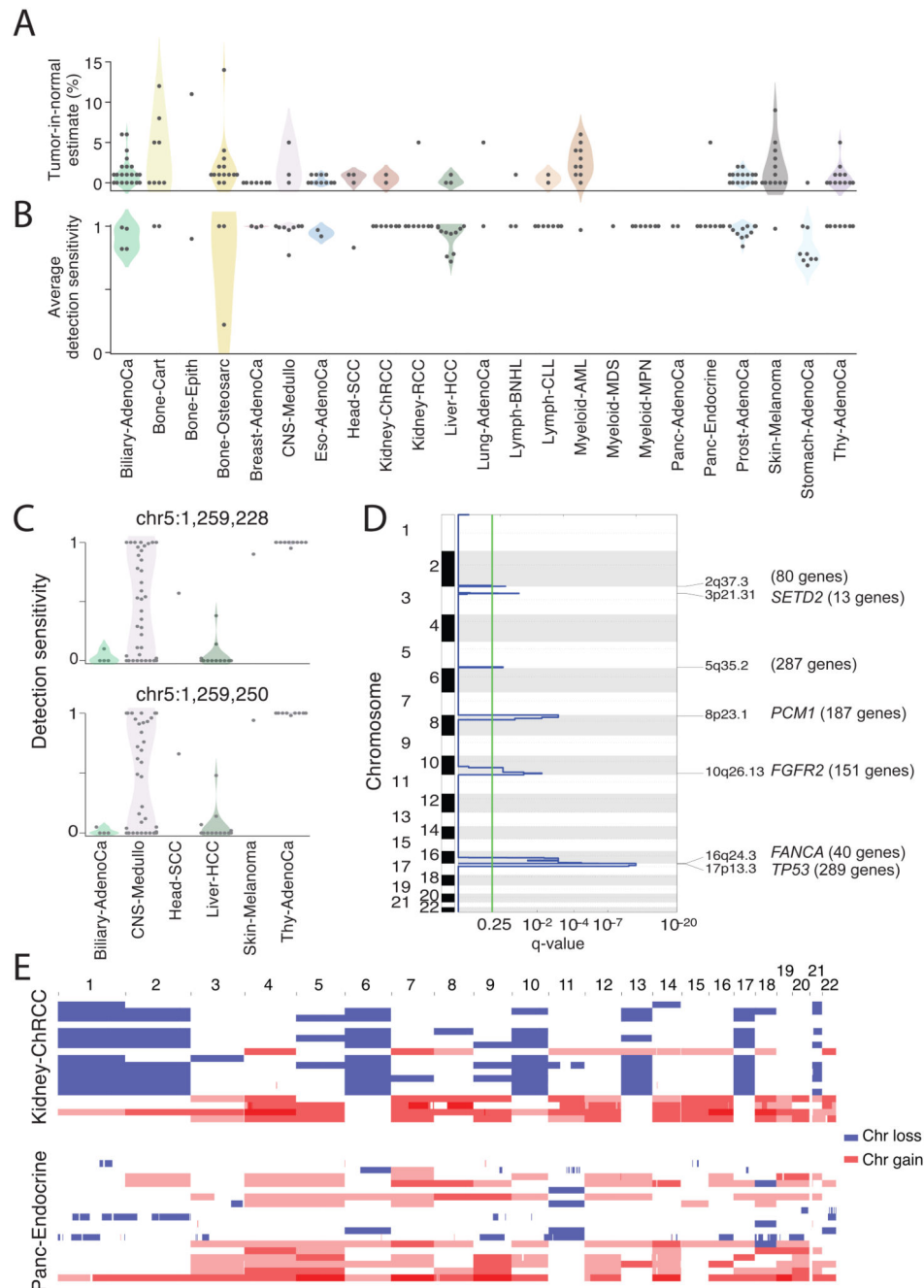


Figure 3. Analysis of patients with no detected driver mutations.

(A) Individual estimates of percentage of tumour-in-normal contamination across no-driver patients in PCAWG (n=181). No data were available for Myeloid-MDS and Myeloid-AML. Points represent estimates for individual patients, and the coloured areas beneath the points are estimated density distributions (violin plots). (B) Average detection sensitivity by tumour type for tumours without known drivers (n=181). Each dot represents a given sample and represents the average sensitivity for detecting clonal substitutions across the genome. Coloured areas beneath the points are estimated density distributions, shown for cohorts

with 5 cases. **(C)** Detection sensitivity for *TERT* promoter hotspots in tumour types where *TERT* is frequently mutated. Coloured areas beneath the points are estimated density distributions. **(D)** Significant copy number losses identified by two-sided hypothesis testing using GISTIC2.0, corrected for multiple hypothesis testing. Numbers in parentheses are the number of genes in significant regions when analysing missing-driver tumours (n=181). Significant regions with known cancer genes are labelled with a representative cancer gene. **(E)** Aneuploidy in Kidney-ChRCC and Panc-Endocrine cancers without known drivers. Patients are ordered in the y axis by tumour type and then by presence of whole genome duplication (bottom) or not (top).

PCAWG vs their genomic position. Lymphoid tumours (khaki for Lymph-BNHL and orange for Lymph-CLL) harbour hypermutation hot spots (3 foci with distance 1kb; pale red zone), many near known cancer genes (red annotations) and with associated SVs (10kb from the focus; shown as internal arcs). **(C)** Circos rainfall plot as in **B** showing distance vs position for consecutive chromoplexy and reciprocal translocation footprints across PCAWG. Lymphoid, prostate and thyroid cancers exhibit recurrent events (2 footprints with distance 10kb; pale red zone) likely to be driver structural variants and are annotated with nearby genes and associated SVs shown as bold and thin arcs for chromoplexy and reciprocal translocations, respectively (colours as in **A**). **(D)** Impact of chromothripsis along the genome and involvement of PCAWG driver genes. **Top.** Number of chromothripsis-induced gains/losses (grey) and amplifications/deletions (blue/red). Within the identified chromothripsis regions, selected recurrently rearranged (light grey), amplified (blue) and homozygously deleted (red) driver genes are indicated. **Bottom.** Inter-breakpoints distance between all subsequent breakpoints within chromothripsis regions across cancer types, coloured by cancer type. Regions with an average inter-breakpoint distance <10kb are highlighted.

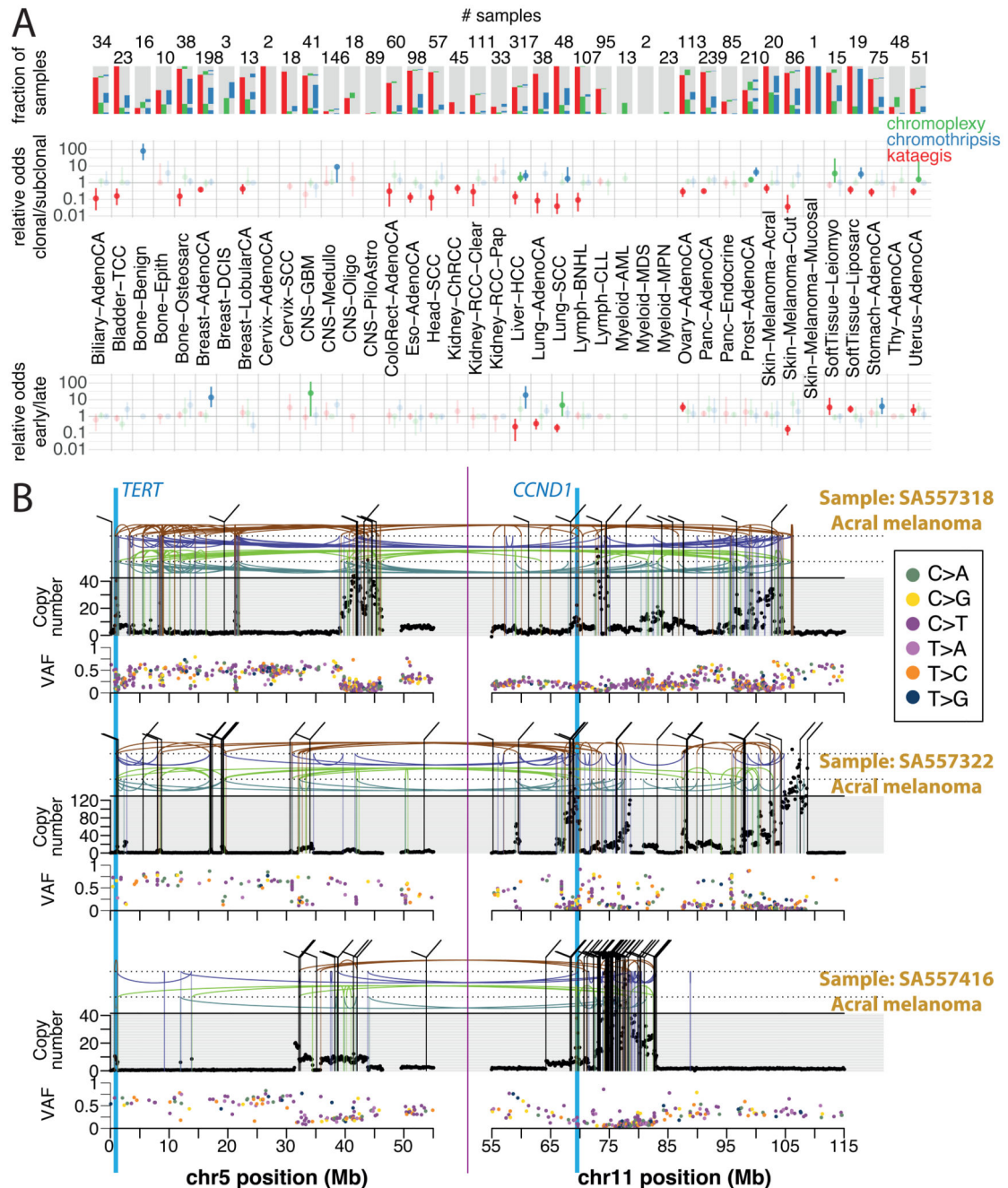


Figure 5. Timing of clustered events in PCAWG.

(A) Extent and timing of chromothripsis, kataegis and chromoplexy across PCAWG. (top) Stacked bar-charts illustrate co-occurrence in samples. (middle) Relative odds of clustered events being clonal vs subclonal are plotted with bootstrapped 95% confidence intervals. Point estimates are highlighted when they do not overlap 1:1 odds. (bottom) Relative odds of the events being early vs late clonal are plotted as above. Sample sizes (number of patients) are shown across the top panel. (B) Three representative patients with melanoma and chromothripsis-induced amplification simultaneously affecting *TERT* and *CCND1*. The

black points in the upper panel represent sequence coverage from individual genomic bins, with structural variants shown as coloured arcs (translocation in black, deletion in purple, duplication in brown, tail-to-tail inversion in cyan, head-to-head inversion in green). The lower panel shows the variant allele fraction (VAF) of somatic point mutations.

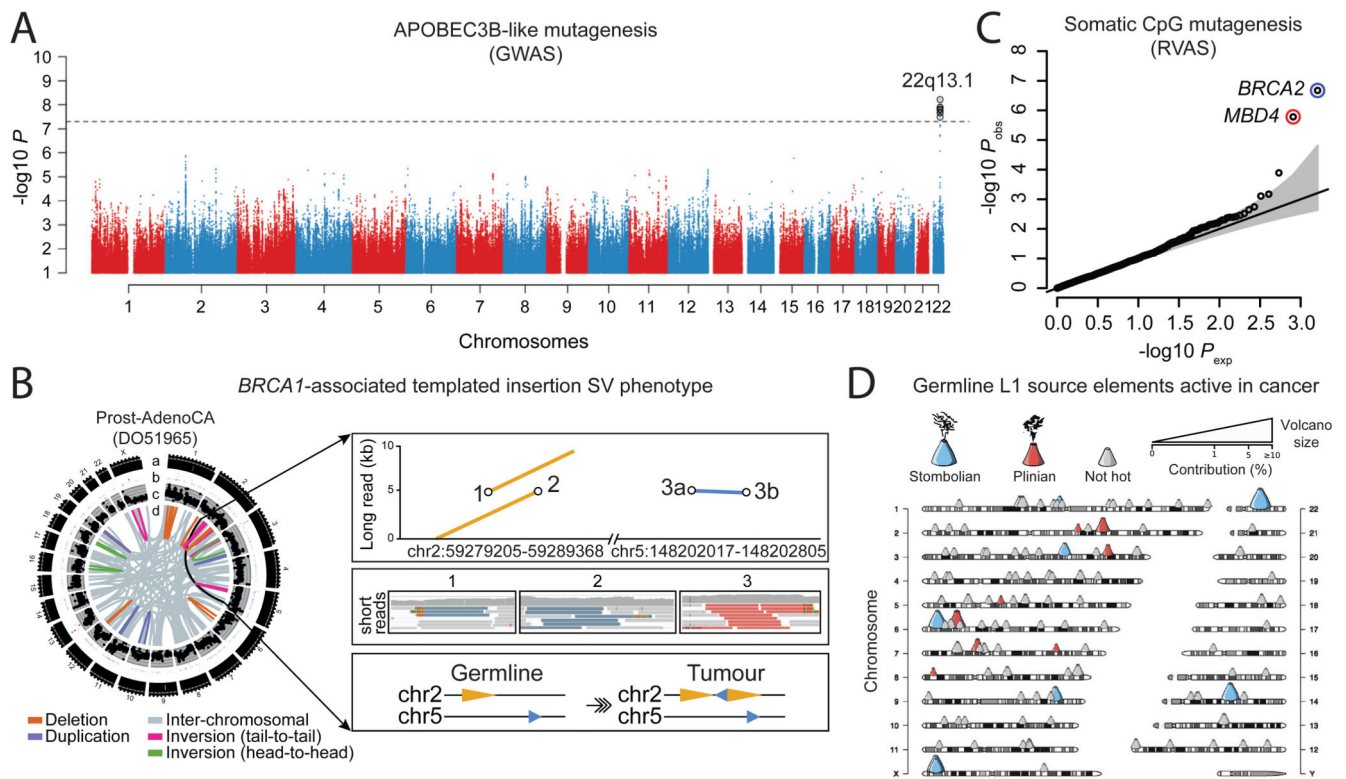


Figure 6. Germline determinants of the somatic mutation landscape.

(A) Association between common ($MAF > 5\%$) germline variants and somatic APOBEC3B-like mutagenesis in individuals of European ancestry ($n = 1201$). Two-sided hypothesis testing was performed with PLINK v1.9. To mitigate multiple hypothesis-testing, the significance threshold was set at genome-wide significance ($p < 5 \times 10^{-8}$). (B) Templated insertion SVs in a *BRCA1*-associated prostate cancer. Left panel: chromosome bands (a); SVs 10Mbp (b); 1kb read-depth from CN 0-6 (c); inter- and intra-chromosomal SVs (> 10 Mbp) (d). Right panel: complex somatic SV composed of a 2.2 kb tandem duplication on chr2 together with a 232 bp inverted templated insertion SV that is derived from chr5 and inserted in-between the tandem duplication (bottom panel). Consensus sequence alignment of locally assembled ONT long-reads to chr2 and 5 of the human reference genome (top panel). Breakpoints are circled and marked as 1 (beginning of tandem duplication), 2 (end of tandem duplication), and 3 (inverted templated insertion). For each breakpoint, the middle panel shows Illumina short reads at SV breakpoints. (C) Association between rare germline PTVs ($MAF < 0.5\%$) and somatic CpG mutagenesis (approx. with Signature 1) in individuals of European ancestry ($n = 1201$). Genes highlighted in blue/red were associated with lower/higher somatic mutation rates. Two-sided hypothesis testing was performed using linear regression models with sex, age at diagnosis, and ICGC project as variables. To mitigate multiple hypothesis-testing, the significance threshold was set at exome-wide significance ($p < 2.5 \times 10^{-6}$). The black line represents the identity line which would be followed if the observed p values followed the null expectation, with shaded area showing 95% confidence intervals. (D) Catalogue of polymorphic germline L1 source elements active in cancer. Chromosomal map shows germline source L1 elements as volcano symbols. Each volcano is

colour-coded according to the type of source L1 activity. The contribution of each source locus (expressed as percentage) to the total number of transductions identified in PCAWG tumours is represented in a size gradient, with top contributing elements exhibiting larger sizes.

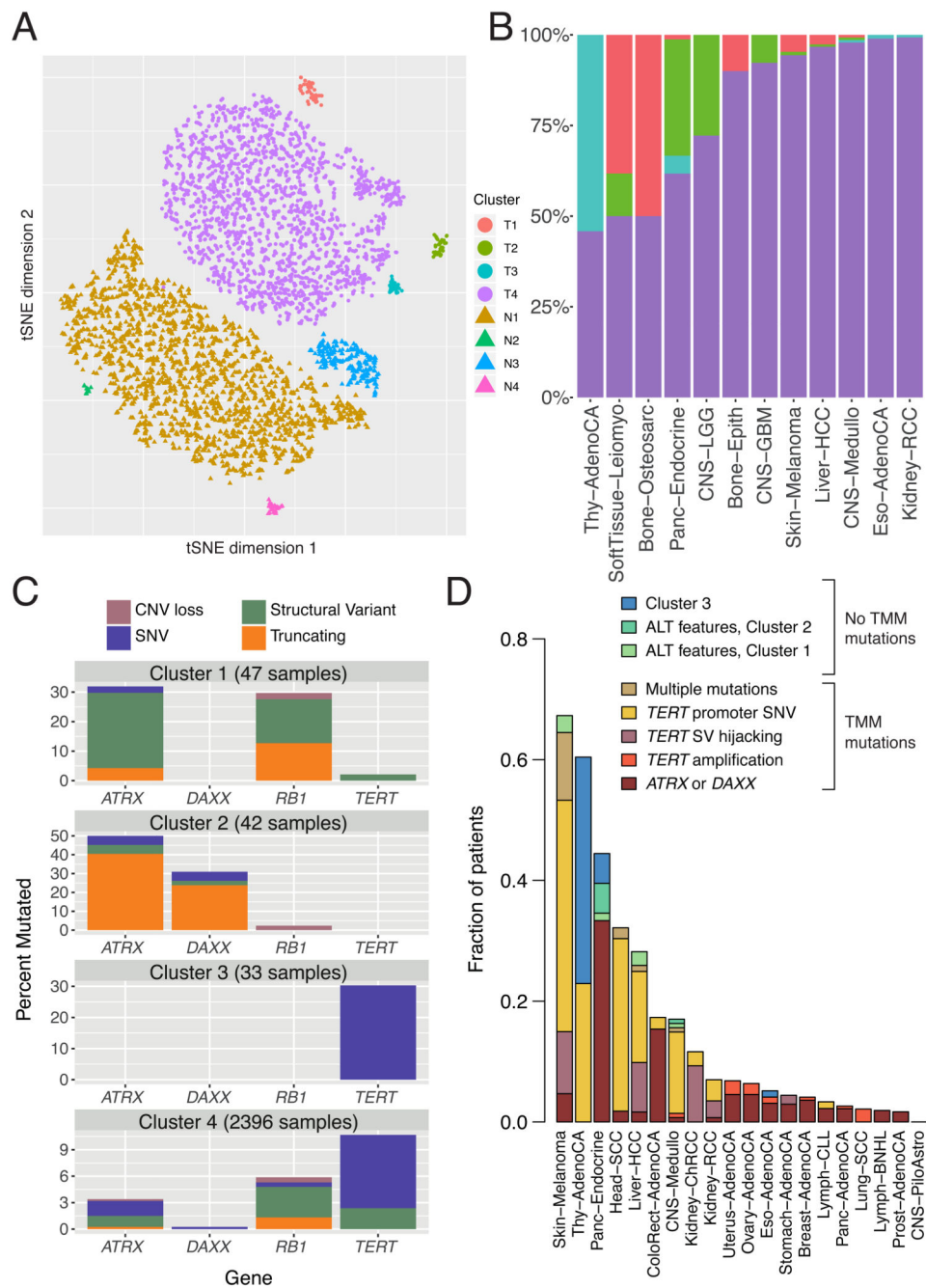


Figure 7. Telomere sequence patterns across PCAWG.

(A) Scatter-plot showing clusters of telomere patterns identified across PCAWG by t-Distributed Stochastic Neighbour Embedding (tSNE), based on $n=2,518$ tumour samples and their matched normal samples. Axes have arbitrary dimension such that samples with similar telomere profiles are clustered together and samples with dissimilar telomere profiles are far apart with high probability. (B) Distribution of the four tumour-specific clusters of telomere patterns in selected tumour types from PCAWG. (C) Distribution of relevant driver mutations associated with alternative lengthening of telomere and normal telomere

maintenance across the four clusters. **(D)** Distribution of telomere maintenance abnormalities across tumour types with more than 40 patients in PCAWG. Samples classified as tumour cluster 1-3 if they fall into a relevant cluster without mutations in *TERT*, *ATRX* or *DAXX* and have no ALT phenotype.